Characterization of the Dnmt2 homolog Pmt1 in *Schizosaccharomyces pombe*

Inaugural-Dissertation

zur

Erlangung des Doktorgrades

Dr. rer. nat.

der Fakultät für

Biologie

an der

Universität Duisburg-Essen

vorgelegt von

Maria Becker

aus Berlin

Februar 2012

Die der vorliegenden Arbeit zugrunde liegenden Experimente wurden in der Abteilung für Genetik der Universität Duisburg-Essen durchgeführt.

1. Gutachter: Prof. Dr. Ann Ehrenhofer-Murray

2. Gutachter: Prof. Dr. Bernhard Horsthemke

3. Gutachter: -

Vorsitzender des Prüfungsausschusses: Prof. Dr. Markus Kaiser

Tag der mündlichen Prüfung: 21.05.2012

TABLE OF CONTENTS

Abbreviations

^{3}H-SAM	S-[methyl-3H]-Adenosyl-L-Methionine
A	adenine
ADD	ATRX-DNMT3-DNMT3L
BAH	bromo adjacent homology
bp	base pair
C	cytosine or cysteine
CBP	calmodulin binding protein
CFU	colony-forming unit
cM	Centimorgan
CR	cysteine-rich
DNA	desoxyribonucleic acid
Dnmt	DNA nucleotide methyltransferase
DTT	dithiothreitol
EDTA	ethylenediaminetetraacetic acid
EGTA	ethylene glycole tetraacetic acid
EMM	Edinburgh Minimal Medium
EST	expressed sequence tag
EtBr	ethidium bromide
G	guanin or glycine
GFP	green fluorescent protein
HDAC	histone deacetylase
ICF	immunodeficiency-centromeric instability-facial anomalies
IgG	immune globulin G
IMAC	immobilized metal affinity chromatography
IPTG	isopropyl β-D-1-thiogalactopyranoside

kDa	Kilodalton
KPi	potassium phosphate buffer
LB	Luria-Bertani broth
m^5C	5-methylcytosine
m^7G	7-methylguanin
mRNA	messenger RNA
nmt	no message in thiamine
N	nitrogen
OD	optical density
ORF	open reading frame
PBHD	polybromo homology domain
PCNA	proliferating cell nuclear antigen
PCR	polymerase chain reaction
PEM	pombe epistasis mapper
Pmt1	pombe methyltransfease 1
PWWP	proline-tryptophan-tryptophan-proline
RNA	ribonucleic acid
RNAi	RNA interference
RTD	rapid tRNA decay
S. cerevisiae	*Saccharomyces cerevisiae*
S. pombe	*Schizosaccharomyces pombe*
SAM	S-adenosyl-methionine
SDS	sodium dodecyl sulfate
SGA	synthetic genetic array
SH-	thiol-
T	thymine or threonine
TAP	tandem affinity purification

TEV	tobacco etch virus
TOR	target of rapamycin
TRD	Target recognition domain
Tris	trizma base
tRNA	transfer RNA
$tRNA^{Asp}$	tRNA coding for aspartate
TSS	transcription start site
U	uracil
YES	Yeast Extract + Supplements, *S. pombe* complete medium
YPD	Yeast extract Peptone Dextrose, *S. cerevisiae* complete medium

1 Lists of figures and tables

1.1 Figures

1.2 Tables

2 Introduction

DNA and RNA can be methylated by a broad variety of methyltransferases. The best studied of these methylations is the methylation at position 5 in cytosine bases that is carried out by DNA or RNA m^5C methyltransferases.

2.1 Cytosine methylation

2.1.1 DNA methylation

The first evidence for methyl groups in DNA was found in calf thymus DNA (Hotchkiss 1948). The significance of this DNA modification was discussed controversially for quite a while, but nowadays DNA methylation is established as a key epigenetic process that is involved in the control of gene expression (Lande-Diner et al. 2007), imprinting (Delaval and Feil 2004; Hore et al. 2007), X-chromosome inactivation (Chang et al. 2006) and maintenance of genome integrity through protection against mobilization of retrotransposons (Howard et al. 2008).

DNA nucleotide bases are methylated at three different positions. In bacteria and most eukaryotes, adenine can be modified at position N6 and cytosine can be methylated at the N4 position in thermophilic bacteria. In eukaryotes, the most commonly found modification of DNA is the methylation of the C5 position of cytosines (Jeltsch 2002). DNA methylation is carried out by DNA methyltransferases that all contain a set of conserved catalytic motifs (see below).

Methylation of cytosines in the mammalian genome occurs primarily in the context of CpG dinucleotides. This dinucleotide is statistically underrepresented in the genome compared to other possible dinucleotides, a phenomenon termed CpG suppression (Robertson and Wolffe 2000). The reason for that is probably the hydrolytic deamination of methylcytosine, which creates a thymine in a TpG mismatch situation. The repair of this mismatch is much less efficient than the repair of the UpG mismatch that would result from the (much slower) deamination of unmethylated cytosine, because for uracil there exists a specialized repair mechanism (Shen et al. 1994). This is due to the fact that uracil is not found in natural DNA. Thus, the DNA

methylation process probably led to the reduction of CpG dinucleotides during evolution.

This reduction of the frequency of CpG dinucleotides can be observed especially in intergenic and intronic regions. On the other hand, repetitive sequences, like transposons and endogenous retroviruses, and CpG islands display less depletion of the CpG dinucleotide (Bird et al. 1985). CpG islands are found in the majority of human promoter regions and are often unmethylated in germ cells. This fact might have prevented these CpG dinucleotides from being lost during molecular evolution (see above). CpG islands can adopt tissue-specific methylation patterns without changes in the germ line cells (Lister et al. 2009), which leads to tissue-specific gene expression through differential promoter activity. Genes that are actively transcribed usually show hypomethylation at the transcription start site (TSS) and hypermethylation in the gene body (Laurent et al. 2010).

DNA methylation is one possible mechanism for long-term silencing of genomic sequences (Robertson and Wolffe 2000), since repressive histone marks and chromatin structure can be altered dynamically upon environmental changes. DNA methylation is less dynamic and it is inherited through cell divisions and can prevent the reactivation of silent genes when it is present in the promoter regions, even when the repressive histone marks are reversed. In cancer cells, promoters of tumor suppressor genes are often also hypermethylated, which leads to repression of the respective gene (Jeltsch 2002).

DNA methylation is especially important for the maintenance of genome integrity and the protection against potentially mobile DNA sequences (Howard et al. 2008). Since “selfish” genetic elements like transposons, retrotransposons and viruses are usually relatively enriched in CpG dinucleotides, they are heavily methylated (Yoder et al. 1997b). This protects them from transcription and subsequent translocation. In some kinds of cancer cells, DNA is often hypomethylated, which might lead to the reactivation of transposable elements and to subsequent mutations.

2.1.2 RNA methylation

RNA molecules are modified much more extensively than DNA. More than 100 different modifications (http://rna-mdb.cas.albany.edu/RNAmods/ (Rozenski et al. 1999)) have been found in many types of cellular RNA, e.g. acetylation (Feldmann et

al. 1966; Johansson and Bystrom 2004) and methylation at various positions of different bases (Jackman et al. 2003; Kalhor and Clarke 2003), and some RNA species carry multiple modifications per molecule (Phizicky and Alfonzo 2010). These modifications stabilize the functional structure of RNAs and can even induce alternative folding under certain circumstances (Helm et al. 1999).

Similar to DNA nucleotides, cytosines in RNA can also be methylated at position 5. This modification is found in many cellular RNAs and in all three living domains (Sprinzl and Vassilenko 2005). RNA m^5C methyltransferases therefore are a large protein family that can be divided into several subfamilies (Motorin et al. 2009). The eukaryotic RNA m^5C methyltransferases alone can already be divided into at least 4 subfamilies: the Trm4 family, the Nop2/p120 family, the family of NSUN/NOP2/NOL2 related proteins, and the unusual Dnmt2 family.

The function of RNA methylation beyond the stabilization of 3D structures is not well established. An importance for the maintenance of proper translation has been suggested for methylation of tRNA molecules, and m^5C in ribosomal RNA may participate in tRNA recognition (Wu et al. 1998; Vicens and Westhof 2001). Some evidence also points to an involvement of RNA methylation in the innate immune system, because methylated RNAs show a reduced activation of toll-like receptors, compared to their unmethylated counterparts (Kariko et al. 2005). There are also speculations about an involvement of RNA methylation in the regulation of epigenetic inheritance patterns (Rassoulzadegan et al. 2006).

2.1.3 tRNA methylation

Most of the known RNA modifications so far are found in tRNA molecules, which are among the most stable RNA molecules. tRNAs were the first small RNAs that were discovered, and their function in translation is well established. They fold into a characteristic secondary structure that is determined by the Watson-Crick base pairs in the sequence, and which is termed “cloverleaf” structure (Figure 1A). Furthermore, tRNAs form a L-shaped 3D structure through hydrogen bonds within the molecule. The tertiary structure can have multiple conformations, and base modifications contribute to the stabilization of a certain folding.

Cellular tRNAs are also among the most strongly modified RNAs, and the modifications are predominantly found in the core of the L-shaped 3D structure as

well as in the anticodon loop. The core modifications are known to increase the thermal stability of tRNAs and lower the conformational flexibility (Helm 2006). Therefore, the core modifications are mostly “structural modifications”. In contrast, the modifications in the anticodon loop can also be “functional”. They contribute to codon recognition and frame shifting, with positions 34 and 37 being of special importance (reviewed in (Helm 2006)).

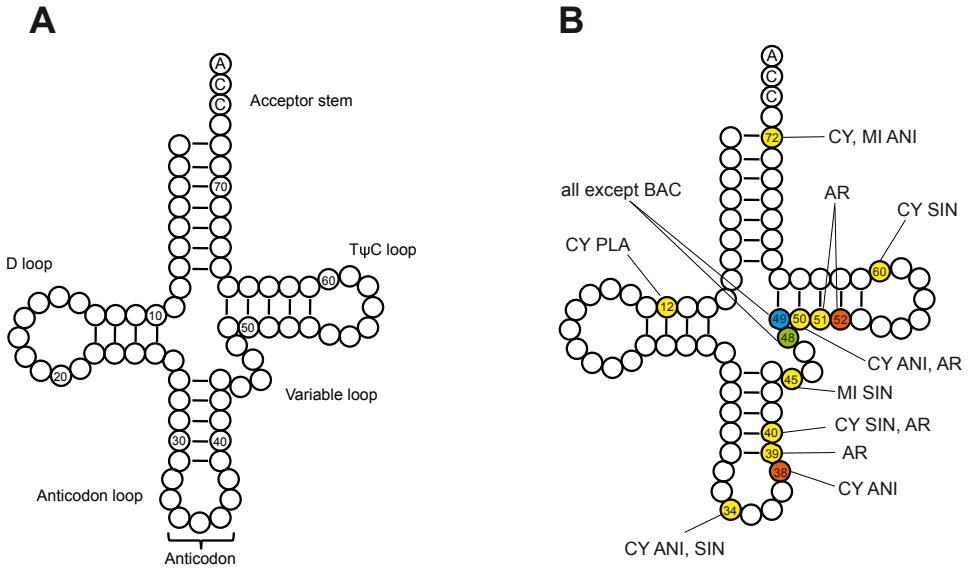

Figure 1: tRNA structure and methylation sites
(A) Secondary cloverleaf structure of tRNA. Circles represent single nucleotides. (B) Global distribution of methylation sites in different tRNAs. The frequency of m^5C occurrence is color-coded: <10% = yellow, 10-30% = red, 30-60% = green, >60% = blue. Abbreviations: CY = cytoplasm, MI = mitochondria, ANI= animals, SIN = single cell eukaryotes, AR = archaea, BAC = bacteria, PLA = plants (modified after (Motorin et al. 2009)).

Despite the high abundance of tRNA modifications, a number of these modifications were found to be non-essential, and the absence of these modifications often displays no or only weak phenotypes (Bjork 1995). Only a few modifications have a strong impact on tRNA structure, and it rather seems that many modifications contribute in a limited way to the stabilization of the structure (Alexandrov et al. 2006). The combination of all the modifications improves the functionality and probably also the lifetime of tRNA molecules.

A modification that can be studied more easily than many other modifications is the methylation at position 5 of cytosines (Helm 2006; Motorin et al. 2009). Although other bases can also be methylated, the cytosine methylation can be detected by bisulfite treatment and subsequent analysis of the methylation pattern after sequencing (Schaefer et al. 2009b). For many tRNAs, it was shown that m^5C is clustered at the junction between the variable region and the TψC-stem, with

positions 48 and 49 being most frequently methylated (Figure 1B). Furthermore, positions in the anticodon loop were also identified as methylation sites (reviewed in (Motorin et al. 2009)).

Methylation of cytosines in tRNA has a significance in structural stabilization, as was demonstrated for m^5C at position 40 in $tRNA^{Phe}$ in *S. cerevisiae*. This modification is important for binding of Mg^{2+} ions and can induce conformational changes of the anticodon loop (Chen et al. 1993). Furthermore, cytosine methylation of tRNA can stabilize tRNA molecules and function to protect them from degradation via an exosome-independent pathway (RTD, rapid tRNA decay (Phizicky and Alfonzo 2010)). This pathway degrades m^5C-deficient tRNA in yeast, when cells are deleted for Trm4 (m^5C) and Trm8 (m^7G). Thus, the degradation is not dependent on the lack of m^5C alone, but it is rather assumed that the lack of more than one modification leads to a destabilization of tRNA structure below a certain threshold, which subsequently leads to the degradation of destabilized tRNAs (Alexandrov et al. 2006).

Cytosine methylation is also important for the translation function of some tRNAs. This function is supported by the finding that the disruption of *TRM4* leads to an increased sensitivity to the antibiotic paromomycin, which affects the precision of ribosome decoding. The m^5C modification might therefore be involved in low error translation in yeast cells (Wu et al. 1998; Motorin et al. 2009).

A recent study also provided evidence for the protection against stress-induced cleavage of tRNA molecules by cytosine methylation in the anticodon loop (Schaefer et al. 2010). Upon heat shock, tRNAs lacking m^5C at position C38 were cleaved in *D. melanogaster* S2 cells. When m^5C was present in these cells, the tRNA integrity was not affected (see below).

2.1.4 The mechanism of cytosine methylation

The methylation of cytosines in DNA and RNA requires distinct properties of the enzymes catalyzing the reaction, due to the differential nature of the two nucleic acids. However, the reaction mechanism of cytosine methylation is the same in both cases. The methylation of cytosines at position 5 of the aromatic ring is a chemically unusual reaction. Although the cofactor S-adenosyl-methionine (SAM) contains a highly reactive methyl group at the methionine sulfur atom and therefore is an effective methyl group donor, this reaction is not trivial. This is due to the fact that the

C5-position of cytosines is situated in an electron poor heterocyclic aromatic ring system, which reduces the reactivity of this carbon atom, compared to electron rich ring systems or non-aromatic compounds. Cytosine contains a carbonyl function and an amino function that have a negative inductive effect on the ring system. Accordingly, position 5 of this ring system is not able to perform a nucleophilic attack on the methyl group of the cofactor.

To solve this problem, m^5C methyltransferases developed a catalytic mechanism that activates the C5 position of the cytosine (Santi et al. 1984; Wu and Santi 1987). For this purpose, the enzyme has to gain access to both sides of the cytosine molecule. To this end, methyltransferases that modify the C5 position of pyrimidines developed a mechanism to flip the target base out of the nucleotide strand and embed it in the catalytic pocket of the enzyme (Klimasauskas et al. 1994; Reinisch et al. 1995).

When the target base is located in the catalytic pocket, the reaction follows the pathway of a Michael addition (Figure 2). In a first step, a cysteine residue in the active centre provides a SH-group for a nucleophilic attack at position 6 of the target cytosine. This results in a covalent complex between the base and the enzyme as an intermediate. The nucleophilic attack is facilitated by transient protonation of the cytosine ring at the endocyclic nitrogen at position N3. This results in a highly reactive 4-5 enamin, which is an efficient nucleophile. Thus, the position C5 is activated and can attack the methyl group of the cofactor SAM. The methyl group is transferred to the base and the covalent base-enzyme complex is dissolved by deprotonation at position C5 by an unknown base within the enzyme and subsequent elimination of the SH-group from the initial cysteine (reviewed in (Jeltsch 2002)).

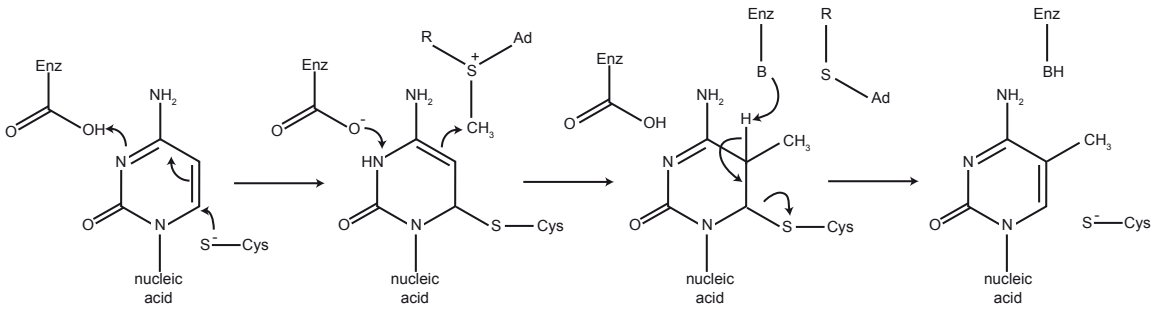

Figure 2: Catalytic mechanism of m^5C methyltransferases
The reaction mechanism is based on the structure of the M.HhaI-DNA complex and was modified after the proposal of (Santi et al. 1984). The base within the enzyme, that abstracts the proton at C5 is unknown Enz=enzyme, Cys=cysteine, Ad=AdoMet, B=base(modified after (Jeltsch 2002)).

RNA methyltransferases utilize different amino acid residues than DNA methyltransferases to catalyze the methylation of cytosines (Liu and Santi 2000).

They use a cysteine residue in motif VI (TCS peptide) to initiate the methylation reaction instead of the one in motif IV (PCQ) that is used by DNA methyltransferases. The cysteine in motif IV of RNA methyltransferases is not directly involved in the reaction (Figure 3). The transient protonation of the substrate that is performed by a glutamate residue in motif VI in DNA methyltranserases is carried out by an aspartate located in motif IV in RNA methyltransferases. Thus, the location of the two important catalytic residues is opposite to the location of those residues in DNA methyltransferases (Bujnicki et al. 2004). Only Dnmt2-type RNA methyltransferases methylate tRNA using a mechanism that is usually used by DNA methyltransferases (see below).

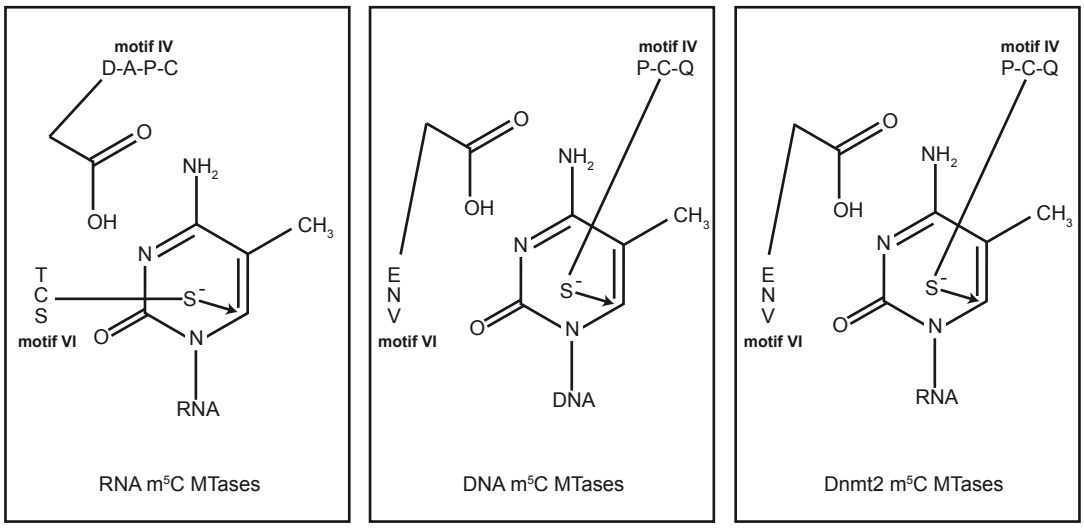

Figure 3: Differences between RNA and DNA methyltransferases
Canonical RNA m^5C methyltransferases use the DAPC peptide in motif IV for protonation and the TCS peptide of motif VI for the initial nucleophilic attack on the C6 position. DNA m5C methyltransferases use an ENV peptide in motif VI for protonation and a PCQ peptide in motif IV for initiation. Dnmt2 methylates a RNA substrate using the DNA methyltransferase mechanism (modified after (Schaefer and Lyko 2009)).

2.2 DNA methyltransferases

In eukaryotes, there are three distinct families of DNA methyltransferases (Dnmt1, Dnmt2 and Dnmt3). They all utilize specific amino acid residues from conserved motifs to catalyze the transfer of a methyl group from the cofactor SAM to the target DNA base, or in the case of Dnmt2 the target RNA base.

In the ternary structure of DNA methyltransferases, the motifs I and X are folded together, so that they form the binding site for the cofactor SAM (Figure 4 (Cheng et al. 1993)). The catalytic cysteine that initiates the reaction is located in motif IV. This

motif is highly conserved and contains a PC-dipeptide in most of the known enzymes (Santi et al. 1984; Wu and Santi 1987). The glutamate residue that stabilizes the intermediate by transient protonation of the base is situated in motif VI (ENV tripeptide) of DNA methyltransferases. Another important amino acid residue is the arginine in motif VIII (Gowher et al. 2006).

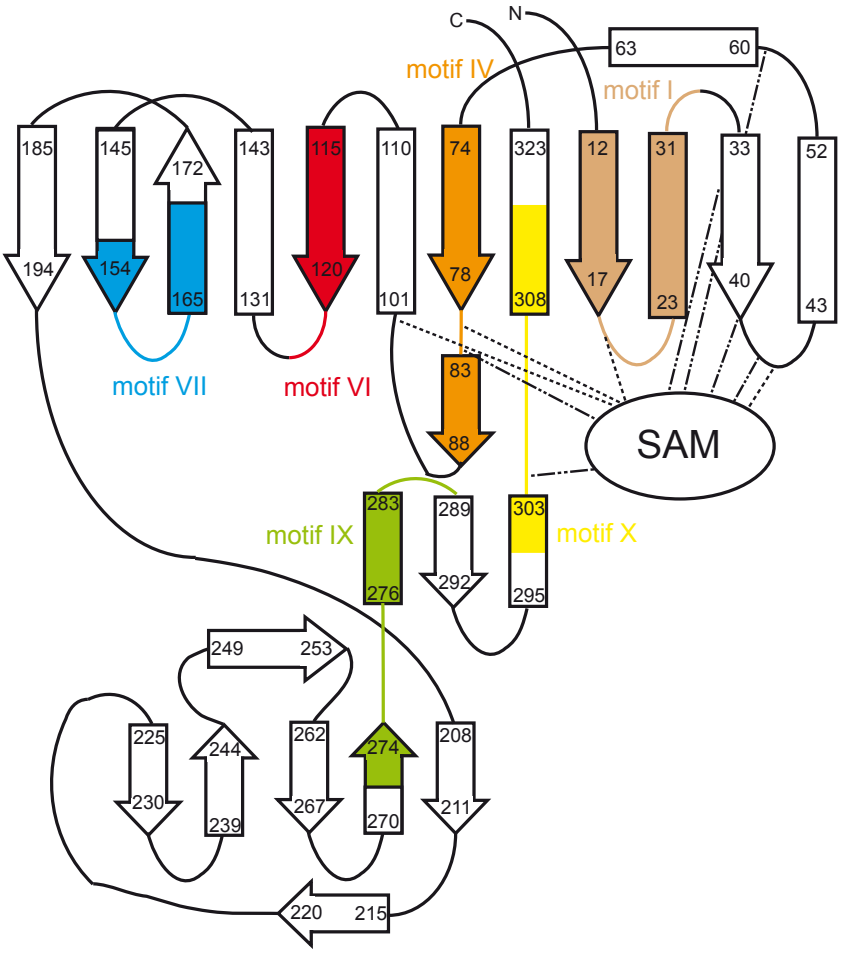

Figure 4: Topology of DNA methyltransferases
Schematic drawing of the secondary structure of the prokaryotic methyltransferase M.HhaI. Boxes represent α-helices, arrows represent β-strands. The regularly dashed lines indicate hydrophobic interactions, the irregularly dashed lines indicate electrostatic interactions or hydrogen bonds. The methyltransferase motifs are colored: brown=motif I, orange=motif IV, red=motif VI, blue=motif VII, green=motif IX, yellow=motif X (modified from (Cheng et al. 1993)).

DNA double strands can be found in three distinct states of methylation; they can be either unmethylated, hemimethylated, or they can be completely methylated on both strands. Therefore, two types of DNA methylation have to be distinguished (Riggs 1975). One is *de novo* methylation that establishes methylation marks on unmethylated DNA (Okano et al. 1998a), and the second one is maintenance methylation that reestablishes methylation patterns after replication of methylated DNA (Bestor et al. 1988). In mammalian cells, two separate families of DNA

methyltransferases execute these distinct functions. Dnmt1 serves as a maintenance methyltransferase, because it has a preference for hemimethylated DNA (Pradhan et al. 1999), and Dnmt3 enzymes are responsible for *de novo* methylation, because they show no preference for hemimethylated over unmethylated DNA (Okano et al. 1998a). However, despite the separation of the two functions of DNA methylation, the activities of the DNA methyltransferases responsible for each function partially overlap. Dnmt1 has a higher *de novo* methylation activity than Dnmt3a and 3b, and Dnmt3 family members have been implicated in maintenance methylation as well.

2.2.1 The DNA nucleotide methyltransferase 1 (Dnmt1)

The first eukaryotic DNA methyltransferase to be cloned and biochemically analyzed was murine Dnmt1 (DNA nucleotide methyltransferase 1 (Bestor et al. 1988)). In comparison to prokaryotic DNA methyltransferases, the protein is large, as it comprises 1620 amino acids and has an N-terminal regulatory domain. In initial studies, the *de novo* methyltransferase activity of Dnmt1 was identified (Bestor et al. 1988), but later work discovered a pronounced preference for hemimethylated DNA (Yoder et al. 1997a; Fatemi et al. 2001). This property suggested that Dnmt1 was the methyltransferase responsible for the maintenance of methylation patterns. For this purpose, Dnmt1 is associated with the replication machinery through its interaction with PCNA (proliferating cell nuclear antigen), where it methylates the newly synthesized strand before the chromatin is reassembled.

Disruption of Dnmt1 function results in global demethylation of genomic DNA. This leads to embryonic lethality in mice (Li et al. 1992), loss of imprinting (Li et al. 1993; Howell et al. 2001) and alterations in X chromosome inactivation (Beard et al. 1995; Panning and Jaenisch 1996; Sado et al. 2000). Embryonic stem cells without Dnmt1 are viable, but unable to differentiate (Li et al. 1992). Other cell lines undergo apoptosis when Dnmt1 is missing (Jackson-Grusby et al. 2001; Takashima et al. 2009). Taken together, these findings indicate an essential role for Dnmt1 in mammalian development, cell proliferation and survival.

Dnmt1 contains all 10 catalytic motifs typical for m^5C methyltransferases in the C-terminal part of the enzyme. The large N-terminal domain is linked to the C-terminus by a lysine-glycine-rich domain and contains several functional domains (Figure 5). These domains include interaction domains with other proteins as well as nuclear

localization signals, BAH (bromo-adjacent homology) domains that are included in the PBHD (polybromo homology domain), and cysteine rich (CR) zinc-binding repeats that are involved in binding to unmethylated CpGs (Allen et al. 2006) and that are essential for the catalytic activity of Dnmt1 (Pradhan et al. 2008).

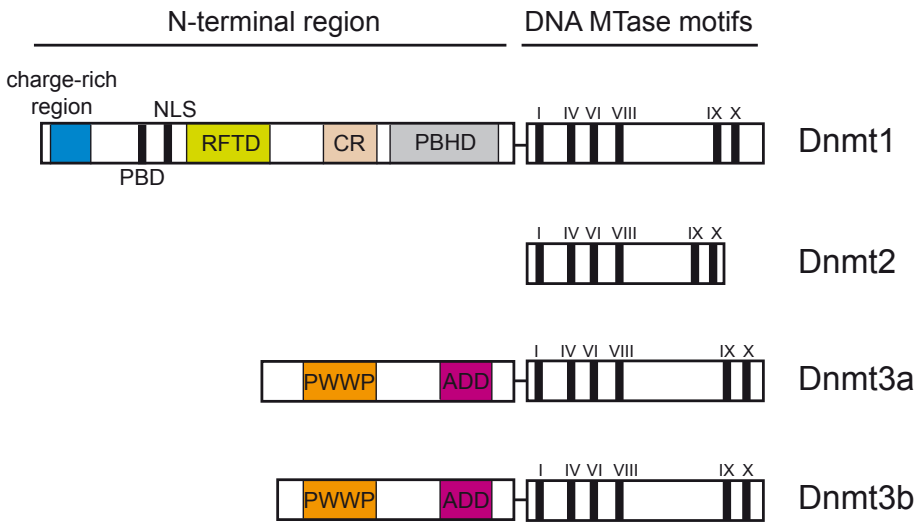

Figure 5: DNA methyltransferase domains
The domain architecture of mammalian DNA methyltransferases is shown. Functional domains of the regulatory N-terminal domains are coloured and labeled. The catalytic motifs in the C-terminal region are numbered. PBD=PCNA binding domain, NLS=nuclear localization signal, RFTD=replication foci targeting domain, CR=cysteine-rich domain, PBHD=polybromo homology domain, PWWP=proline-tryptophan-tryptophan-proline, ADD= ATRX-DNMT3-DNMT3L (modified from (Jurkowska et al. 2011)).

The enzyme is localized in the nucleus, where it is diffusely distributed when cells are not replicating during interphase. In S-phase, Dnmt1 is found at replication foci, where it methylates CpG dinucleotides, if the cytosine in the parental strand is methylated (Tatematsu et al. 2000). Interestingly, there is a slightly shorter oocyte-specific isoform (Dnmt1o) that is located in the cytoplasm and only transiently found in the nucleus (Mertineit et al. 1998).

The highly processive enzyme Dnmt1 is allosterically regulated by its own N-terminal domain. The catalytic C-terminal domain is not active without the N-terminus (Margot et al. 2000). When the N-terminus is bound to methylated DNA, the activity of Dnmt1 on neighbouring cytosine target sites is increased, and its specificity shifts slightly from hemimethylated to unmethyated DNA (Fatemi et al. 2001; Goyal et al. 2006). When the N-terminus is bound to unmethylated DNA, the activity of the enzyme is inhibited (Bacolla et al. 1999; Flynn et al. 2003). This observation corresponds to the fact that methylation patterns in the human genome are bimodal, i.e. genomic regions are either highly methylated or not methylated at all. When the binding to

methylated DNA activates Dnmt1, then it is logical that during evolution methylated regions attract more methylation. On the other hand, poorly methylated regions would tend to loose methylation, when Dnmt1 is inhibited by unmethylated DNA (Jurkowska et al. 2011). The allosteric control of Dnmt1 activity by the N-terminal region would also provide an explanation for the fact that the isolated C-terminal domain is inactive, although it contains all the catalytic motifs. This mechanism would also prevent the genome from uncontrolled DNA methylation when Dnmt1 is fragmented by proteolysis.

As a part of the epigenetic network, Dnmt1 interacts with a broad variety of proteins involved in epigenetic gene regulation. Among others HDAC1 (Fuks et al. 2000) and HDAC2 (Rountree et al. 2000), Dnmt3a and b (Kim et al. 2002), several transcription factors (Robertson et al. 2000), histone lysine methyltransferases and silencing effectors like HP1 and MeCP2 were shown to interact with Dnmt1 (Fuks et al. 2003; Kimura and Shiota 2003). Dnmt1 is associated to the replication machinery through its interaction with the processivity factor PCNA (Chuang et al. 1997). Another important interaction partner is UHRF1 (Bostick et al. 2007), which binds to hemimethylated DNA and thereby targets Dnmt1 to replicated DNA. Thus, UHRF1 is required for the maintenance of DNA methylation.

It should also be noted that despite its maintenance function, Dnmt1 has a significant *de novo* methylation activity. This activity is even higher than the *de novo* methylation activity of Dnmt3. Furthermore, Dnmt1 probably plays a role in assisting Dnmt3 in *de novo* methylation by methylating hemimethylated DNA generated by Dnmt3 (Fatemi et al. 2001).

2.2.2 The Dnmt3 family

Due to the fact that Dnmt1 displays a preference for hemimethylated DNA and that in cells lacking Dnmt1 there is still some DNA methylation present, it was suggested that there exists at least one other DNA methyltransferase that carries out *de novo* methylation of unmethylated DNA double strands. This enzymatic activity was found when Dnmt3 methyltransferases were discovered (Okano et al. 1998a). This family of DNA methyltransferases comprises three members in mammals: Dnmt3a, Dnmt3b and Dnmt3L. Of these three, only Dnmt3a and Dnmt3b are active methyltransferases, and they display no preference for unmethylated or

hemimethylated DNA (Gowher and Jeltsch 2001). The amino acid sequence of Dnmt3L has several non-conservative mutations in the catalytic residues and it also lacks the catalytic motifs IX and X.

Both Dnmt3a and 3b are divided into a catalytically active C-terminal domain and a regulatory N-terminal domain ((Xie et al. 1999), Figure 5). The N-terminal regions of the Dnmt3-familiy proteins are unrelated to the respective regions of Dnmt1. The C-terminal region contains all 10 conserved motifs representing m^5C-methyltransferases and, in contrast to Dnmt1, the catalytical part is active in the absence of the N-terminus. Dnmt3a and Dnmt3b are also shown to methylate cytosines in a non-CpG context, but the biological significance of this methylation is unknown (Gowher and Jeltsch 2001).

The N-terminal region of both enzymes contains a cysteine-rich domain (ADD (ATRX-DNMT3-DNMT3L) domain) and a PWWP (proline-tryptophan-tryptophan-proline) domain. The ADD domain forms an interface for several interactions with other proteins. All Dnmt3 proteins have been shown to interact with the N-terminal tail of histone H3 through the ADD domain, but only when lysine 4 of histone H3 is unmodified (Ooi et al. 2007; Otani et al. 2009). The PWWP domain is essential for the targeting of Dnmt3a and 3b to pericentric chromatin, where they are involved in the methylation of different subsets of repeats.

Dnmt3a and 3b are essential for embryonic development, and accordingly, the expression of both enzymes is high in embryonic tissues and undifferentiated embryonic stem (ES) cells and is down-regulated in differentiated cells (Okano et al. 1998a). They both interact with the catalytically inactive Dnmt3L protein.

Despite the numerous similarities of the Dnmt3 proteins, they also exhibit various differential properties; $Dnmt3a^{-/-}$ mice die shortly after birth, whereas the Dnmt3b knockout is lethal already at embryonic day 9.5 and causes multiple developmental defects (Okano et al. 1999). Dnmt3a interacts with the catalytically inactive Dnmt3L and is required for the establishment of imprints during gametogenesis. In contrast, Dnmt3b is not required for this process, but it methylates minor satellite repeats in embryos and ES cells, which does not require Dnmt3a. Furthermore, specific CpG islands on the inactive X chromosome seem to be methylated by Dnmt3b specifically, because inactivation of Dnmt3b in the human ICF (immunodeficiency-centromeric instability-facial anomalies) syndrome is the only human disease associated to a mutated DNA methyltransferase (Okano et al. 1999). Other results indicate a participation of Dnmt3b in maintenance DNA methylation. Taken together, these

results implicate only partially overlapping biological functions for Dnmt3a and Dnmt3b.

Dnmt3L is the only Dnmt3 family member that is expressed specifically in germ cells during gametogensis and embryonic stages (Bourc'his and Bestor 2004). The localization of this protein depends on the distribution of the other Dnmt3s, because it is only found concentrated in chromatin foci, when Dnmt3a is present (Hata et al. 2002) and it was shown to interact with both Dnmt3 methyltransferases (Margot et al. 2003). The knockout of Dnmt3L results in viable mice with no morphological abnormalities. However, male knockouts are sterile, and female mutants are unable to deliver viable offspring. Loss of Dnmt3L leads to a loss of maternal imprints, which leads to biallelic expression of genes normally transcribed from the paternal allele (Hata et al. 2002).

2.2.3 The unusual Dnmt2 enzymes

All organisms that contain members of the Dnmt1 and Dnmt3 families, additionally contain a member of the Dnmt2 family of methyltransferases (Goll and Bestor 2005). On the other hand, organisms that contain a Dnmt2 homolog do not necessarily have Dnmt1 or Dnmt3 proteins. There are several species that contain a Dnmt2 homolog as the sole m^5C-methyltransferase, e.g. *Drosophila melanogaster*, *Dictyostelium discoideum*, *Entamoeba histolytica* and *Schizosaccharomyces pombe*. Therefore, enzymes belonging to the Dnmt2 family are the most widely distributed enzymes of the eukaryotic DNA methyltransferases (Schaefer and Lyko 2009).

Dnmt2 was identified by an EST (expressed sequence tag) database search as a new candidate DNA methyltransferase (Yoder and Bestor 1998). Sequence homology revealed that Dnmt2 is related to the putative DNA methyltransferase that was annotated in the fission yeast genome (Wilkinson et al. 1995). In search for an explanation for the residual DNA methylation in Dnmt1 null mutant mouse embryonic stem cells, Dnmt2 was found to belong to the DNA methyltransferase family, because it contains all 10 conserved motifs that are characteristic for DNA methyltransferases in the canonical order. Although it lacks the large N-terminal domains that are present in Dnmt1 and Dnmt3, the catalytic domain is well conserved. The assumption that Dnmt2 belonged to the DNA methyltransferase family was further supported by the observation that the crystal structure of Dnmt2 is

essentially superimposable with the structure of the bacterial restriction methyltransferase M.HhaI (Figure 6). This indicated that the calatytic motifs of Dnmt2 are well organized and in the correct orientation for a DNA methyltransferase (Dong et al. 2001). However, no DNA methyltransferase activity could be detected in initial studies of mammalian Dnmt2 homologs, although denaturant resistant binding to DNA has been observed for Dnmt2 *in vitro* (Okano et al. 1998b; Dong et al. 2001). Other laboratories were able to detect Dnmt2 dependent DNA methylation, but the level was very low and close to the backgound of the assays applied (Hermann et al. 2003; Tang et al. 2003). Recombinant human Dnmt2 was shown to methylate a low amount of cytosines in DNA substrates in a nonprocessive manner and without sequence specificity (Hermann et al. 2003). DNA bisulfite sequencing suggested methylation of isolated cytosines in *Drosophila* DNA that was also not sequence specific (Lyko et al. 2000). Thus, the DNA methylation activity under the conditions that were examined was residual. More recently, a specific methylation activity on certain retroelements has been observed. Locus specific methyltransferase activity on selected retroelements in the genomes of *Drosophila* and *Dictyostelium* has been reported by independent groups (Kuhlmann et al. 2005; Phalke et al. 2009), but these results are controversially discussed (Schaefer and Lyko 2010) and need further investigation.

Sequence comparisons show that the target recognition domain (CFTXXYXXY) is highly conserved among Dnmt2 family members, but that this motif is not found in other DNA methyltransferases. When DNA is modeled into the crystal structure of Dnmt2, the second tyrosine (Y) of the CFT motif is in significant steric conflict with the non-target strand of double stranded DNA (Goll and Bestor 2005).

When purified human Dnmt2 was used for *in vitro* methylation of DNA and RNA extracts from Dnmt2$^{-/-}$ mouse tissues, a small RNA was detected that could be methylated by Dnmt2 that was not methylated in extracts from wild type tissues (Goll et al. 2006). This small RNA was identified as tRNA^{Asp}, and the methylation was localized specifically to the cytosine base at position 38 in the anticodon loop of the tRNA. This tRNA can also be methylated, if the substrate is an *in vitro* transcribed RNA that lacks any other modification (Hengesbach et al. 2008; Jurkowski et al. 2008).

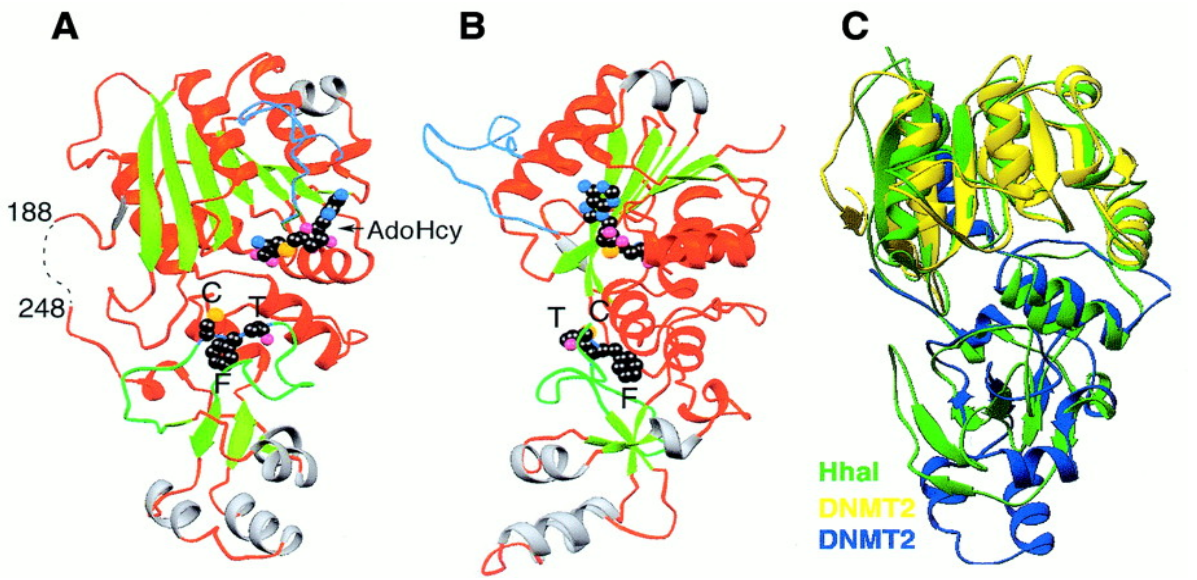

Figure 6: Structure of Dnmt2
(A) Ribbon diagram of the Dnmt2Δ47-AdoHcy complex in the front view. (B) Ribbon diagram of the Dnmt2Δ47-AdoHcy complex in the right side view. Helices and loops in (A) and (B) are coloured red, unique helices of Dnmt2 are coloured gray, strands are green the PC loop is light blue and the TRD loop is green. AdoHcy and the CFT of the TRD are shown as balls with carbon atoms in black, nitrogen in light blue, oxygen in magenta and sulfur atoms in orange. (C) Superimposition of the Dnmt2Δ47 in yellow and blue and M.HhaI in green (Dong et al. 2001).

When purified human Dnmt2 was used for *in vitro* methylation of DNA and RNA extracts from Dnmt2$^{-/-}$ mouse tissues, a small RNA was detected that could be methylated by Dnmt2 that was not methylated in extracts from wild type tissues (Goll et al. 2006). This small RNA was identified as tRNA^{Asp}, and the methylation was localized specifically to the cytosine base at position 38 in the anticodon loop of the tRNA. This tRNA can also be methylated, if the substrate is an *in vitro* transcribed RNA that lacks any other modification (Hengesbach et al. 2008; Jurkowski et al. 2008).

Thus, Dnmt2 is an unusual enzyme. Sequence and homology data imply a DNA methyltransferase activity, but experimental data suggest that the tRNA methyltransferase activity of Dnmt2 is much more robust than any detectable activity on DNA. On the other hand, Dnmt2 does not share significant sequence similarities with typical RNA methyltransferases. The unique position of Dnmt2 as a tRNA methyltransferase became even more pronounced when it was shown that Dnmt2 uses a DNA methyltransfease-like mechanism to methylate tRNA (Jurkowski et al. 2008). Typical RNA methyltransferases use a peptide in motif IV for protonation of the substrate and a peptide in motiv VI for catalysis, whereas the role of the two different motifs is reversed in DNA methyltransferases. Dnmt2 uses the motifs like DNA methyltransferases do, but the substrate is RNA.

The subcellular localization of the enzyme varies significantly. It was found in the nucleus (Kunert et al. 2003; Kuhlmann et al. 2005), in the cytoplasm (Goll et al. 2006; Rai et al. 2007) or both (Schaefer et al. 2008) and also associated to the nuclear matrix (Banerjee et al. 2005; Schaefer et al. 2008). The nuclear localization is in agreement with both the DNA and the tRNA methyltransferase activity, whereas a cytoplasmic localization would rather point towards the tRNA methyltransferase activity.

Despite the knowledge about the localization of the protein and the targets of methylation, it has been difficult to determine the biological function of Dnmt2 or the tRNA methylation at position C38. Although Dnmt2 is highly conserved through evolution, which indicates an important cellular function, mutant organisms mostly show no or only very subtle phenotypes under standard laboratory conditions. *S. pombe*, *D. melanogaster*, *A. thaliana* and mouse mutants were indistinguishable from wild-type (Wilkinson et al. 1995; Kunert et al. 2003; Goll et al. 2006) and *D. discoideum* showed a minor developmental phenotype (Katoh et al. 2006). Surprisingly, zebrafish displayed lethal defects in the differentiation of retina, liver and brain when Dnmt2 was knocked down (Rai et al. 2007).

More detailed analysis of Dnmt2 mutants in different “Dnmt2-only” organisms implied several interesting possibilities for biological function. The overexpression of the *Drosophila* homolog was found to cause increased resistance to various stresses like starvation or oxidative stress and furthermore to increase the mean lifespan of the flies (Lin et al. 2005). These observations were supported by a second study that was able to reproduce the aging phenotype and the resistance to oxidative stress (Schaefer et al. 2010). This study furthermore identified additional methylation targets of *Drosophila* Dnmt2, $tRNA^{Gly}$ and $tRNA^{Val}$, and discovered the protection of methylated tRNAs against stress induced cleavage. Other studies on this Dnmt2 homolog concentrated on the DNA methylation activity and reported methylation of retrotransposons that was detected using DNA bisulfite sequencing (Phalke et al. 2009). However, these findings were questioned and require further investigation (Schaefer and Lyko 2010; Krauss and Reuter 2011).

The *Dictyostelium* homolog (DnmA) has been shown to be responsible for the small amount of DNA methylation found in the *D. discoideum* genome (Kuhlmann et al. 2005). This organism also exhibits morphological defects in late development that were attributed to the DNA methylation activity of DnmA that occurs at specific retrotransposons (Katoh et al. 2006). However, later studies have also identified

robust $tRNA^{Asp}$ methyltransferase activity for DnmA, equivalent to the activity of the other known Dnmt2 homologs (Sara Müller, Wolfgang Nellen, unpublished data). Additionally to the $tRNA^{Asp}$ methylation, DnmA was able to methylate $tRNA^{Glu}$ of *Dictyostelium*.

Another "Dnmt2-only" organism like *Drosophila* and *Dictyostelium* is the protozoan parasite *Entamoeba histolytica*. The Dnmt2 homolog in this organism is named Ehmeth and was shown to exhibit a weak DNA methyltransferase activity when genomic DNA was used as a substrate. Additionally, the amoeba showed impaired ability to kill mammalian cells when the activity of Dnmt2 was inhibited by 5-azacytidine (Fisher et al. 2004). Surprisingly, Ehmeth was shown to interact with the glycolytic enzyme enolase, which causes inhibition of Ehmeth $tRNA^{Asp}$ methylation activity. The inhibition of Ehmeth by enolase could be influenced by the enolase substrate (Tovy et al. 2010a). These findings suggest regulation of Ehmeth by enolase outside of its glycolytic function.

Studies on the substrate recognition of the human Dnmt2 enzyme suggest that a tRNA is a "good" substrate, if it contains a cytosine at position 38 and additionally carries a cytosine at position 32, an adenine at position 37 and another cytosine at position 40. These bases are present in the $tRNA^{Asp}$ sequences of *H. sapiens*, *S. pombe*, *D. discoideum* and probably most of the other Dnmt2 containing organisms. The respective bases that are present in the *S. cerevisiae* $tRNA^{Asp}$ (U32, G37, U40) are antideterminants and are probably the reason why the *S. cerevisiae* $tRNA^{Asp}$ is not a substrate for methylation by Dnmt2, although it contains a cytosine at position C38 (M. Helm, personal communication).

2.3 The fission yeast *Schizosaccharomyces pombe* as a model organism

The fission yeast *Schizosaccharomyces pombe* is a unicellular eukaryotic organism. It was isolated from east-african millet beer and named "pombe" after the Swahili word for beer (Lindner 1893). It was established as a model organism in the 1950s (Leupold 1950) and has been used for genetic studies as well as cell cycle research.

S. pombe's rod-shaped cells are usually 3-4 µm in diameter and 7-14 µm in length. In contrast to the baker's yeast *Saccharomyces cerevisiae*, fission yeast grows exclusively at the tips and divides by medial fission instead of budding. Under normal

conditions, the cells are haploid, and diploids are obtained only under starvation conditions. The 13.8 Mbp genome of the fission yeast was completely sequenced (Wood et al. 2002), and it contains about 5000 ORFs distributed on three chromosomes. The localization of all proteins was determined using GFP-tagged proteins (Matsuyama et al. 2006).

Despite its small genome, the fission yeast displays significant similarities to higher eukaryotes like the centromere structure, the presence of introns in gene sequences and the utilization of an RNA interference system. Furthermore, cell cycle and cellular structure are comparable to higher eukaryotes. In contrast to higher eukaryotes, however, *S. pombe* has the advantages of simple cultivation, short replication time and easy accessibility of the genome for mutations. The fact that this organism is well investigated and that methods for genetic manipulation are well established provides versatile possibilities for research on genetics and protein function.

Fission yeast was chosen for this study, because it contains an annotated putative DNA methyltransferase that belongs to the Dnmt2 family of DNA methyltransferases. Besides this protein, there are no other putative DNA methyltransferases annotated in the *S. pombe* genome. Therefore, the fission yeast is a “Dnmt2-only” organism. This fact makes it an ideal organism to study the function of a Dnmt2 homolog. The absence of other DNA methyltransferases obviates the necessity of excluding the possibly overlapping DNA methyltransferase activity of similar enzymes when studying Dnmt2 activity.

2.4 The pombe methyltransferase 1 (Pmt1)

The fission yeast *Schizosaccharomyces pombe* contains a single gene encoding for a putative DNA methyltransferase. The pombe methyltransferase 1 (Pmt1) was identified based on its sequence homology to bacterial m^5C methyltransferases (Wilkinson et al. 1995). It contains all 10 conserved motifs that are characteristic for m^5C methyltransferases in the correct order. In contrast to the previously known eukaryotic m^5C methyltransferases (Dnmt1 family), it lacks the large N-terminal domain and was therefore more similar to the prokaryotic methyltransferases than to Dnmt1. After the identification of mammalian Dnmt2, it was recognized that Pmt1 shared high similarity with this eukaryotic DNA methyltransferase family and thus was the first Dnmt2 homolog to be identified (Yoder and Bestor 1998).

Already in the first study on Pmt1, it was observed that the protein sequence deviates from the consensus sequence of DNA methyltransferases in the catalytic motif IV. Other m^5C methyltransferases contain the peptide PPCQ, which includes the catalytic cysteine that initiates the methyl group transfer (Figure 7). In Pmt1, this sequence is altered to PSCQ. Recombinant Pmt1 was able to bind to specific DNA sequences, but was not able to methylate DNA substrates, which was attributed to the mutation in the catalytic motif IV, and which was consistent with the lack of detectable DNA methylation in the fission yeast (Antequera et al. 1984). One further study reported an activation of the *pmt1*$^+$ gene product by deletion of the serine residue in the PSCQ motif IV (Pinarbasi et al. 1996). This deletion “reestablishes” a PCQ tripeptide in the catalytic motif IV that is also found in other DNA methyltransferases like Dnmt1. Wild type and mutant protein were able to bind to specific DNA fragments at a CCAGG sequence, but only the mutant protein displayed specific DNA methyltransferase activity. These results suggest a sequence specificity for the mutant protein that is equivalent to the restriction methyltransferase M.EcoRII and are discussed controversially.

Initial studies provided evidence that the *pmt1*$^+$ gene is transcribed at a significant level. However, the deletion of the *pmt1*$^+$ gene resulted in cells that were indistinguishable from wild type cells (Wilkinson et al. 1995). Therefore, *pmt1*$^+$ is not essential for vegetative growth, conjugation or meiosis of the fission yeast. It was also mentioned that the function of the *pmt1*$^+$ gene might only be required under certain conditions, because strains grown in a laboratory are not a subject to the same environmental stresses as cells that inhabit their natural environment. Furthermore, the presence of the proline to serine mutation next to the catalytic cysteine can be found in certain tRNA methyltransferases, which could indicate that a proline to serine mutation does not automatically render the enzyme inactive and may suggest a tRNA methyltransferase activity for Pmt1 (Wilkinson et al. 1995). Especially due to the findings on activity of the human homolog Dnmt2 (Goll et al. 2006), a tRNA methyltransferase activity can be postulated for Pmt1 in *S. pombe*. Despite this notion, the tRNA methyltransferase activity of Pmt1 to date has not been investigated.

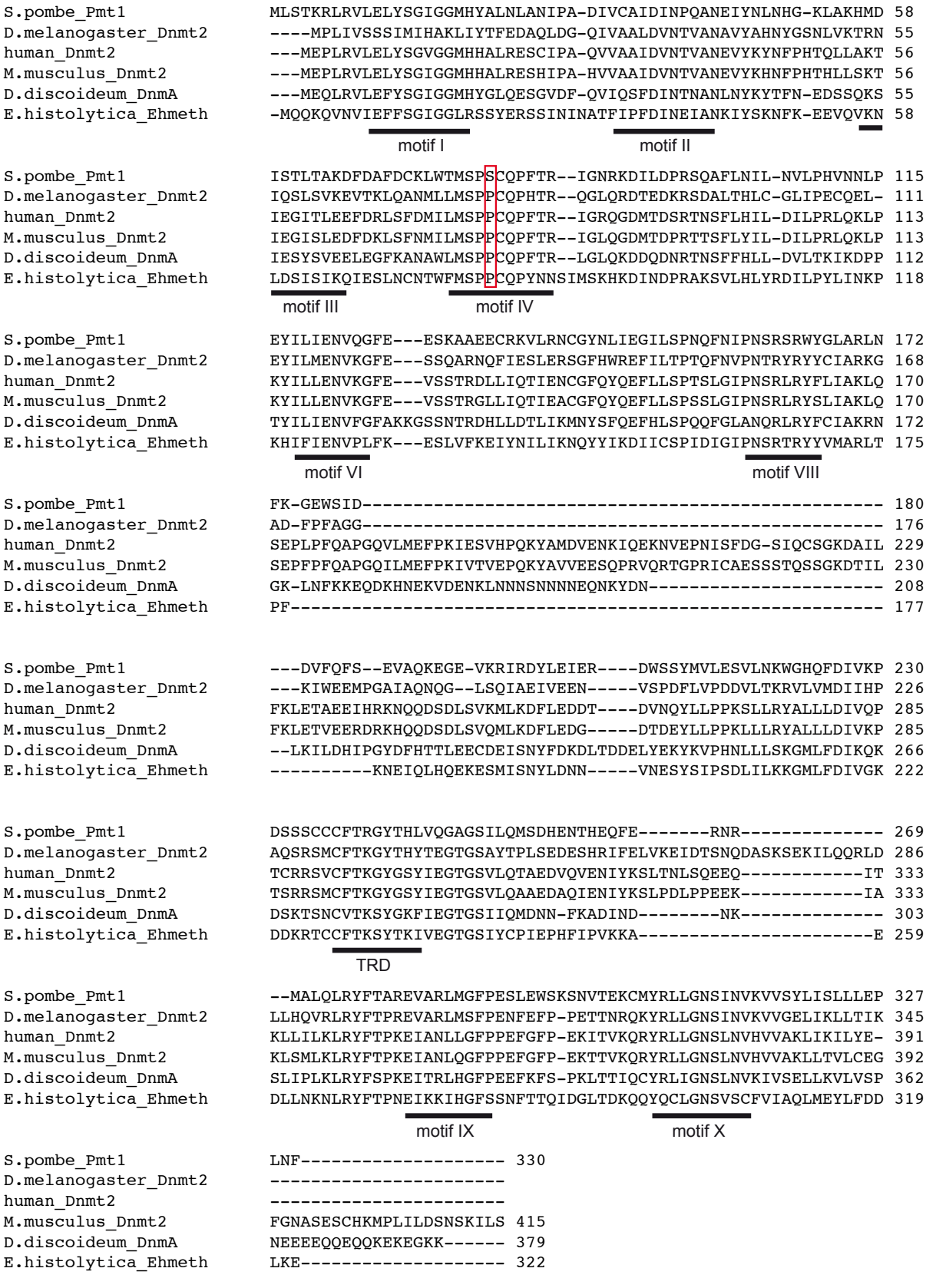

Figure 7: Multiple sequence alignment of Dnmt2 proteins
Alignment of the amino acid sequences of the Dnmt2 homologs from *S. pombe*, *D. melanogaster*, *H. sapiens*, *M. musculus*, *D. discoideum* and *E. histolytica* using the ClustalW2 algorithm. The mutation motif IV of Pmt1 is marked with a box. Catalytic motifs and the target recognition domain are labeled with black bars.

3 Aim of this thesis

The identification of the tRNA methyltransferase activity of the DNA methyltransferase homolog Dnmt2 has highlighted the exceptional role of this enzyme among the eukaryotic DNA methyltransferases. The strong conservation of Dnmt2 proteins, along with the existence of Dnmt2-only organisms, suggests an important biological function of Dnmt2 activity. However, the nature of this function is only poorly understood. Therefore, Dnmt2 enzymes and the biological role of this tRNA methyltransferase activity has raised increasing interest in the scientific community.

The fission yeast *Schizosaccharomyces pombe* provides favorable circumstances to investigate the function of a Dnmt2 homolog, because it contains such a homolog, but lacks any additional DNA methyltransferases. Therefore, we chose to investigate the function and biological role of the fission yeast Dnmt2 homolog Pmt1. This homolog has not been investigated for its tRNA methyltransferase activity and was claimed to be inactivated by a mutation in its catalytic motif IV. Insights into Pmt1 function could lead to a better understanding of the mammalian homolog that has already been implicated as a possible biomarker for monitoring azacytidine treatment of cancer patients (Schaefer et al. 2009a). Research in other organisms indicated an involvement of Dnmt2 function in aging (Lin et al. 2005; Schaefer et al. 2010), development (Rai et al. 2007) and stress resistance (Schaefer et al. 2010), all of which are important research fields associated with human diseases.

In the course of this study, we sought to determine whether Pmt1 is an active tRNA methyltransferase both *in vitro* and *in vivo*. Our observations concerning Pmt1-dependent *in vivo* methylation prompted us to investigate the influence of nutrient availability on the activity of the fission yeast Dnmt2 homolog and led to the discovery of an unexpected link between Pmt1-dependent tRNA methylation and cellular signaling pathway involving the serine/threonine kinase Sck2. Based on results from other Dnmt2 homologs, we furthermore sought to identify the role of Pmt1 in the process of chronological aging.

In summary, the aim of this study was the unbiased characterization of Pmt1 activity, based on previous results on Pmt1 (no detectable DNA methyltransferase activity) and Dnmt2 ($tRNA^{Asp}$ methyltransferase activity) using genetic as well as biochemical

approaches. In the course of this study we were able to identify an activity for Pmt1 that was specific for cytosine 38 of $tRNA^{Asp}$. The *S. pombe* $tRNA^{Glu}$ was an additional target of Pmt1 methylation. Surprisingly, we discovered a nutrient dependency of Pmt1 activity *in vivo* and were able to determine a factor that regulates Pmt1 activity. The involvement of the serine/threonine kinase Sck2 in Pmt1 regulation suggested that tRNA methylation might be regulated by nutrient availability via the TOR signaling pathway. Additional results implied a role for Pmt1 activity in chronological aging.

4 Materials and methods

4.1 *E. coli* strains

Rosetta (DE3)	F^- *omp*T *hsd*SB(r_B^- m_B^-) *gal dcm* pRARE (CamR) (Merck)
TOP10	F^- *mcr*A Δ(*mrr-hsd*RMS-*mcr*BC) φ80*lac*ZΔM15 Δ*lac*X74 *rec*A1 *ara*Δ139Δ(*ara-leu*)7697 *gal*U *gal*K *rps*L (Str^R) *end*A1 *nup*G (Invitrogen)
DH5α	F^- φ80*lac*ZΔM15 Δ(*lac*ZYA-*arg*F)U169 *rec*A1 *end*A1 *hsd*R17(r_k^-, m_k^+) *pho*A *sup*E44 *thi*-1 *gyr*A96 *rel*A1 λ- (Invitrogen)

4.2 Media and growth conditions

All *E. coli* strains used for plasmid purification were cultured at 37 °C in Luria-Bertani (LB) medium containing 100 µg/mL ampicillin according to standard procedures (Sambrook et al. 1989).

S. pombe strains were cultured according to standard protocols (Moreno et al. 1991). Media that were used in this study are given in Table 1. If not stated otherwise, yeast cells were grown in standard complete medium (YES) or in minimal medium (EMM) with 2 % glucose and the required supplements at 30 °C. For selection for antibiotic resistance, YES medium was supplemented with 100 mg/L G418 (Gerbu), 100 mg/L cycloheximide (Carl Roth) or 100 mg/L nourseothricin (ClonNat, Werner Bioagents). *S. cerevisiae* standard complete medium (YPD) and standard minimal medium (YM) supplemented with 2% glucose and the required supplements was also used for *S. pombe* cultures in this study. Solid media were prepared by addition of 2 % agar.

Table 1: Media used in this study

Medium	Composition
YES	5 g/L yeast extract 30 g/L glucose 250 mg/L adenine 250 mg/L histidine 250 mg/L leucine 250 mg/L uracil

	250 mg/L lysine
EMM	3 g/L potassium hydrogenphtallate 2.2 g/L Na_2HPO_4 5 g/L NH_4Cl 20 g/L glucose 20 mL/L 50x salt stock 1 mL/L 1000x vitamine stock 100 µL/L 10000x mineral stock
YPD	10 g/L yeast extract 20 g/L peptone 20 g/L glucose
SPAS	10 g/L glucose 1 g/L KH_2PO_4 1 mL/L 1000x vitamine stock 45 mg/L adenine 45 mg/L histidine 45 mg/L leucine 45 mg/L uracil 45 mg/L lysine
YM	6.7 g/L yeast nitrogen base w/o amino acids

Stock solutions for *S. pombe* media were prepared according to standard protocols (Moreno et al. 1991), filter sterilized and stored at 4 °C. The composition of these solutions is given in Table 2.

Table 2: Stock solutions for *S. pombe* media

Stock solution	**composition**
50x salt stock	52.5 g/L $MgCl_2$*6 H_2O 0.735 g/L $CaCl_2$*2 H_2O 50 g/L KCl 2 g/L Na_2SO_4
1000x vitamine stock	1 g/L pantothenic acid 10 g/L nicotinic acid 10 g/L inositol 10 mg/L biotin

10000x mineral stock	5 g/L boric acid 4 g/L $MnSO_4$ 4 g/L $ZnSO_4$*7 H_2O 2 g/L $FeCl_2$*6 H_2O 0.4 g/L molybdic acid 1 g/L KI 0.4 g/L $CuSO_4$*5 H_2O 10 g/L citric acid

4.3 *Schizosaccharomyces pombe* strains

S. pombe strains used in this study are given in Table 3. The strains originated from the laboratory collection or from a deletion library that contained deletions of nearly all non-essential genes (Bioneer). Additional deletions were obtained by direct deletion of the respective gene using genomic integration of either a kanMX or a natMX cassette (Janke et al. 2004). Additional strains were kindly provided by the indicated sources.

Table 3: *S. pombe* used in this study

Name	Genotype	Source
AEP1	*h^- leu1-32 ura4-D18 his3-D3*	YGRC
AEP8	*h^- leu1-32 ura4-D18 his3-D3 pmt1Δ::kanMX*	this study
AEP10	*h^- leu1-32 ura4-D18 his3-D3 pmt1-TAP/kanMX*	this study
AEP11	*h^- leu1-32 ura4-D18 his3-D3 pmt1-GFP/kanMX*	this study
AEP37	*h^- leu1-32 ade6-210 ura4-D18 mat1_m-cyhS smt0 rpl42::cyhR(sP56Q) pmt1Δ::natMX*	this study
AEP57	*h^+ leu2-32 ura4-D18 ade6-210*	Bioneer
AEP61	*h^- leu2-32 ura4-D18 his7-366 ade6-216 sck1Δ::LEU2*	Kurt Runge
AEP62	*h^- leu2-32 ura4-D18 his7-366 ade6-216 sck2Δ::LEU2*	Kurt Runge
AEP117	*h^+ leu2-32 ura4-D18 ade6-216 pka1Δ::kanMX*	Bioneer
AEP119	*h^+ leu2-32 ura4-D18 ade6-216 sck2Δ::kanMX*	Bioneer
AEP120	*h^+ leu2-32 ura4-D18 ade6-216 tor1Δ::kanMX*	Bioneer

AEP125	*h*$^+$ *leu2-32 ura4-D18 ade6-216 pka1*Δ*::kanMX pmt1*Δ*::natMX*	this study
AEP126	*h*$^+$ *leu1-32 ura4-D18 ade6-216 sck2*Δ*::kanMX pmt1*Δ*::natMX*	this study

4.4 Molecular cloning

Plasmids used in this study originated from or were derived from the laboratory collection (Table 4). Plasmids were generated according to standard cloning techniques (Sambrook et al. 1989). Kits for plasmid isolation and gel purification of PCR fragments were purchased from Qiagen. Restriction enzymes and the respective buffers were used from NEB.

For the exchange of single amino acids, the PCR sewing technique was used. With this method in a first step short complementary overhangs were created that contain the desired mutation. These PCR products served as polymerase start sites in a second PCR reaction. The intron-less sequence of *pmt1*$^+$ was generated by reverse transcription of *S. pombe* RNA with randon hexamers. PCR using the cDNA as template and *pmt1*-specific primers with overhangs containing XhoI and BamHI restriction sites amplified intron-less *pmt1*-fragments that were cloned into the pET15b vector. The resulting pET15b-pmt1 plasmid (pAE1372) served as a template for the generation of other *pmt1*-containing vectors (pAE1462, pAE1590, pAE1666, pAE1890, pAE1891). For the replacement of the *nmt1* promoter by the *pmt1* promoter in pAE1891, the *nmt1* sequence was excised from pAE1890 using XhoI and PstI restriction sites. The *pmt1* promoter that was generated from the 400 bp upstream of the genomic *pmt1* locus by PCR was inserted into the vector using the same restriction sites. The Dnmt2 expression vector pAE1385 was a kind gift from A. Jeltsch (Jurkowski et al. 2008). The *in vitro* transcription vectors were generated as described below.

Table 4: Plasmids used in this study

Name	**Vector**	**Description**
pAE1372	pET15b-pmt1	XhoI-pmt1-BamHI (intron-less pmt1$^+$-sequence)
pAE1385	pET28a(+)-hDnmt2	HindIII-hDnmt2-XhoI (T. Jurkowski)

pAE1429	REP4X	nmt1-promoter, ars1, ura4^{+} marker
pAE1434	pSLF172	Designed to tag expressed protein at C-terminus with 3xHA-tag, nmt1-promoter
pAE1445	pSGP572a	nmt1-promoter, ars1, ura4+ marker, NotI-TTG-GFP-TAG-SalI
pAE1462	REP4X-pmt1	BamHI-pmt1-SmaI (intron-less *pmt1*$^{+}$-sequence)
pAE1587	pJET1-tRNAAsp (*D. discoideum*)	XhoI-T7pr-GCG-tRNAAsp-BamHI
pAE1588	pJET1-tRNAAspC38A (*D. discoideum*)	XhoI-T7pr-GCG-tRNAAspC38A-BamHI
pAE1590	pSGP572a-pmt1	BglII-pmt1-SacII (intron-less *pmt1*$^{+}$-sequence)
pAE1666	pET15b-pmt1C81A	XhoI-pmt1C81A-BamHI (intron-less *pmt1*$^{+}$-sequence)
pAE1688	pJET1-tRNAAsp (*S. pombe*)	XhoI-T7pr-GCG-tRNAAsp-NcoI
pAE1736	pJET1-tRNAAsp C38A (*S. pombe*)	XhoI-T7pr-GCG-tRNAAspC38A-NcoI
pAE1758	pJET1-tRNAGlu (*S. pombe*)	XhoI-T7pr-GCG-tRNAGlu-NcoI
pAE1820	pJET1-tRNALys (*S. pombe*)	XhoI-T7pr-GCG-unspliced tRNALys-NcoI
pAE1890	pSLF172-pmt1	nmtpr-XhoI-pmt1-BglII-HA-tag (intron-less *pmt1*$^{+}$-sequence)
pAE1891	pSLF172-prpmt1-pmt1	PstI-pmt1pr-XhoI-pmt1-BglII-HA-tag (intron-less *pmt1*$^{+}$-sequence)

Oligonucleotides used for gene deletions and plasmid constructions are listed in Table 5. Oligonucleotides were designed using ApE software and synthesized by Metabion.

Table 5: Oligonucleotides used for gene deletion or plasmid generation

Oligonucleotides	**Sequence**
K2	GCCCCTGAGCTGCGCACGTC
K3	CTGCCCAGATGCGAAGTTAAGTGCGC

pJET-Seq.fw	GGTATTATCTCTATTTTTAACTTGGAGCAGG
pJET-Seq.rev	GCCACCTACAACGGTTCC
pmt1-BamHI.rev	TCACGCGGATCCTTAGAAATTTAGAGGTTCCAGTAATAGAGA
pmt1-BglII.fw	AACGGAAGATCTATGCTTAGTACAAAAAGATTACGGGTCCT
pmt1-C81A.fw	GTAAATTATGGACTATGAGTCCCAGTGCTCAACCTTTTACTA GAATAGGAAACC
pmt1-C81A.rev	CGGTTTCCTATTCTAGTAAAAGGTTGAGCACTGGGACTCATA GTCCATAATTTAC
pmt1-check.fw	AACATTCCTAATTCTCGCAGTAGAT
pmt1-check.rev	GAGCCTAGCCAATCCATACC
pmt1-KO.up	GGTTACATTCAATGCTTAGTACAAAAAGATTACGGGTCCTGG AGCTATATTCTGGCGTACGCTGCAGGTCGAC
pmt1-NotI.rev	TTTTCCTTTTGCGGCCGCCGAAATTTAGAGGTTCCAGTAATA GAGAAATC
pmt1-PCR1.fw2	GCCAATCTCTGTGAACGGG
pmt1-PCR1.rev2	GGACCCGTAATCTTTTTGTACTAAGC
pmt1-S2	AATATTAATTTCCTTTCATTTTAAAAAAATAGTTTTGACTTCTA ACCGCTTTTAATCGATGAATTCGAGCTCG
pmt1-S3	CGTTAAAGTTGTTTCATACTTGATTTCTCTATTACTGGAACCT CTAAATTTCCGTACGCTGCAGGTCGAC
pmt1-SacII neu.rev	CGATCCCCGCGGCTGAAATTTAGAGGTTCCAGTAATAGAGA AATC
pmt1-Sew.fw2	CGAGCTCGAGATGTTCGTG
pmt1-Sew.rev	CCAGTGGAGGTTGGATGATTC
pmt1-SmaI.fw	ACTTCCCCCGGGATGCTTAGTACAAAAAGATTACGGGTCCT
pmt1-XhoI.fw	ACTCCGCTCGAGATGCTTAGTACAAAAAGATTACGGGTC
pmt1.fw	AAATCTAATGCAGGTAGGTC
pmt1.rev	GTCTTGAAATTAGTCCTGG
REP.fw	GATATGGATATTTATTAAATCAGGAAAAACGTAAC
REP.rev	GTGGTTTATAAAAATTCTTAACTACACCACT

For the generation of the pJET1 vectors for the *in vitro* transcription of tRNAs, the genes for $tRNA^{Asp}$ (SPATRNAASP.01), $tRNA^{Glu}$ (SPATRNAGLU.01), $tRNA^{Lys}$ (SPBTRNALYS.07) and the mutant $tRNA^{Asp}$C38A were cloned into an *in vitro* transcription vector. For this purpose, the PCR fragments with the sequences of *S. pombe* tRNAs were generated using four overlapping oligonucleotides in a single PCR reaction (Table 6). The resulting PCR fragments additionally contained XhoI and NcoI restriction sites, a T7 promoter sequence and a GCG trinucleotide that served as a start site for the T7 RNA polymerase. The DNA fragments were integrated into the pGEM-T easy vector (Promega), and subsequently cloned into pJET1-tRNAAsp (*D. discoideum*) vector (kind gift from W. Nellen) after excision of the *Dictyostelium* $tRNA^{Asp}$ sequence using XhoI and NcoI restricton sites.

Table 6: Oligonucleotides used for transcription vector generation

$tRNA^{Asp}$	
Asp1	CTCGAGTTTTTCAGCAAGATTTGTAATACGACTCACTATAGCGTCTCC
Asp2	CGAACCCGGGCTGCAAGCGTGACAGGCTTGTGTACTACCCCTATACTAAAGGAGACGCTATAGTGAGTCG
Asp3	GCAGCCCGGGTTCGAATCCCGGAGGGAGAGCCATGG
Asp4	CCATGGCTCTCCCTCC
$tRNA^{Asp}$C38A	
Asp1	CTCGAGTTTTTCAGCAAGATTTGTAATACGACTCACTATAGCGTCTCC
AspC38A2	CGAACCCGGGCTGCAAGCTTGACAGGCTTGTGTACTACCCCTATACTAAAGGAGACGCTATAGTGAGTCG
Asp3	GCAGCCCGGGTTCGAATCCCGGAGGGAGAGCCATGG
Asp4	CCATGGCTCTCCCTCC
$tRNA^{Glu}$	
Glu1	CTCGAGTTTTTCAGCAAGATTTGTAATACGACTCACTATAGCGTCCG
Glu2	GAACCCCGACCGCGTCGGTGAAAGCGACGAATCCTAGCCGTTGGACCACAACGGACGCTATAGTGAGTCG
Glu3	CGCGGTCGGGGTTCGACTCCCCGCAACGGAGCCATGG

Glu4	CCATGGCTCCGTTGC
$tRNA^{Lys}$ (unspliced)	
Lys1	CTCGAGTTTTTCAGCAAGATTTGTAATACGACTCACTATAGCGTCCC
Lys2	CGACTCACTATAGCGTCCCGAGTGGCTCAATCGGTTTAGAGCGTCTGACTCTTACGAATGGTATCAGAAGGTTGCGAG
Lys3	TGGTATCAGAAGGTTGCGAGTTCGAGTCTCGCCTTGGGAGCCATGG
Lys4	CGGAACCCTCGGTACC

4.5 RNA purification

Yeast cells were grown to an optical density OD_{600} of 0.5 - 0.9 in 50 mL cultures. Cells were harvested and the pellets were either stored at -20 °C or directly used for RNA preparation. Small sample numbers were prepared using 8 mL TriZol (Invitrogen) reagent per sample and glass beads. After vigorous shaking for 5 minutes, the samples were centrifuged for 20 minutes at 12000xg to clear them from debris. The RNA was extracted using chloroform and precipitated with isopropyl alcohol.

Larger sample numbers were prepared using 8 mL TriFast (PeqLab) reagent per sample and glass beads. After vigorous shaking for 5 minutes, the samples were transferred to PhaseTrap tubes (Peqlab), and an equal amount of chloroform was added. Centrifugation at 1500xg lead to a stable phase separation, and the RNA was precipitated from the supernatant with isopropyl alcohol.

4.6 Transcription and purification of tRNAs

In vitro transcribed tRNAs were obtained using T7 transcription kit (Fermentas) according to the suppliers instructions. Briefly, the vector containing the tRNA gene was linearized using NcoI (NEB) and 0.5 µg of this template DNA were incubated for 2 hours at 37 °C with nucleotides and T7-RNA polymerase in the reaction buffer. The transcripts were treated with TURBO DNase (Ambion) for 15 min at 37 °C and

subjected to phenol/chloroform extraction and gel filtration using Sephadex G50 (GE Healthcare).

4.7 *In vitro* RNA methylation Assay

The activity of methyltransferases that use S-adenosyl-methionine (SAM) as a cofactor can be detected in an *in vitro* methylation assay, if the methyl group of SAM is labeled with a radioactive atom, e.g. with tritium. The labeled methyl group will be transferred to the appropriate substrate by an active methyltransferase. The radioactivity of the substrate can then be detected by autoradiography after gel electrophoresis of the reaction products. This assay also provides the possibility to analyze different proteins for their methylation activity and different RNA samples for their ability to be methylated.

In vitro methylation of RNA samples was performed as described previously (Jurkowski et al. 2008). RNA extracts from *S. pombe* cells or *in vitro* transcribed tRNA were incubated with 3 µM of purified recombinant protein. The amounts of RNA varied from 2 µg to 10 µg of total RNA extracts, depending on the concentration of the sample, or were 0.5 µg for *in vitro* transcribed tRNA. The methylation reaction was composed as follows:

X µL RNA
2 µL 10x methylation buffer (50 mM Tris HCl pH 7.5, 50 mM NaCl, 5 mM $MgCl_2$, 1 mM DTT)
1 µL Ribolock RNase Inhibitor (20 u/µL, Fermentas)
2 µL S-[methyl-3H]-adenosyl-L-methionine (1 mCi/mL, Hartmann Analytic)
Y µL recombinant DNA methyltransferase (final concentration 3 µM)
Add water to 20 µL

After 90 minutes of incubation at 22 °C, the reaction was stopped by the addition of 1.2 u/µL Proteinase K (NEB) and 1 mM non-radioactive SAM (Sigma) and further incubated for 30-60 minutes. The samples where stored at -20 °C over night after addition of the RNA loading buffer (10 mL formamide, 100 µL 0.5 M EDTA, Bromophenol blue).

The denaturating 7 M urea 12 % polyacrylamide gel (5 mL 10x TBE, 21 g urea, 15 mL Rotiphorese Gel 40 (19:1), 15 mL water, 100 µL TEMED, 100 µL 10 % APS) was run for 30 minutes at 24-28 mA before loading the samples. The samples were

heated to 80 °C for 5 minutes, loaded onto the gel and separated for 3-5 hours at 24-28 mA. The gel was then stained with EtBr for 20 minutes and documented before it was fixed with a solution containing 10 % acetic acid and 10 % methanol twice for 10 minutes. Incubation in amplify solution for 1 hour was followed by drying the gel in a gel dryer at 70 °C. An autoradiography film (GE Healthcare) was then exposed to the gel at -80 °C over night up to several days.

4.8 RNA bisulfite sequencing

When RNA is treated with bisulfite, non-methylated cytosines will be deaminated to uracil, whereas methylated cytosines will not be affected by the treatment. When the bisulfite-treated RNA is then converted into cDNA, amplified by PCR and sequenced, methylated cytosines will be sequenced as cytosines in the sequence, whereas unmethylated RNA-cytosines will appear as thymines after sequencing. This method thus allows the detection of RNA methylation in a given substrate.

RNA bisulfite sequencing was performed according to protocols published elsewhere (Schaefer et al. 2009b). Briefly, 2 µg of total RNA were treated with 2 u/µL TURBO DNase (Ambion) in a total sample volume of 10 µL for 30 minutes at 37 °C. The DNase was inactivated with DNase inactivation reagent (Ambion) by incubation at room temperature for 5 minutes and centrifugation at 10000xg. 42.5 µL Bisulfite Mix (Epitect Bisulfite Kit, Qiagen) and 17.5 µL stabilization solution (Qiagen) were added to the 10 µL of each sample to give a final volume of 70 µL, and it was incubated for the bisulfite reaction (5 minutes at 70 °C, 3 hours at 60 °C, cool down to 20 °C). The samples were desalted using Micro-Bio-Spin columns (Bio-Rad) and then incubated with 70 µL of 1 M Tris (pH 9) at 37 °C for 1 hour for desulphonation of RNA adducts. After addition of 1/10 sample volume 3 M sodium acetate, 20 µg glycogen and 420 µL ethanol, the RNA was precipitated at -80 °C over night.

The precipitated RNA was pelleted, washed and dissolved in 10 µL DEPC treated water. The concentration of the RNA was determined using a spectrophotometer. For cDNA synthesis, 500 ng of bisulfite-treated RNA were mixed with 2 µL of 10 mM dNTP mix (Superscript III, Invitrogen) and 1 µL of 10 µM tRNA-specific RT-primer in a total volume of 13 µL and incubated at 70 °C for 5 minutes. After addition of 2.3 µL of 10x RT buffer, 4 µL of 25 mM $MgCl_2$, 2 µL of 0.1 M DTT, 1 µL RNase inhibitor and 1 µL Superscript III reverse transcriptase (total volume of 23 µL), the samples were

incubated for 10 minutes at 25 °C, 50 minutes at 50 °C, 15 minutes at 94 °C and cooled down to 4 °C. 1 µL of cDNA was then used for PCR amplification [3 min 96 °C, (30 sec 96 °C, 45 sec 45 °C, 45 sec 68 °C) x35 cycles, 5 min 70 °C, cool down to 4 °C], the amplicon was purified from an agarose gel using the QiaQuick Gel extraction Kit (Qiagen) and cloned into the pGEM-T easy vector (Promega) for sequencing. Individual clones were purified using QiaPrep Spin Miniprep Kit (Qiagen) and sequenced at GATC Biotech. The five nucleotides with random sequences that were included in the primers used for reverse transcription (Table 7) provided a possibility to identify independent clones in the RNA methylation analysis.

Table 7: Oligonucleotides used for RNA bisulfite sequencing

Name	**Sequence**
stemloop.rev	CTCAACTGGATTGGCT
tRNA^{Asp}	
Asp RT-Primer	CTCAACTGGATTGGCTNNNNNGATAAATCCAGTTGAGTGGCT CTCCCTC
Asp bisulfite.fw	TTAGTATAGGGGTAGTATAT
tRNA^{Glu}	
Glu RT-Primer	CTCAACTGGATTGGCTNNNNNGATAAATCCAGTTGAGTGGCT CCATTACA
Glu bisulfite.fw	TTTGTTGTGGTTTAATGGT
tRNA^{His}	
His RT-Primer	CTCAACTGGATTGGCTNNNNNGATAAATCCAGTTGAGTGGTA CCCACACCA
His bisulfite.fw	ATATGGTTTAGTGGTTAAGAT
tRNA^{Leu}	
Leu RT-Primer	CTCAACTGGATTGGCTNNNNNGATAAATCCAGTTGAGTGGTA AAAAATAT
Leu bisulfite.fw	TTGTTTGAGTGGTTATGGAGT
tRNA^{Lys}	
Lys RT-Primer	CTCAACTGGATTGGCTNNNNNGATAAATCCAGTTGAGTGGCT CCCAAAA

Lys bisulfite.fw	GTGGTTTAATTGGTTTAGAGT
$tRNA^{Val}$	
Val RT-Primer	CTCAACTGGATTGGCTNNNNNGATAAATCCAGTTGAGTGGTA CATCTAC
Val bisulfite.fw	AGTTTAGTGGTTATGATTTT

4.9 SDS-PAGE and Western Blotting

Proteins were separated by SDS-PAGE in Tris-glycine buffer at 120 V according to standard protocols (Laemmli 1970). Gels were stained using coomassie blue or silver staining (SilverStain Plus, Bio-Rad) according to the manufacturer's instructions. Protein transfer to nitrocellulose membranes (Bio-Rad) was accomplished by blotting with the Bio-Rad Tank Transfer System in blot buffer (25 mM Tris, 52 mM glycine, 10 % methanol) at 120 V for 90 min. The membrane was blocked for 2 hours in 5 % milk/TBS-T (50 mM Tris/HCl pH 7.5, 150 mM NaCl, 0.1 % Tween-20, 5 % dry milk powder). Incubation with the primary antibody was over night at 4 °C in 5 % milk/TBS-T, and incubation with the secondary antibody was for 2 hours at room temperature in 5 % milk/TBS-T (concentrations see below). The blot was washed 5 times for 5 minutes with TBS-T (50 mM Tris/HCl pH 7.5, 150 mM NaCl, 0.1 % Tween-20), and the western blot signals were detected using ECL Western Blotting Analysis System (GE Healthcare) and Hyperfilm ECL (GE Healthcare).
Primary epitope tag antibodies were obtained from Sigma (Peroxidase Anti-Peroxidase complex 1:1000, α-polyHistidine 1:3000) and Millipore (α-CBP 1:2000). Secondary antibodies conjugated to horseradish peroxidase were purchased from Sigma (sheep α-mouse 1:1000, goat α-rabbit 1:1000)

4.10 Purification of recombinant Dnmt2 proteins

Proteins carrying a hexa-histidine peptide tag can efficiently be purified using immobilized metal affinity chromatography (IMAC (Hochuli 1988)). This purification relies on the affinity of a molecule for a certain metal, which is immobilized onto a chelating surface, and allows for purification under native as well as denaturating conditions.

For protein purification, 500 mL of LB medium containing 100 µg/mL ampicillin and 34 µg/mL chloramphenicol were inoculated with Rosetta *E. coli* strains carrying the expression vector. The cells were grown to an OD_{600} of 0.6, and protein expression was subsequently induced with 1 mM IPTG for 1-3 hours before the cells were harvested at 4000 rpm and stored at -20 °C. The cells were lysed in sonication buffer (30 mM potassium phosphate buffer (KPi) pH 7.0, 300 mM KCl, 10 % glycerol, 0.1 mM DTT, complete Protease Inhibitor Cocktail (Roche)) by repeated addition of small amounts of lysozyme and sonification for 10 minutes using 30 sec intervals until the lysate was almost clear.

The protein was purified using Profinity IMAC Ni-charged resin (Bio-Rad) in sonication buffer containing 10 mM imidazole and eluted from the beads using elution buffer containing 200 mM imidazole (30 mM KPi pH 7.0, 300 mM KCl, 10 % glycerol, 0.1 mM DTT, 200 mM imidazole). Purification was followed by dialysis in dialysis buffer I (30 mM KPi pH 7.0, 200 mM KCl, 20 % glycerol, 0.1 mM EDTA, 1 mM DTT) and dialysis buffer II (30 mM KPi pH 7.0, 100 mM KCl, 50 % glycerol, 0.1 mM EDTA, 1 mM DTT), and the final protein concentration was determined using Bradford reagent (Bio-Rad) according to the manufacturer's instructions. Typical protein concentrations ranged from 20 µM to 90 µM.

4.11 Purification of native protein by Tandem-Affinity Purification (TAP)

The Tandem Affinity Purification (TAP) method is based on a protein tag that consists of three essential parts (Rigaut et al. 1999; Puig et al. 2001). The protein A part of the TAP tag is able to bind to IgG columns, whereas the CBP (calmodulin binding protein) module is able to bind calmodulin beads. The two protein sequences are separated by a TEV (tobacco etch virus) protease cleavage site that allows for elution from an IgG column by TEV cleavage, which shortens the protein tag by the protein A part. The major advantage of this purification is the possibility of purifying a protein under mild native conditions, which allows for copurification of associated factors.

S. pombe cells were cultured in 6 L YES medium to an OD_{600} of 1.5-2. The cells were harvested, the pellet was washed with ice-cold water, resuspended in buffer A (10 mM HEPES pH 7.9, 10 mM KCl, 1.5 mM $MgCl_2$, 0.5 mM DTT, 2 mM

benzamidine, complete Protease Inhibitor Cocktail (Roche)) and frozen at -80 °C. For protein extraction, the pellet was thawed, and the cells were lysed using a French-Press. Subsequently, the amount of KCl was adjusted to a final concentration of 260 mM. Debris and supernatant were separated by ultracentrifugation (30 min at 21000 rpm, 2 h at 30000 rpm). TAP-tagged proteins were extracted using two sequential column materials. The first purification was with rabbit IgG agarose beads (Sigma) that were equilibrated with IPP150 buffer (10 mM Tris/HCl pH 8.0, 150 mM NaCl, 0.1 % Nonidet (NP-40)). The protein was eluted from the column using AcTEV-protease (Invitrogen) at a final concentration of 0.1 u/µL in a final volume of 1 mL TEV cleavage buffer (10 mM Tris/HCl pH 8.0, 150 mM NaCl, 0.1 % Nonidet, 0.5 mM EDTA, 1 mM DTT) for 2 hours at 16 °C. The eluate was then applied to a calmodulin sepharose column (GE healthcare) that had been equilibrated with calmodulin binding buffer (10 mM Tris/HCl pH 8.0, 10 mM 2-mercaptoethanol, 150 mM NaCl, 1 mM magnesium acetate, 1 mM imidazole, 2mM $CaCl_2$, 0.1 % Nonidet). The protein was eluted with EGTA using Calmodulin elution buffer (10 mM Tris/HCl pH 8.0, 10 mM 2-mercaptoethanol, 150 mM NaCl, 1 mM magnesium acetate, 1 mM imidazole, 0.1 % Nonidet, 2mM EGTA pH 8.0). The eluate was concentrated by centrifugation in Centricon tubes (Millipore) according to the supplier's instructions. The concentrated eluate was then analyzed by SDS-PAGE, Western Blot analysis and Silver staining.

4.12 Chronological lifespan assay

For a quantitative determination of chronological lifespan, *S. pombe* cells were cultured in 50 mL or 100 mL complete medium or minimal medium for several weeks at 30 °C. After 2-3 days, when the culture had reached stationary phase according to the measured OD_{600}, samples of the aged culture were taken at regular intervals and serially diluted. At least 4 different dilutions for every culture were plated onto YES medium plates and incubated at 30 °C for 3 days. The number of colonies on each plate was counted, and the amount of colony-forming units (CFU) was determined for each culture.

For qualitative determination of chronological lifespan, *S. pombe* cells were cultured in 6 mL complete medium or minimal medium for several weeks at 30 °C. After 2-3 days, when the culture had reached stationary phase according to the measured

OD_{600}, samples of the aged culture were taken at regular intervals and serially diluted in 1:6 dilution steps, spotted onto YES plates and incubated at 30 °C for 3 days.

4.13 Synthetic Genetic Array

Synthetic lethality describes the phenomenon that two non-essential mutations become essential when they are combined. This effect gives indications as to overlapping functions of the two mutant genes and genetically places them in parallel pathways.

In a Synthetic Genetic Array (SGA), the combination of a certain mutation with many different other mutations is screened for synthetic lethality. This can be achieved by utilization of a collection of strains that contain deletions of non-essential genes (deletion library). Each of the mutations from the library is combined with a deletion of the gene of interest. Such high-throughput screens require special features in the strain background of the yeast cells that allow for large-scale selection of haploid single and double mutants. The establishment of the Pombe Epistasis Mappers and the availability of an *S. pombe* deletion library (Bioneer) that contained deletions of approximately 3000 non-essential genes provided all the necessary features for a synthetic genetic array (Roguev et al. 2007).

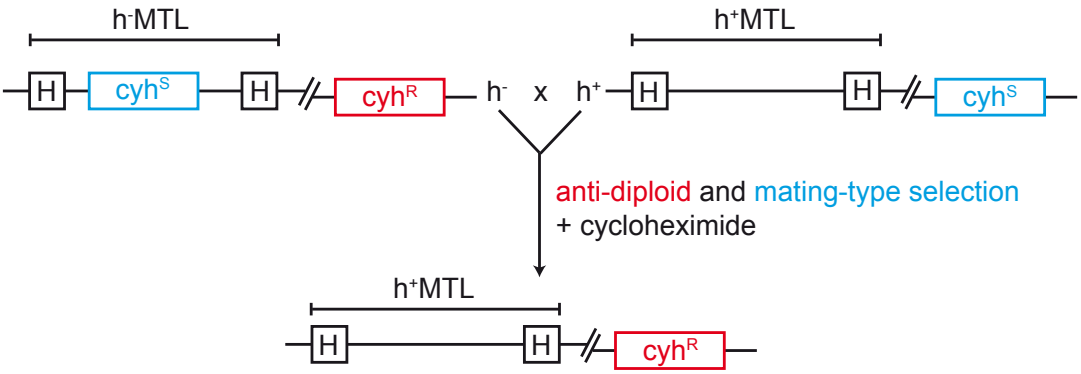

Figure 8: Selection strategy applied in this study
The cycloheximide sensitive (cyh^S) allele that was inserted in the h^- mating type locus (MTL) allowed for selection against h^- cells after the cross. The combination of the cyh^S allele with a recessive cycloheximide resistance allele (cyh^R) in this h^- strain mimics the genotype of a heterozygous diploid cell and allows for anti-diploid and mating-type selection after the cross (modified from (Roguev et al. 2007)).

The selection of haploid double deletion strains of a specific mating type is based on the genotype of the Pombe Epistasis Mapper (PEM) strains (Roguev et al. 2007). For this study we chose to perform the selection using the strain PEM2. PEM2 has an h^-

mating type and is modified with the insertion of a wild type rpl42 (cyh^S) allele into the mating type locus, which causes cycloheximide sensitivity. This strain additionally has a recessive rpl42(sP56Q) allele that provides cycloheximide resistance inserted in the genome. When this strain is crossed with an h^+ strain that is cycloheximide sensitive and the sporulation products are selected for cycloheximide resistance, only haploid cells that contain the cycloheximide resistance allele can survive. These haploids also have to be h^+ cells, because cycloheximide selects against the sensitive h^- mating type locus.

The gene deletions in the deletion library were marked with the kanMX marker gene that provides resistance to the antibiotic G418. The *pmt1*$^+$ deletion was introduced into in the PEM2 strain and marked with the natMX marker gene that provides resistance against the antibiotic nourseothricin. When the selection against one or both of these deletions was combined with the cycloheximide selection, the surviving cells were either haploid single mutants carrying the deletion from the library (cycloheximide + G418), or haploid double mutants carrying the deletion from the library and the *pmt1*$^+$ deletion (cycloheximide + G418 + nourseothricin). When the sporulation products contained viable single mutants, but no viable double mutants, this indicated a synthetic lethal interaction.

The SGA was performed according to the protocol published by (Roguev et al. 2007). Briefly, yeast cells of opposing mating types (AEP37 x Bioneer deletion library) were mixed in microtiter plates and transferred to sporulation plates (SPAS, Table 1) using a replica tool. The plates were incubated for 4 days at 23 °C. Next, the cells were transferred to complete medium plates (YES) for spore germination and incubated for one day at 30 °C, before the cells were replica plated onto complete medium containing cycloheximide and G418 (YES+GC) for selection for haploid single mutants (incubation at 30 °C for two days). In a final step, the yeast cells were transferred to complete medium containing cycloheximide, G418 and nourseothricin (YES+GNC) for double mutant selection. The plates were incubated at 30 °C for two days and documented. Comparison of growth on YES+GC and growth on YES+GNC identified gene deletions that affected cell growth in combination with a *pmt1*$^+$ deletion.

4.14 *S. pombe* crosses and tetrad dissection

Cell material of the two strains to be crossed was mixed on a SPAS plate and incubated at room temperature for two days. *S. pombe* cells mate and sporulate spontaneously under these conditions. Asci were transferred to YES plates, identified under a microscope, separated and incubated at 37 °C for 3-5 hours or over night at room temperature to allow for break-down of the ascus wall. Afterwards, the spores were separated by micromanipulation and incubated at 30 °C for 2-3 days. The markers of the segregants were tested by replica plating onto appropriate selective medium.

5 Results

5.1 Pmt1 methylated heterologous tRNA^{Asp} *in vitro*

Dnmt2 homologs from various species have tRNA methyltransferase activity. Despite the fact that Pmt1 was the first member of the Dnmt2 family to be identified, the RNA methyltransferase activity of the *S. pombe* homolog has not yet been investigated. In this study we wanted to investigate the activity of Pmt1 based on the findings on other Dnmt2 homologs.

In a first approach, we sought to determine *in vitro* methylation activity of Pmt1 on substrates that are methylated by other Dnmt2 homologs. Recombinant Dnmt2 proteins can be used to methylate tRNA substrates in an *in vitro* methylation reaction. We therefore sought to determine whether recombinant Pmt1 could methylate known Dnmt2 substrates *in vitro*. To this end, we purified 6xHis-tagged Pmt1 from *E. coli*. The protein was soluble and could be purified under native conditions in sufficient amounts for the application in an *in vitro* methylation assay. Coomassie staining and western blot analysis confirmed the purification of a 39 kDa protein (Figure 9A) – the expected size for hexa-histidine-tagged Pmt1 – that was detectable using an eptitope tag antibody (Figure 9B).

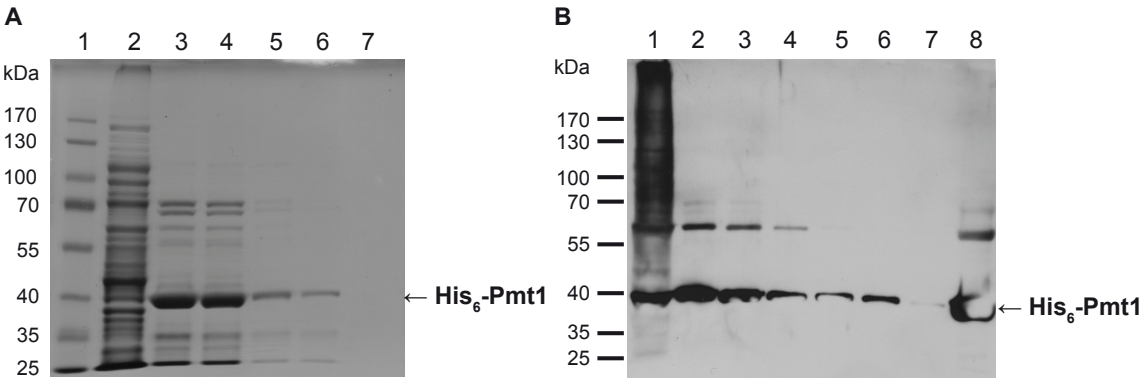

Figure 9: Purification of hexa-histidine tagged Pmt1
(A) Samples from different steps of the His_6-purification were separated by SDS-PAGE in an 8 % SDS-gel. Coomassie staining visualized the protein bands. His_6-tagged Pmt1 is expected at 39 kDa. 1= Marker, 2=Flowthrough after Ni-beads, 3=Concentrated eluate, 4=Eluate 60 mM imidazole fraction 1, 5=Eluate 60 mM imidazole fraction 5, 6=Eluate 100 mM imidazole fraction 1, 7=Eluate 100 mM imidazole fraction 5 (B) Samples from different steps of the His_6-purification were separated by SDS-PAGE and visualized by Western blotting. Anti-histidine-tag antibody detected His_6-Pmt1 at 39 kDa. 1=Flowthrough after Ni-beads, 2=Eluate 60 mM imidazole fraction 1, 3=Eluate 60 mM imidazole fraction 3, 4=Eluate 60 mM imidazole fraction 5, 5=Eluate 100 mM imidazole fraction 1, 6=Eluate 100 mM imidazole fraction 3, 7=Eluate 100 mM imidazole fraction 5, 8=Concentrated eluate.

Dictyostelium discoideum $tRNA^{Asp}$ has been identified as a substrate for the *D. discoideum* homolog of Dnmt2, DnmA. This $tRNA^{Asp}$, like all other known Dnmt2 substrates, contains a cytosine at position 38 in the anticodon loop, which is the methylation target of tRNA methylation by Dnmt2 enzymes. In an *in vitro* methylation assay, not only DnmA, but also human Dnmt2 can methylate the $tRNA^{Asp}$ from *D. discoideum* (S. Müller, W. Nellen, unpublished data). Therefore, we used *in vitro* transcribed $tRNA^{Asp}$ from *D. discoideum* as a substrate to ask whether Pmt1 can also methylate this tRNA (in collaboration with Sara Müller and Wolfgang Nellen, Department for Genetics, University of Kassel).

The *in vitro* methylation assay is based on the fact that m^5C-methyltransferases use S-adenosyl-methionine (SAM) as a cofactor. In the assay, a radioactively labeled SAM was used that contained a tritiated methyl group. During the methylation reaction, this radioactive methyl group is transferred to the substrate, and the radioactively labeled substrate can then be detected by autoradiography (Jurkowski et al. 2008). As expected, the previously characterized methylation activity of DnmA and human Dnmt2 on $tRNA^{Asp}$ could be detected (Figure 10). Significantly, Pmt1 was able to methylate the $tRNA^{Asp}$ substrate to a similar degree as DnmA and hDnmt2. This demonstrated that Pmt1, like other Dnmt2 enzymes, has *in vitro* tRNA methyltransferase activity. This activity was found on an *in vitro* transcribed $tRNA^{Asp}$ substrate that carried no other modifications, implicating that previous modification of the substrate is not required for *in vitro* activity of Pmt1. Furthermore, this showed that the mutation in the amino acid sequence of the catalytic motif IV (PPCQ → PSCQ), which was thought to be responsible for the absence of a detectable DNA methyltransferase activity in Pmt1 did not abrogate $tRNA^{Asp}$ methylation activity *in vitro*.

The activity of Dnmt2 enzymes is specific to a cytosine residue at position 38 of the anticodon loop, and this is the only position known to be methylated by Dnmt2 enzymes. To determine the methylation site within the *D. discoideum* $tRNA^{Asp}$ sequence, we also tested the ability to methylate a mutated $tRNA^{Asp}$ substrate ($tRNA^{Asp}$C38A), which did not contain the cytosine at position 38. Pmt1 was unable to methylate this tRNA (Figure 10), showing that Pmt1 methylated the *D. discoideum* $tRNA^{Asp}$ at position C38.

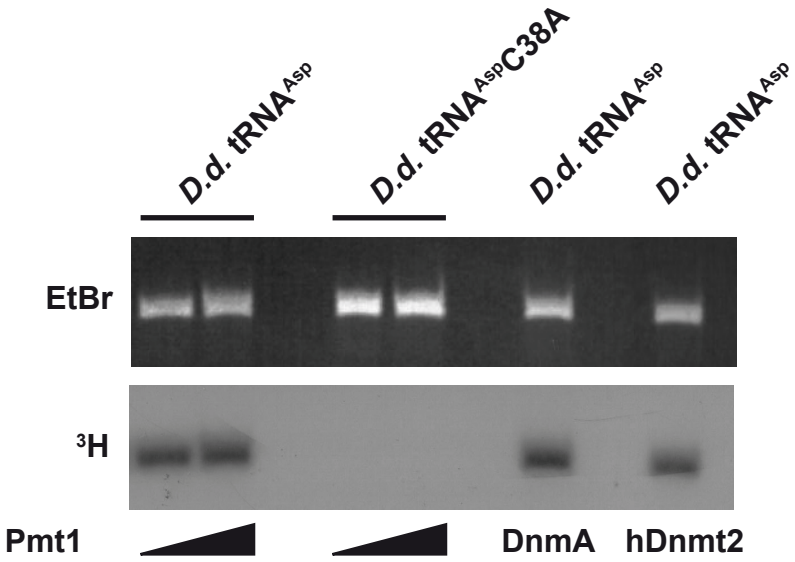

Figure 10: Pmt1 methylates *D. discoideum* tRNA^{Asp} at position C38.
In vitro transcribed tRNA^{Asp} (500 ng) or tRNA^{Asp}C38A (500 ng) from *Dictyostelium discoideum* was incubated with different Dnmt2 homologs (Pmt1: 3-12 µM, DnmA: 3 µM, hDnmt2: 3 µM). The samples were separated by urea-PAGE and *in vitro* methylation was detected by autoradiography. Recombinant DnmA and Dnmt2 were courtesy of Sara Müller and Wolfgang Nellen.

5.2 Pmt1 methylated *S. pombe* tRNA^{Asp} *in vitro*

We next sought to determine whether the ability of Pmt1 to methylate tRNAs is extended to the native tRNA^{Asp} from *S. pombe*. Therefore, we analyzed the tRNA^{Asp} gene of *S. pombe* for the properties required for Dnmt2 target recognition. As in other known Dnmt2 substrate tRNAs, we found that *S. pombe* tRNA^{Asp} also contains a cytosine at position 38 in the anticodon loop. Thus, it could in principle be a substrate for a Dnmt2 homolog.

The *S. pombe* tRNA^{Asp} sequence or a mutated sequence coding for tRNA^{Asp}C38A were transcribed *in vitro* and applied as substrates in the methylation assay. Recombinant Pmt1 was able to methylate the *S. pombe* tRNA^{Asp} substrate, as detected by a strong methylation signal. In contrast, the mutated tRNA could not be methylated (Figure 11A). This demonstrated that recombinant Pmt1 methylates *S. pombe* tRNA^{Asp} at position C38 *in vitro*. As for the *D. discoideum* tRNA^{Asp}, no previous modifications on the tRNA were necessary to detect Pmt1 activity on the substrate.

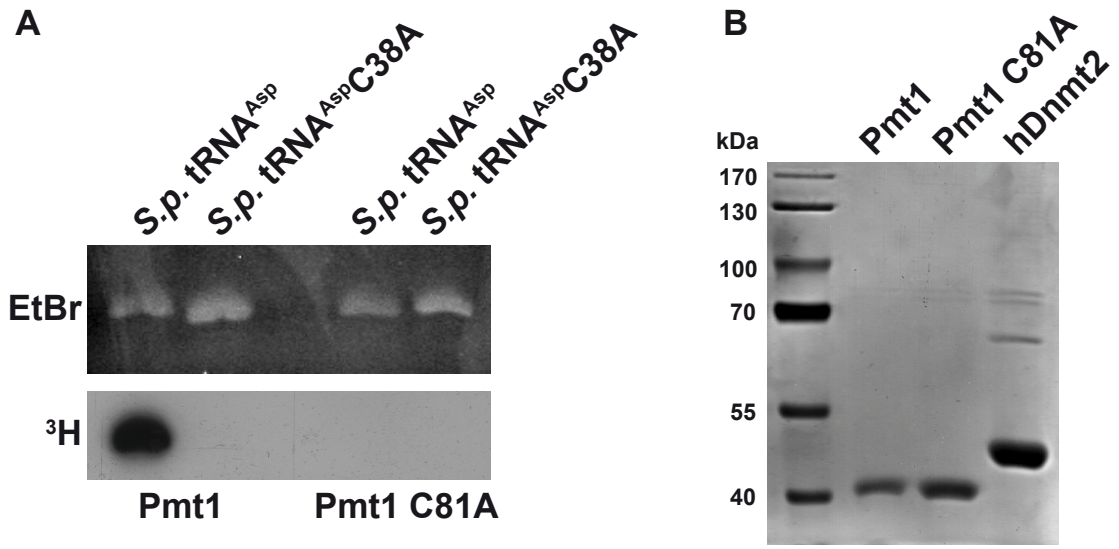

Figure 11: Pmt1 methylates *S. pombe* tRNA^{Asp} at position C38.
(A) *In vitro* transcribed tRNA^{Asp} (500 ng) or tRNA^{Asp}C38A (500 ng) from *Schizosaccharomyces pombe* was incubated with 3 µM Pmt1 or 3 µM Pmt1C81A. The samples were separated by urea-PAGE and *in vitro* methylation was detected by autoradiography. (B) The amounts of purfied protein were compared by SDS-PAGE. Coomassie staining visualized His$_6$-Pmt1 and His$_6$-Pmt1C81A at 39 kDa and His$_6$-hDnmt2 at ~46 kDa.

When recombinant proteins are used for activity assays, there is always the possibility that the detected activity originates from a contaminant that has been copurified with the enzyme of interest. To investigate the methylation activity of possible contaminants, we constructed a catalytically inactive Pmt1 mutant. In this protein, the catalytic cysteine in motif IV was exchanged by an alanine, which is expected to abrogate the methyltransferase activity of Pmt1. The mutant protein was purified from *E. coli* and used in the methylation assay. The amounts of protein used in the assay were compared using SDS-PAGE and coomassie staining (Figure 11B). Importantly, the mutant protein was not able to methylate any of the tRNA^{Asp} substrates (Figure 11A). This result showed that the methylation activity detected on tRNA^{Asp} resided in Pmt1 and not in a copurifying contaminant.

5.3 Pmt1 methylated *S. pombe* tRNA^{Glu} *in vitro*

Dnmt2 homologs have the ability to methylate tRNAs other than tRNA^{Asp} that contain a cytosine at position 38. In *Drosophila*, tRNA^{Gly} and tRNA^{Val} are methylated at position C38 (Schaefer et al. 2010), and in *D. discoideum*, tRNA^{Glu} is a target for methylation by the *Dictyostelium* Dnmt2 homolog DnmA (W. Nellen, personal communication). To determine whether Pmt1 is also able to methylate other

S. pombe tRNAs, we identified all tRNAs of the fission yeast containing a C38 (Table 8). Due to a proposed "target recognition motif" that includes the bases at the positions 32, 37, 38 and 40 (M. Helm, unpublished data), we also compared the C38-containing tRNA sequences for the bases at these positions. According to the proposed motif, Dnmt2 enzymes require a cytosine at position 32 in the anticodon loop, an adenine at position 37, a cytosine at position 38 and another cytosine in the anticodon stem at position 40.

Table 8: *S. pombe* tRNAs containing a C38

tRNA	C32	A37	C38	C40
Asp	+	+	+	+
Glu	+	+	+	
Lys unspliced	+	+	+	
Val		+	+	+
Leu			+	+
His			+	
Lys	+	+		

We chose to investigate $tRNA^{Glu}$ and the unspliced $tRNA^{Lys}$ as substrates for recombinant Pmt1, because they contain all but one of the bases hypothesized to be important for target recognition and subsequent activity of Dnmt2 enzymes. The only tRNA in *S. pombe* with a perfect match to the pattern is $tRNA^{Asp}$. *In vitro* transcripts of these two tRNAs were used as substrates in the methylation reaction. As a result, we found that $tRNA^{Glu}$ can be methylated by Pmt1, but to a much lesser extent than $tRNA^{Asp}$ (Figure 12). Pmt1 was unable to methylate the unspliced $tRNA^{Lys}$ (Figure 12), although it contains all the same bases of the recognition pattern as $tRNA^{Glu}$. This suggested that proper folding of the tRNA, which is probably not present in the unspliced $tRNA^{Lys}$, is another important factor of Pmt1 target recognition.

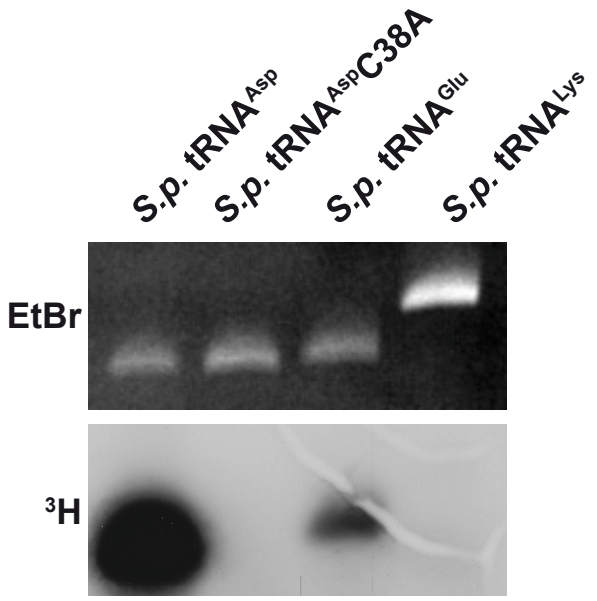

Figure 12: Pmt1 methylates *S. pombe* tRNA^{Glu}.
In vitro transcribed tRNAs (500 ng) were incubated with Pmt1 (3 µM). The samples were separated by urea-PAGE and *in vitro* methylation was detected by autoradiography.

5.4 Pmt1 had methyltransferase activity *in vivo*

Since we had observed that Pmt1 has tRNA methyltransferase activity *in vitro*, we next asked whether the enzyme is also active in the yeast cells. To this end, we used RNA bisulfite sequencing. This method has been derived from the commonly used DNA bisulfite sequencing method, but adapted to the needs of RNA samples (Schaefer et al. 2009b). It allows for direct analysis of methylation patterns on native RNA. We extracted RNA from *S. pombe* strains, treated it with bisulfite and generated PCR amplicons of tRNA^{Asp}. Individual independent clones were analyzed by sequencing to determine methylation at cytosine residues.

To ensure high cellular Pmt1 protein levels (and for reasons that will become obvious below), we expressed *pmt1*$^+$ from the *nmt1* overexpression promoter by using a *pmt1Δ*-strain that carried either a control vector or an overexpression vector and cultured them in *S. pombe* minimal medium (EMM) to ensure maintenance of the plasmids. The *pmt1Δ* background was used to provide a situation with unmethylated tRNA^{Asp} as a control. The overexpression of the protein should force Pmt1 into action. The RNA isolated from these strains was treated with bisulfite, reverse transcribed, amplified by PCR and cloned for sequencing.

Significantly, upon *pmt1*$^+$-overexpression, the methylation of position C38 of tRNA^{Asp} was 100 % (Figure 13). We detected methylation at positions C48, C49, C60, C61

and C62, which are carried out by other tRNA-methyltransferases, which indicated that the bisulfite reaction was successful and that methylated cytosines are not converted to uracil by the bisulfite treatment. This provided further evidence for the methylated state of cytosine 38 in this strain. As expected, we found no methylation at position C38 in the *pmt1Δ*-strain. The other methylation sites of $tRNA^{Asp}$ were unaffected by the change in $pmt1^{+}$-expression. This result for the first time demonstrated *in vivo* Pmt1 activity on a $tRNA^{Asp}$ substrate.

We also wanted to determine the level of methylation in a wild-type strain. Thus, $tRNA^{Asp}$ from a wild-type strain carrying either a control or an overexpression vector was also analyzed by RNA bisulfite sequencing. We were able to detect cytosine methylation at position C38 in 23 % of the analyzed clones when the cells carried the control plasmid. As expected from the results above the methylation level was 100 % upon $pmt1^{+}$-overexpression. This result provided evidence for *in vivo* Pmt1 activity on $tRNA^{Asp}$ at the endogenous expression level (Figure 13).

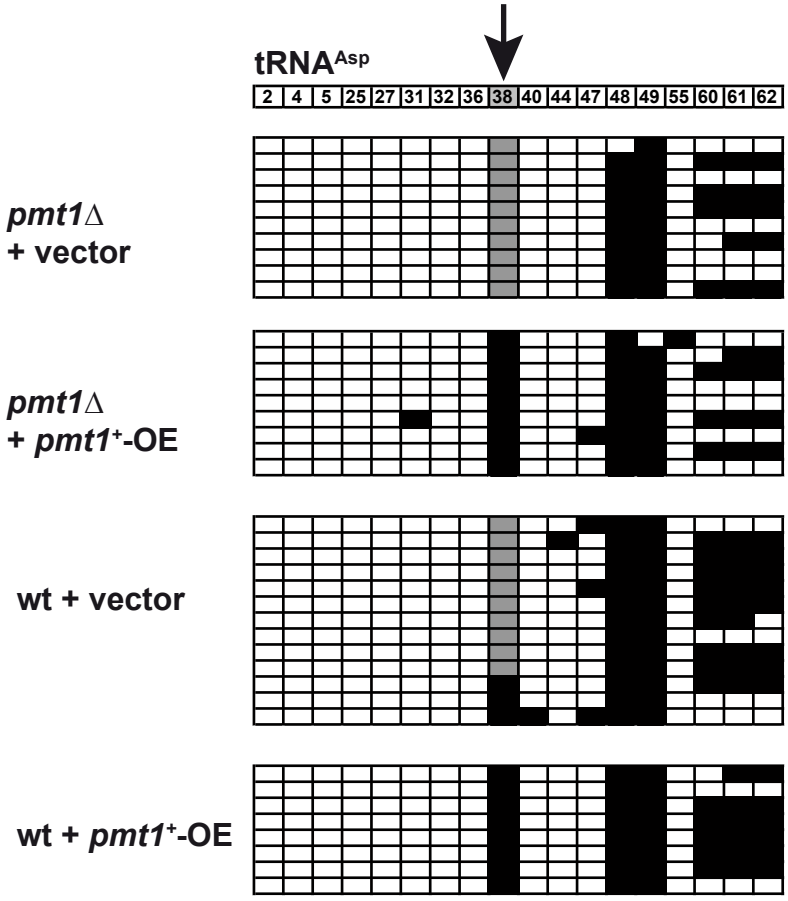

Figure 13: Pmt1 methylates $tRNA^{Asp}$ *in vivo*.
Bisulfite analysis of $tRNA^{Asp}$ from wild type or *pmt1Δ* cells carrying either a control plasmid or a $pmt1^{+}$-overexpression plasmid. Each column represents a cytosine of $tRNA^{Asp}$, each line represents an individual clone. Methylated cytosines are indicated by black boxes, grey boxes mark unmethylated C38.

To validate these findings with an independent method, we used the *in vitro* methylation assay to detect RNA methylation in cellular RNA. The recombinant Pmt1 enzyme in the *in vitro* methylation reaction was able to methylate – and therefore radioactively label – all substrates in the total RNA sample that are unmethylated upon extraction from the yeast cells. RNA substrates that have already been methylated *in vivo* in the cells cannot be methylated in the *in vitro* reaction. Consequently, completely unmethylated RNA samples are expected to give a detectable band in the *in vitro* methylation, whereas RNA fully methylated *in vivo* is expected to give no detectable signal for the *in vitro* methylation. If only a fraction of the RNA substrates was methylated *in vivo*, a reduced methylation signal is expected in the *in vitro* methylation reaction. We used total RNA isolated from a wild-type strain and a *pmt1*$^{+}$-overexpression strain as substrates for an *in vitro* methylation reaction (Figure 14).

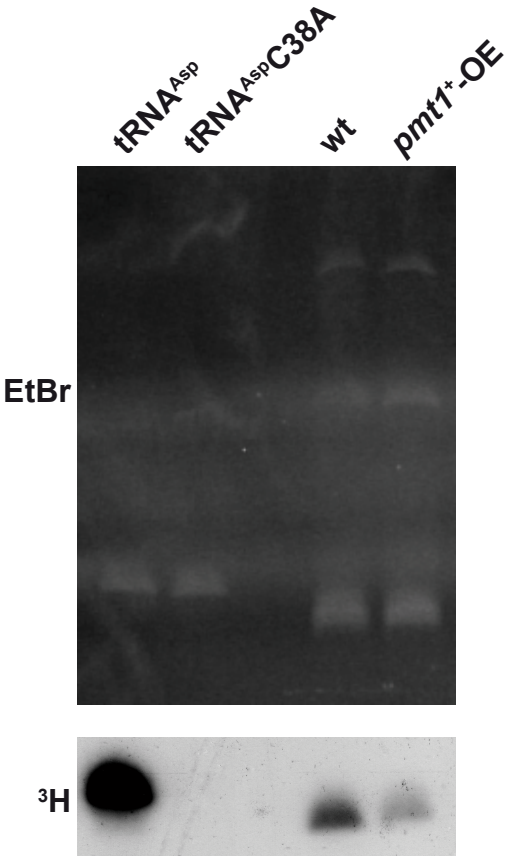

Figure 14: *In vivo* methylation upon *pmt1*$^{+}$-overexpression is confirmed by *in vitro* methylation. Total RNA extracts from wild type or *pmt1*$^{+}$-overexpression strain were incubated with 3 µM Pmt1. The samples were separated by urea-PAGE and methylation signals were detected by autoradiography. tRNA^{Asp} and tRNA^{Asp}C38A served as controls for the methylation reaction.

In agreement with the results from the bisulfite sequencing, we detected a strongly reduced methylation signal for the *pmt1*$^{+}$-overexpression strain compared to the wild-

type strain. The ethidiumbromide (EtBr) stained gel showed that similar amounts of total RNA were used in the *in vitro* methylation reaction (Figure 14). Since equal EtBr signals indicate equal RNA amounts in the samples, changes in the signal strength of the autoradiography indicate changes in the amount of methylated Pmt1 substrates. For this experiment, this suggested that in the *pmt1*$^{+}$-overexpression strain there is *in vivo* methylated RNA that subsequently is unavailable for methylation by the recombinant enzyme in the *in vitro* reaction. Although the observed methylation signal for the *pmt1*$^{+}$-overexpression strain was lower than in the wild-type strain, there was still a detectable signal left. This was surprising, because we found 100 % methylation of tRNA^{Asp} in the overexpression strain by RNA bisulfite sequencing, and it therefore indicated that there are other small RNAs besides tRNA^{Asp} in the total RNA extracts that can be methylated by recombinant Pmt1, but not by the overexpressed enzyme in the cells.

We knew from the previous experiments with the *in vitro* tRNA transcripts that Pmt1 is able to methylate substrates other than tRNA^{Asp}, although to a lesser extent. We therefore hypothesized that the residual signal in the overexpression strain resulted from the *in vitro* methylation of previously unmethylated tRNA^{Glu}. To test this hypothesis, we performed RNA bisulfite sequencing of RNA extracted from the *pmt1*$^{+}$-overexpression strain, and analyzed the methylation level of tRNA^{Glu}. We detected a methylation level of 25 % of the analyzed clones of tRNA^{Glu} (Figure 15). This showed that Pmt1 was able to methylate less favorable substrates *in vivo*, but to a lower level than the tRNA^{Asp} substrate.

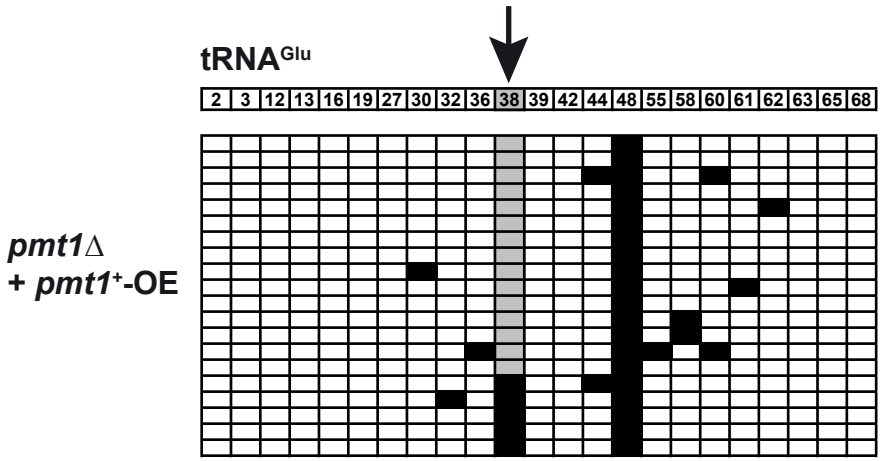

Figure 15: *In vivo* methylation of tRNA^{Glu} upon *pmt1*$^{+}$-overexpression
Bisulfite analysis of tRNA^{Glu} from *pmt1Δ* cells carrying a *pmt1*$^{+}$-overexpression plasmid. Each column represents a cytosine of tRNA^{Glu}, each line represents an individual clone. Methylated cytosines are indicated by black boxes, grey boxes mark unmethylated C38.

These data explained the residual signal in the *pmt1*$^{+}$-overexpression strain in the *in vitro* methylation assay. The recombinant enzyme in the *in vitro* reaction could methylate the residual 75 % of tRNA^{Glu} that was not methylated *in vivo*. Thus, at least a fraction, if not all, of the methylation signal detected after *in vitro* methylation of total RNA from the *pmt1*$^{+}$-overexpression strain could be explained by methylation of previously unmethylated tRNA^{Glu} by the recombinant enzyme.

We also sought to test the methylation status of all the other tRNAs of *S. pombe* that contain a cytosine at position 38 (Table 8). For this purpose, we performed RNA bisulfite sequencing for all of these tRNAs. We were unable to evaluate the data for the methylation in tRNA^{His}, tRNA^{Val}, tRNA^{Lys} and tRNA^{Leu} due to technical reasons (data not shown). The sequences that were cloned after the bisulfite treatment and the reverse transcription were incomplete. The region of interest, the anticodon loop, was missing in most of the analyzed clones. A possible explanation could be the extensive modification of many tRNAs that could interfere with the reverse transcription of the tRNAs.

5.5 *In vivo* tRNA methylation by Pmt1 was depended on nutrient conditions

The previous experiments on the methylation level of tRNA^{Asp} in the yeast cells indicated that tRNA methylation by Pmt1 was limiting under certain conditions, because we detected only approximately 25 % methylation of tRNA^{Asp} at position C38 in the wild-type strain. We hypothesized that nutrient conditions might limit Pmt1-dependent methylation of tRNA^{Asp} *in vivo*.

To test this hypothesis, we cultured wild-type and *pmt1Δ* cells in *S. pombe* complete medium (YES). In this medium, nutrient availability should not be limited. We performed bisulfite sequencing of RNA extracted from these cultures and analyzed tRNA^{Asp} methylation. Positions C48 and C49 were constitutively methylated, regardless of the presence of *pmt1*$^{+}$. This indicated that the bisulfite conversion did not affect methylated cytosines and verified the results that were found for the methylation at position C38. As expected, the *pmt1Δ*-strain showed no methylation at position C38 of tRNA^{Asp}. If limited nutrients would lead to limited Pmt1 activity, the tRNA methylation in a wild-type strain should increase in a complete medium. To our

surprise, the RNA extracted from wild-type cells also had no methylated cytosines at position C38 of $tRNA^{Asp}$ (Figure 16).

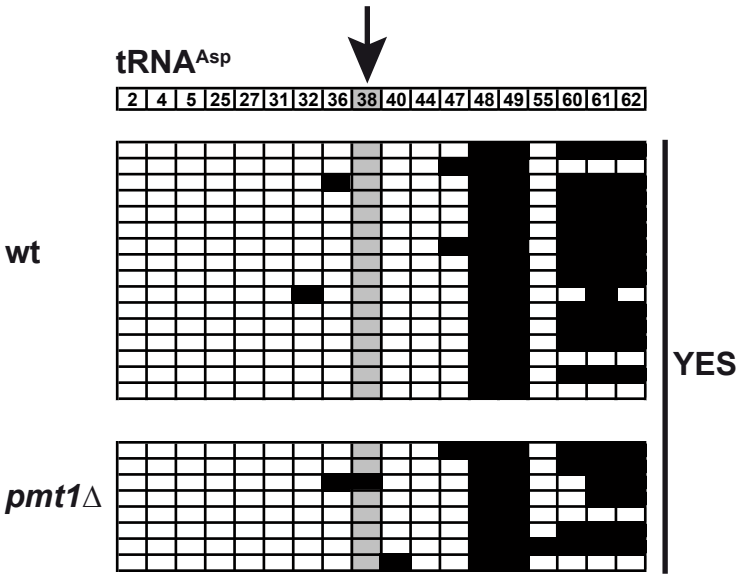

Figure 16: $tRNA^{Asp}$ is not methylated in cells cultured in *S. pombe* complete medium
Bisulfite analysis was performed for $tRNA^{Asp}$ from wild type or *pmt1Δ* cells cultured in YES medium. Each column represents a cytosine of $tRNA^{Asp}$, each line represents an individual clone. Methylated cytosines are indicated by black boxes, grey boxes mark unmethylated C38.

Serendipitously, preliminary experiments on RNA methylation in *S. pombe* cells in our laboratory were carried out on RNA that was extracted from cells cultured in complete medium from another yeast species, *Saccharomyces cerevisiae*. These experiments suggested that there was Pmt1-dependent tRNA methylation under these conditions. Thus, we cultured wild-type and *pmt1Δ* cells in *S. cerevisiae* complete medium YPD and analyzed RNA extracted from these cultures for $tRNA^{Asp}$ methylation using RNA bisulfite sequencing. The methylation at positions C48 and C49, which could be detected reliably, served as an internal control for the results found for the methylation at position C38. The *pmt1Δ*-strain displayed no $tRNA^{Asp}$ methylation at position C38, which was expected due to the absence of Pmt1. Surprisingly, we could detect almost 100 % of $tRNA^{Asp}$ methylation in the wild-type strain in this medium (Figure 17). The strong difference in $tRNA^{Asp}$ methylation between cells cultured in YES (*S. pombe* medium) or YPD (*S. cerevisiae* medium) could be attributed to changes in Pmt1 activity. Whether this alteration in Pmt1 activity was caused by altered $pmt1^{+}$ expression, remained to be investigated (see below). Furthermore, this result implied that one or more components of the YPD medium had a strong influence on Pmt1-dependent tRNA methylation. This medium differs from the *S. pombe* complete medium, although they both contain yeast extract

and glucose. The amount of each ingredient is different in both media. YPD also contains peptone, a component that causes slightly delayed growth of *S. pombe* cells.

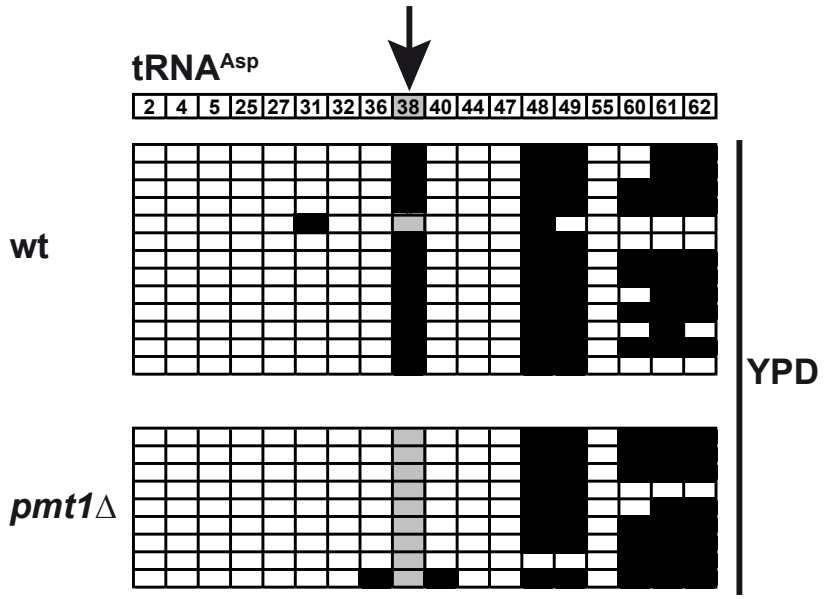

Figure 17: tRNA^{Asp} is methylated in cells cultured in *S. cerevisiae* complete medium
Bisulfite analysis was performed for tRNA^{Asp} from wild type or *pmt1Δ* cells cultured in YPD medium. Each column represents a cytosine of tRNA^{Asp}, each line represents an individual clone. Methylated cytosines are indicated by black boxes, grey boxes mark unmethylated C38.

In the experiment that showed complete tRNA^{Asp} methylation upon *pmt1*$^{+}$-overexpression in EMM medium, we also found tRNA^{Glu} to be methylated to about 25 % (Figure 15). This tRNA was also shown to be a Pmt1 target when recombinant Pmt1 methylated *in vitro* transcribed tRNA^{Glu} (Figure 12). Thus, we wanted to investigate, whether tRNA^{Glu} is also methylated when cells are cultured in YPD medium, because the high methylation level of tRNA^{Asp} indicates activity of Pmt1 under these conditions. We performed RNA bisulfite sequencing for tRNA^{Glu} using RNA extracted from wild-type cells cultured in YPD medium. Interestingly, we were unable to detect methylation of tRNA^{Glu} at position C38 (Figure 18). The methylation at position C48 verified the results we detected for the methylation of position C38. This result suggests a differential activity of Pmt1 under the different culture conditions, because despite the similar tRNA^{Asp} methylation in RNA extracted from cells cultured in YPD or with the *pmt1*$^{+}$-overexpression plasmid from EMM medium, the tRNA^{Glu} methylation level differed significantly in these two conditions.

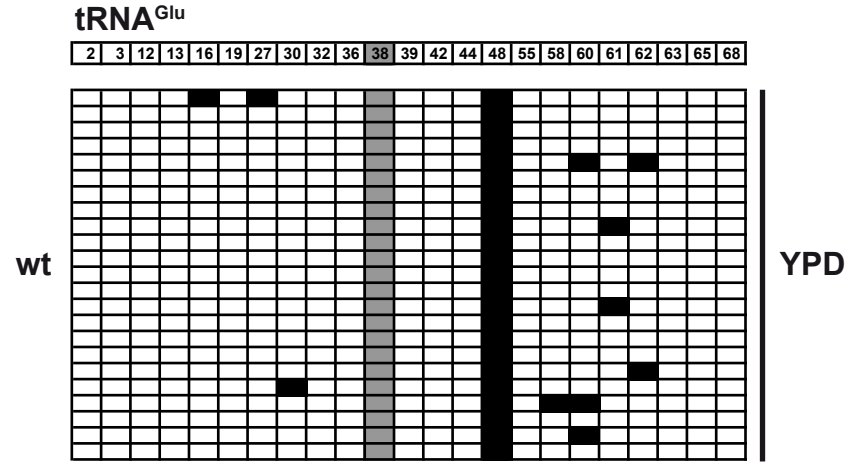

Figure 18: tRNAGlu is not methylated in *S. pombe* cells cultured in YPD.
Bisulfite analysis was performed for $tRNA^{Glu}$ from wild type cells cultured in YPD medium. Each column represents a cytosine of $tRNA^{Asp}$, each line represents an individual clone. Methylated cytosines are indicated by black boxes, grey boxes mark unmethylated C38.

We sought to verify all these results from the bisulfite sequencing using the *in vitro* methylation assay. We used recombinant Pmt1 to methylate RNA from wild-type and *pmt1Δ* cells that were cultured in *S. pombe* complete medium (YES) or *S. cerevisiae* complete medium (YPD). In agreement with the RNA bisulfite sequencing results, we found no difference in the methylation level between wild-type and *pmt1Δ* cells that were grown in YES medium (Figure 19). However, wild-type RNA that was extracted from cells cultured in YPD showed a decreased methylation signal compared to the deletion strain cultured in the same medium. This further supported the results from the bisulfite sequencing, where we found almost 100 % $tRNA^{Asp}$ methylation in the wild-type strain cultured in YPD. This led us to ask which component of the medium was responsible for tRNA methylation in YPD.

Table 9: Composition of YPD and YES medium

	YPD	YES
Supplements	none	250 mg/L
Glucose	2 %	3 %
Yeast extract	1 %	0,5 %
Peptone	2 %	none

A comparison of the composition of the two media (Table 9) showed that the amount of the components that were used in both media were variable. While both media

contained glucose and yeast extract, the amounts of both components differed. YES medium contained 3 % glucose and 0.5 % yeast extract, whereas YPD has 2 % glucose and 1 % yeast extract. Furthermore, YES medium is supplemented with adenine, leucine, histidine, lysine and uracil (250 mg/L each) and YPD contains 2 % peptone and has none of the defined supplements. To test which ingredient was responsible for the altering methylation levels of cellular RNA, we created media that had the amount of one component adapted to the respective other medium. This led us to a total amount of 10 different media, including the two standard media YES and YPD. We then analyzed RNA extracted from wild-type and *pmt1Δ* cells cultured in all of the resulting media in the methylation assay with recombinant Pmt1.

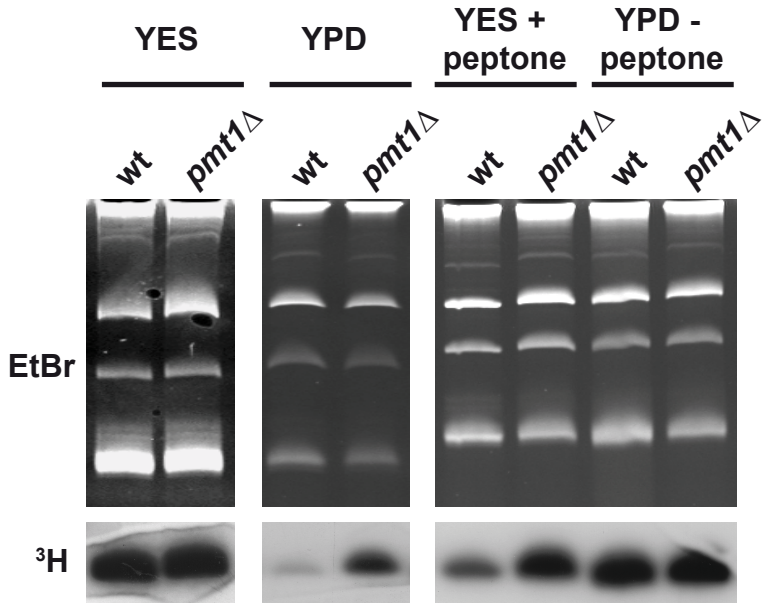

Figure 19: Peptone induces tRNA methylation.
Total RNA extracts from wild type and *pmt1Δ* cells, cultured in YES or YPD medium either with or without peptone, were analyzed using *in vitro* methylation by Pmt1 (3 µM). The samples were separated using urea-PAGE and methylation signals were detected by autoradiography.

We found that the level of tRNA methylation by Pmt1 was not affected by the amount of glucose, the percentage of yeast extract or the presence of supplements (data not shown). However, the addition of peptone to YES medium resulted in an increased *in vivo* methylation of tRNA, which was detected as a reduced methylation signal in the *in vitro* methylation assay (Figure 19). Accordingly, when peptone was omitted from YPD medium, the *in vivo* methylation of the wild type cells was reduced to the level of the *pmt1Δ* strain, as indicated by the strong methylation signal in the *in vitro* assay.
Peptone is a mixture of nutrients that is generated by peptic digestion of animal tissue. Therefore, it contains a broad variety of amino acids, peptides, salts and other

cellular components. It is used as a nitrogen source for the yeast cells, but the exact nitrogen source is not defined. Our results indicated that one or more components of peptone increase Pmt1 activity and induce *in vivo* tRNA methylation.

We hypothesized that perhaps the nitrogen in peptone was the factor activating Pmt1. Since complete media contain the undefined components yeast extract and peptone, we cannot alter the amount of nitrogen in these media without altering many other components. Individual media components can only be varied in completely defined media. For *S. pombe*, such a fully synthetic medium is the Edinburgh Minimal Medium (EMM). The only nitrogen source in this medium is ammonium chloride (NH_4Cl). To test our hypothesis, we therefore changed the normal 0.5 % NH_4Cl to 0 % and to 2.5 %. If Pmt1 was activated by increasing amounts of nitrogen, the tRNA methylation should increase with increasing amounts of NH_4Cl.

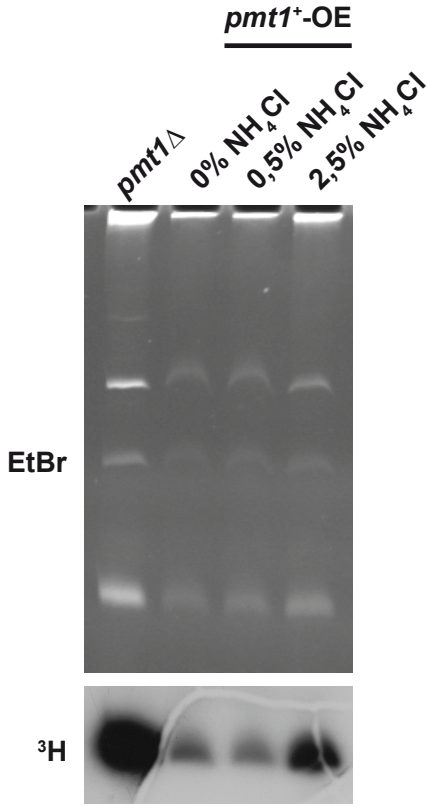

Figure 20: tRNA methylation is inhibited by ammonium chloride
RNA was extracted from *pmt1Δ* cells carrying a control vector or a *pmt1*$^+$-overexpression vector cultured in minimal medium containing varying amounts of NH_4Cl (0%, 0.5% and 2.5%). The RNA was used for *in vitro* methylation by Pmt1. The samples were separated using urea-PAGE and methylation signals were detected by autoradiography.

To test this, we cultured a pmt1Δ strain carrying a control vector or a *pmt1*$^+$-overexpression vector in the media containing the different amounts of NH_4Cl. RNA extracted from these cultures was then analyzed by *in vitro* methylation. Pmt1

activation and subsequent tRNA methylation by increased amounts of ammonium chloride would be indicated by a decreased methylation signal for the RNA extracted from cells grown in 2.5 % NH_4Cl. Contrary to our expectations, the *in vitro* methylation signal increased with increasing amounts of ammonium chloride (Figure 20). Unfortunately, the RNA extracted from cells that were cultured in medium containing 0 % NH_4Cl had a very low concentration and despite the equalization of the used amounts of RNA the EtBr staining showed a significantly lower amount of RNA for this sample. However, the results for the samples from cells cultured in 0.5 % and 2.5 % NH_4Cl indicated that *in vivo* tRNA methylation was reduced upon increasing NH_4Cl in the medium. Reduced tRNA methylation would originate from a reduced activity of Pmt1.

5.6 tRNA methylation by Pmt1 depended on the kinase Sck2

To gain further insight into the nutrient dependence of the tRNA methylation by Pmt1, we hypothesized that the TOR signaling pathway might be involved in activating Pmt1 upon changes in nutrient availability. The mammalian TOR pathway is well known to sense the nutritional status of cells. By phosphorylation of various target proteins, like the serine/threonine kinase S6K that phosphorylates the ribosomal protein S6, the mTOR complex 1 (mTORC1) signals to global mRNA translation, ribosome synthesis, autophagy and aging mechanisms (Sharp and Richardson 2011). These mechanisms help the cells to adapt to dietary restriction and are involved in the regulation of lifespan and healthspan.

In *S. pombe*, there are two homologs of TOR annotated in the genome, *tor1*$^+$ and *tor2*$^+$. *Tor2*$^+$ is an essential gene that is required for normal growth (Kim et al. 2010), whereas *tor1*$^+$ is required only during cell proliferation under stress conditions and for sexual differentiation under nitrogen starvation (Weisman and Choder 2001). Fission yeast also carries a homolog of the S6 kinase called Sck2. Sck2 is a non-essential gene that is involved in the regulation of life span, since *sck2Δ* cells display an elongated lifespan (Roux et al. 2006). The same extended lifespan has been demonstrated for *pka1Δ* cells. Pka1 is a kinase that is involved in the glucose-sensing pathway of *S. pombe* (Byrne and Hoffman 1993).

In a first approach, we investigated the two downstream effector kinases Sck2 (probably downstream of TOR) and Pka1 (downstream of the glucose receptor Git3).

To test whether any of these two kinases are responsible for the activation of Pmt1, we tested whether the deletion of *sck2*$^{+}$ or *pka1*$^{+}$ had an influence on the tRNA methylation level. We first hypothesized that RNA methylation by Pmt1 might be inhibited by one of the nutrient sensing pathways in *S. pombe* standard complete medium (YES). If those pathways would signal a sufficient nutritional status that does not require tRNA methylation, then the tRNA methylation should increase upon deletion of the factor transducing the signal. This would mean that the nutrient signaling pathways under abundant nutrient condition would inhibit Pmt1 activity. This would result in increased Pmt1-dependent RNA methylation when the signaling pathways were interrupted. As a result, the methylation signal after the *in vitro* methylation reaction should be reduced. To test this hypothesis, we used RNA extracted from *pka1Δ* and *sck2Δ* strains that were cultured in *S. pombe* complete medium for *in vitro* methylation by Pmt1. However, we found no change in the methylation level upon deletion of either *pka1*$^{+}$ or *sck2*$^{+}$ (Figure 21). The detected methylation signals were as strong in the two deletion strains as in the wild type, which suggests that there was no Pmt1-dependent RNA methylation in the *pka1Δ* and the *sck2Δ* strain.

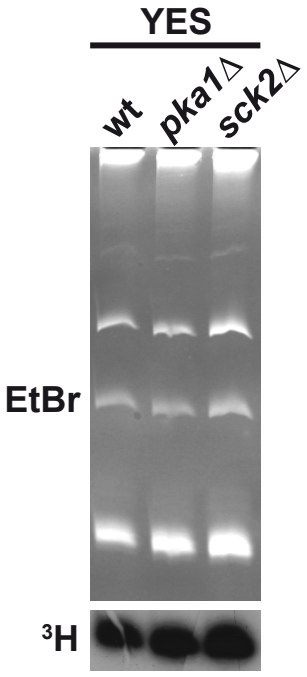

Figure 21: tRNA methylation in YES medium is not affected by deletion of *pka1*$^{+}$ or *sck2*$^{+}$.
RNA was extracted from wild type, *pka1Δ* or *sck2Δ* cells cultured in *S. pombe* complete medium YES. The RNA was subjected to *in vitro* methylation by Pmt1. The samples were separated using urea-PAGE and methylation signals were detected by autoradiography.

Next, we asked whether those nutrient-sensing pathways might activate Pmt1 in YPD medium, which was opposite to our first hyposthesis. Therefore, we performed *in vitro* methylation analysis of RNA extracted from *sck2Δ*, *tor1Δ* (Figure 22A) and *pka1Δ* (Figure 22B) cells that were cultured in YPD medium. A strain deleted for *sck1*$^{+}$, a kinase unrelated to TOR signaling or the glucose-sensing pathway, was used to compare the effect on different signaling pathways. In YPD medium, tRNA^{Asp} is methylated (see above) and an inhibition of Pmt1 should result in reduced methylation levels *in vivo*. This can be detected by observing increased *in vitro* methylation by recombinant Pmt1. The data show weak methylation signals for RNA from *sck1Δ*, *tor1Δ* (Figure 22A) and *pka1Δ* (Figure 22B), which suggested high *in vivo* methylation in these strains, as is also the case in the wild type cells. Therefore, this indicated that those deletions had no effect on tRNA methylation. In contrast, in cells deleted for *sck2*$^{+}$, the *in vivo* methylation was reduced, as indicated by the increased *in vitro* methylation signal (Figure 22A). This suggested that Sck2 is at least partially required for Pmt1-dependent RNA methylation in YPD medium and led us to the assumption that Sck2 either directly or indirectly activated Pmt1.

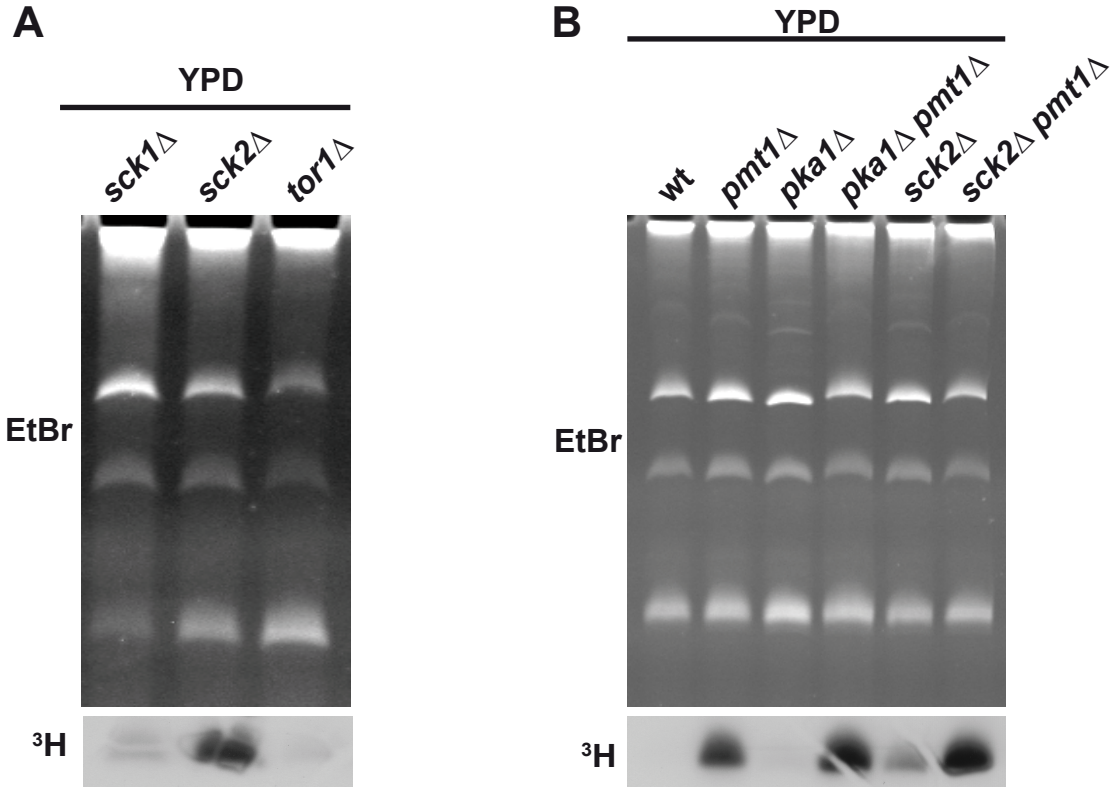

Figure 22: tRNA methylation by Pmt1 is activated by *sck2*$^{+}$.
(A) Total RNA extracts from *sck1Δ*, *sck2Δ* or *tor1Δ* cells cultured in *S. cerevisiae* complete medium YPD were used for *in vitro* methylation by Pmt1. The samples were separated using urea-PAGE and methylation signals were detected by autoradiography. (B) Total RNA extracts from *pka1Δ* or *sck2Δ* cells or double deletions of those genes with pmt1Δ, cultured in *S. cerevisiae* complete medium YPD, were analyzed using *in vitro* methylation by Pmt1. The samples were separated using urea-PAGE and methylation signals were detected by autoradiography.

When *pmt1*$^+$ was additionally deleted in the *pka1Δ* or *sck2Δ* background, the *in vitro* methylation signal was increased. This further validates the dependency of the RNA methylation on *pmt1*$^+$. The *in vivo* methylation level in the *sck2Δ* single deletion is reduced compared to wild type cells, but it is not as low as in an *sck2Δ pmt1Δ* double deletion strain. These results support an involvement of Sck2 in the regulation of Pmt1-dependent tRNA methylation.

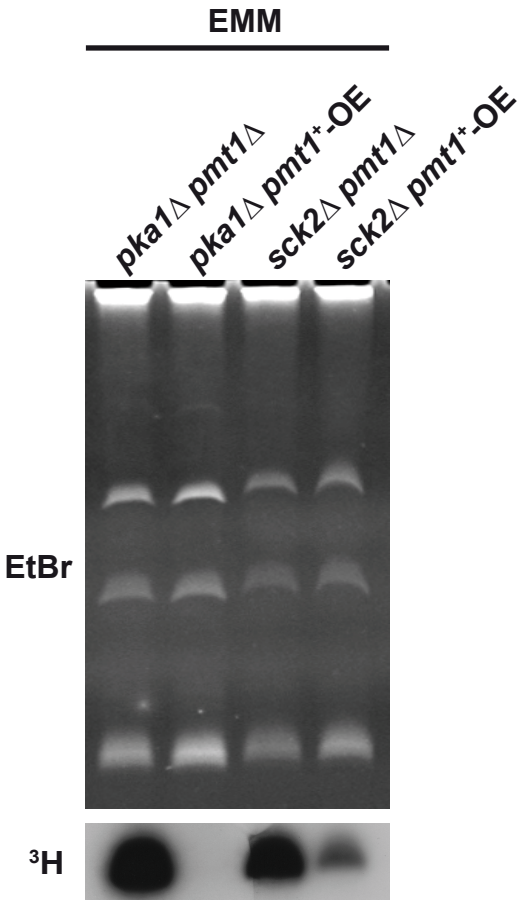

Figure 23: Deletion of *sck2*$^+$ inhibits Pmt1 activity upon *pmt1*$^+$-overexpression.
Total RNA extracts from *pka1Δ pmt1Δ* or *sck2Δ pmt1Δ* cells containing either a control vector or a *pmt1*$^+$-overexpression vector, cultured in *S. cerevisiae* complete medium YPD, were used for *in vitro* methylation by Pmt1. The samples were separated using urea-PAGE and methylation signals were detected by autoradiography.

We also investigated the effect of the deletion of *pka1*$^+$ and *sck2*$^+$ in a situation with increased Pmt1 levels. Therefore, we cultured *pka1Δ pmt1Δ* and *sck2Δ pmt1Δ* cells containing either a control vector or a *pmt1*$^+$-overexpression vector in *S. pombe* minimal medium EMM. RNA extracted from these cells was methylated in the *in vitro* methylation assay. As expected, both double deletions gave strong methylation signals, indicating no *in vivo* methylation (Figure 23). In the *sck2Δ pmt1Δ* strain, an *in vitro* methylation signal was still detectable upon *pmt1*$^+$-overexpression. When *pmt1*$^+$ was overexpressed in the *pka1Δ pmt1Δ* strain, the *in vitro* methylation signal was

almost undetectable. As in the wild-type, this suggested complete $tRNA^{Asp}$ methylation upon *pmt1*$^+$-overexpression. These results indicated that Sck2 was required for full Pmt1 activity, even upon elevated Pmt1 levels. The increased amount of Pmt1 protein could not compensate for the reduced activity that was dependent on *sck2*$^+$. Furthermore, this result supported the assumptions drawn from the results obtained from *sck2Δ* cells cultured in YPD medium. Even upon overexpression of *pmt1*$^+$, there was a detectable signal after the *in vitro* methylation reaction. This could be explained by incomplete methylation of Pmt1 substrates *in vivo*. This supports the hypothesis that Pmt1 activity is inhibited upon *sck2*$^+$ deletion.

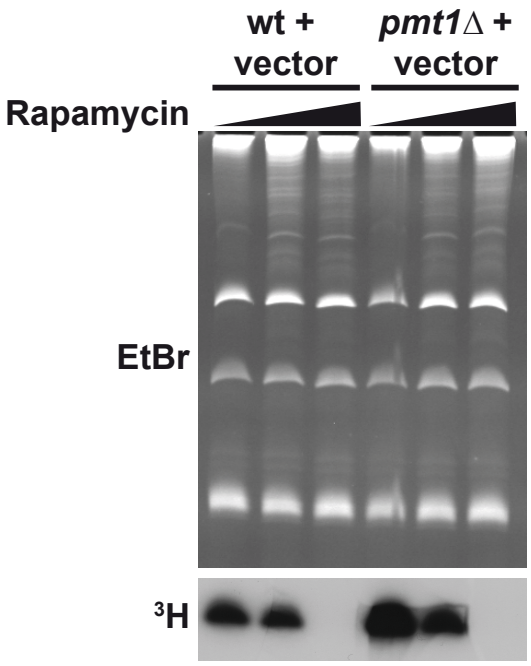

Figure 24: Rapamycin treatment causes loss of methylation signal.
Total RNA extracts from wild type or *pmt1Δ* cells containing a control vector, cultured in *S. pombe* minimal medium EMM, were used for in vitro methylation. The cells were treated with 0 nM, 200 nM or 400 nM rapamycin. The samples were separated using urea-PAGE and methylation signals were detected by autoradiography.

Next, we asked whether the TOR (target of rapamycin) signaling pathway could be involved in the regulation of Pmt1, although the deletion of *tor1*$^+$ had no effect on Pmt1-dependent tRNA methylation. Since there are two homologs of TOR present in *S. pombe*, we hypothesized that maybe Tor2 signals to Sck2. To investigate the effect of Tor2 on Pmt1-dependent RNA methylation, we could not use a *tor2Δ* strain, because the deletion of *tor2*$^+$ is lethal for fission yeast cells (Kim et al. 2010), and we do not have a *tor2* mutant allele at our disposal. Therefore, we sought to inhibit TOR signaling using rapamycin. Thus, we treated wild-type cells and as a control also

pmt1Δ cells with increasing amounts of rapamycin. The RNA isolated from these cells was then used for *in vitro* methylation. Significantly, we observed a decreasing methylation signal for the wild-type cells with increasing amounts of rapamycin (Figure 24), which was opposing to our expectations and indicated that TOR inhibition increased *in vivo* RNA methylation by Pmt1. We also treated *pmt1Δ* cells with rapamycin, and surprisingly we also observed a decrease in the methylation signal upon rapamycin treatment, which is counterintuitive, because it would indicate increased *in vivo* methylation in the absence of Pmt1. This indicated that the observed reduction of the methylation signal in the wild type could not be attributed to increased *in vivo* tRNA methylation caused by elevated Pmt1 activity. A decrease of the *in vitro* methylation signal in the *pmt1Δ* strain could be explained in three ways. The first one would be that another methyltransferase upon rapamycin treatment would methylate *in vivo* the targets of the recombinant enzyme. The second explanation is the degradation of the unmethylated Pmt1 substrates upon treatment with rapamycin. The third reason could be reduced tRNA transcription upon rapamycin treatment (see discussion).

5.7 Pmt1 influenced the chronological lifespan of yeast cells

Factors involved in nutrient sensing are known to have an influence on the maximal lifespan in yeast cells (Kaeberlein 2010). Impaired TOR signaling leads to an increased lifespan in *S. cerevisiae* (Fontana et al. 2010). Studies in *S. pombe* imply a similar lifespan regulation in the fission yeast. Reduced TOR signaling can be achieved either by addition of rapamycin to the yeast cultures or by deletion of downstream targets of the TOR complex. Accordingly, *sck2Δ* cells have been shown to display an elongated lifespan (Roux et al. 2006; Chen and Runge 2009), as is the case for the *S. cerevisiae* homolog of Sck2, Sch9 (Fabrizio et al. 2001). This, together with our observation of reduced tRNA methylation in *sck2Δ* cells, raised the question whether *pmt1*$^{+}$, and therefore also tRNA methylation, are involved in the regulation of lifespan in *S. pombe* cells.

Therefore, we investigated the influence of *pmt1*$^{+}$ on chronological lifespan of *S. pombe* cells. If the lifespan extension of *sck2Δ* cells was at least partially mediated by impaired activation of Pmt1, we would expect *pmt1Δ* cells to have an elongated lifespan compared to wild-type cells. To test this hypothesis, we cultured wild-type

and *pmt1Δ* cells carrying either a control vector or a *pmt1*$^{+}$-overexpression vector in minimal medium. The viability of the cells was measured using the CFU (colony forming units) method. At regular intervals, samples from the aged cultures were plated onto full medium plates, and the number of cells that were able to form colonies was counted after 3 days of incubation at 30 °C.

As a result, we found *pmt1Δ* cells to display an elongated lifespan compared to strains containing the *pmt1*$^{+}$ gene, independent of the gene's expression level (Figure 25). This indicated that Pmt1-dependent tRNA methylation decreased chronological lifespan of the fission yeast cells. Interestingly, we found no significant difference between cells with 100 % tRNA^{Asp} methylation (wt or *pmt1Δ* + *pmt1*$^{+}$-OE) and cells with only about 25 % tRNA^{Asp} methylation (wt + control vector). Taken together, these results suggest that tRNA methylation via Pmt1 shortens chronological lifespan in *S. pombe* and that this pathway might be one component of *sck2Δ*-induced lifespan extension.

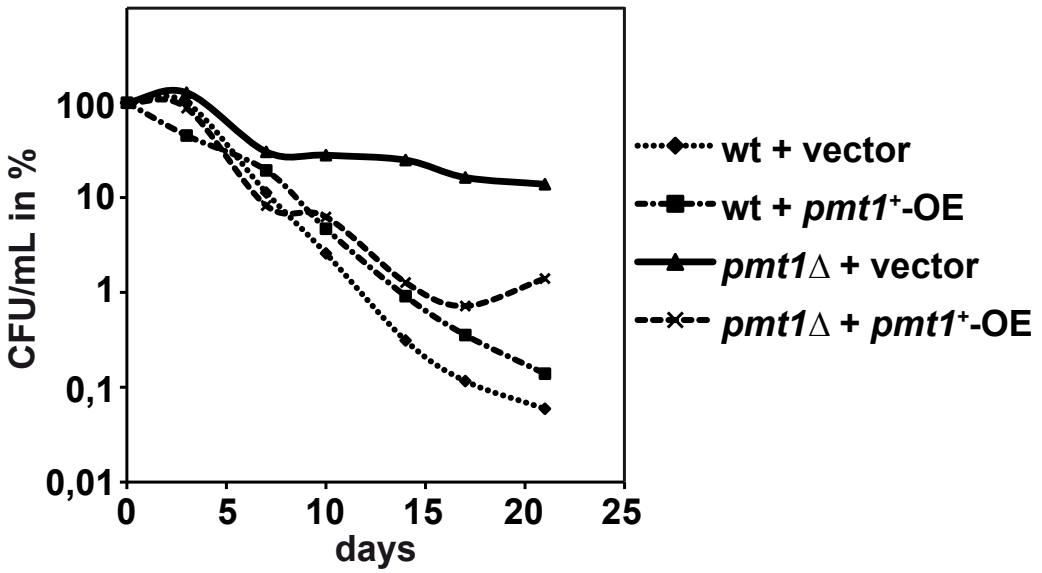

Figure 25: Deletion of *pmt1*$^{+}$ increases chronological lifespan in *S. pombe* cells in EMM.
Wild type and pmt1Δ cells carrying either a control vector or a *pmt1*$^{+}$-overexpression vector were cultured in *S. pombe* minimal medium EMM for several weeks. Viability of the yeast cells was measured by counting colony-forming units at regular intervals.

A change of the culture medium could have strong impact on tRNA methylation levels, as was seen in the RNA bisulfite and *in vitro* methylation experiments. Therefore we asked, whether a change of the medium also had an effect on the lifespan of the yeast cells. We cultured wild-type and *pmt1Δ* cells in YPD medium and measured cell viability using the CFU method. We showed previously that tRNA^{Asp} was methylated to almost 100 % in this medium, which is the same amount

of $tRNA^{Asp}$ methylation as in EMM medium upon *pmt1*$^+$-overexpression. This meant that the tRNA methylation levels were comparable with the previous aging experiment. Thus, we expected the wild-type cells to age more rapidly than the *pmt1Δ* cells. However, the data revealed an increased lifespan of the wild-type compared to the *pmt1Δ* strain in YPD medium (Figure 26A). We also performed a chronological lifespan experiment and did not count colony-forming units, but instead plated serial dilutions of the aged cultures onto full medium plates. The result of this second aging experiment was comparable to the previous one. The wild-type cultures contained more living cells after prolonged incubation than the *pmt1Δ* cultures (Figure 26B). The reason why this result seemed to be contrary to the results obtained in minimal medium remained enigmatic (see discussion).

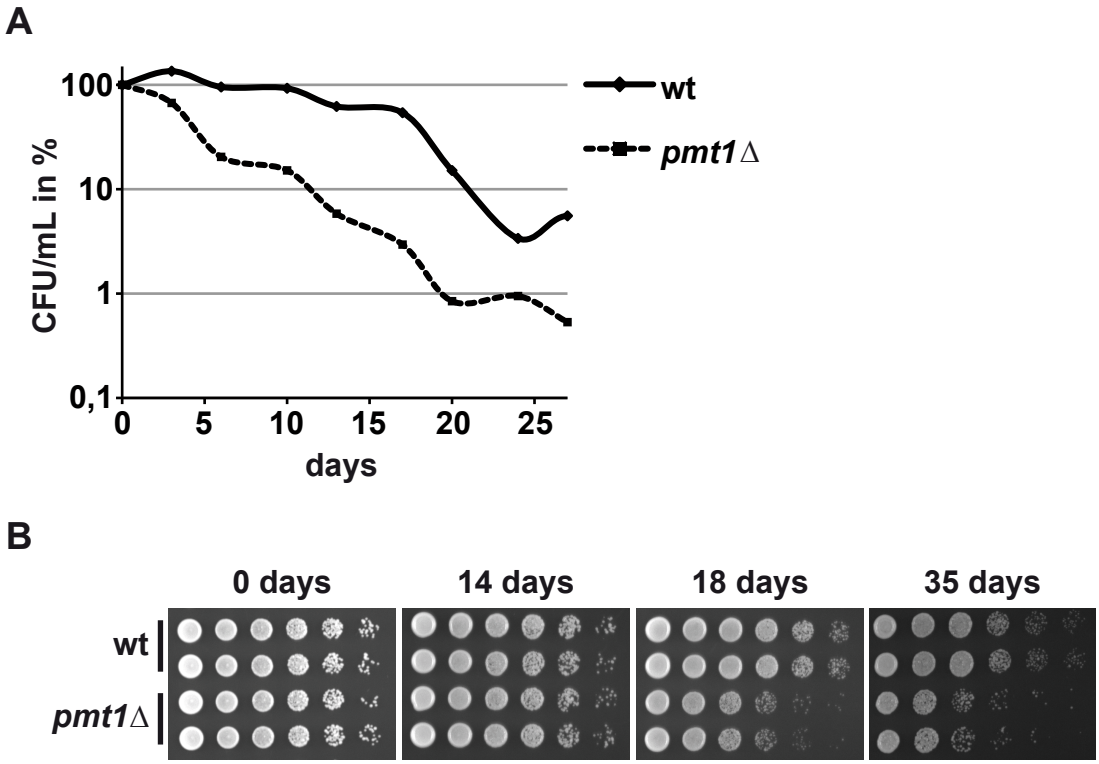

Figure 26: Deletion of *pmt1*$^+$ decreases chronological lifespan of *S. pombe* cultured in YPD.
Wild type and *pmt1Δ* cells were cultured in *S. cerevisiae* complete medium YPD for several weeks. Viability of the yeast cells was measured by counting colony forming units (A) or by plating serial dilutions onto full medium plates (B) at regular intervals.

5.8 The expression of *pmt1*$^+$ was independent of the culture medium

In our previous experiments, we observed strong differences in Pmt1-dependent tRNA methylation and concluded that Pmt1 activity was altered under the different

conditions. Besides inhibition or activation of the catalytic activity of the enzyme, increasing or decreasing protein levels could be a potential cause for variations in Pmt1 activity. Therefore, we analyzed gene expression and protein level to gain insight into the abundance of Pmt1.

To measure the expression of *pmt1*$^+$ on mRNA level, we used RT-PCR followed by qPCR. In this experiment, we wanted to investigate the differential expression of *pmt1*$^+$ when it was transcribed either from an overexpression vector containing the *nmt1*-promoter, from a vector containing the endogenous *pmt1*-promoter or from the genomic locus. Furthermore, we asked whether the endogenous expression of *pmt1*$^+$ was altered when the yeast cells were cultured in YES or YPD medium.

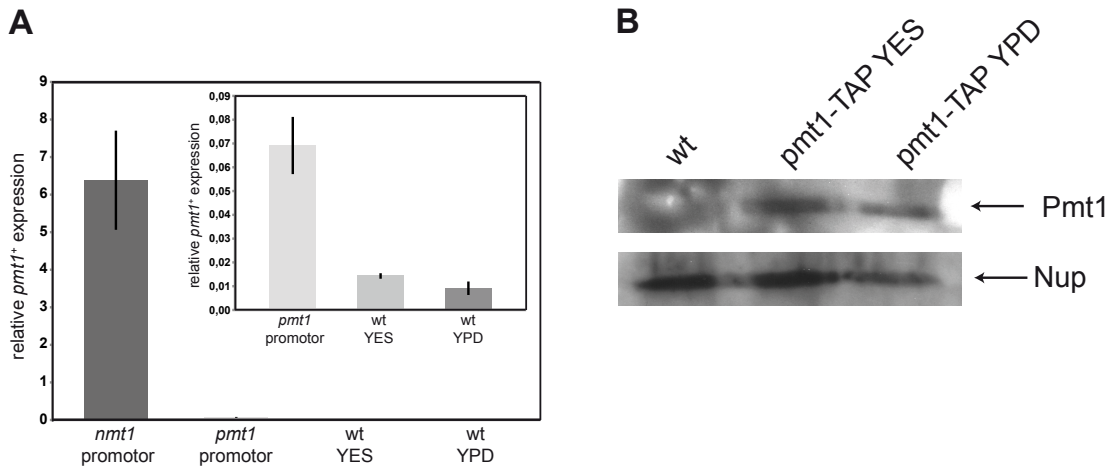

Figure 27: Levels of *pmt1*$^+$ upon expression from its native promoter or the *nmt1* promoter
(A) *pmt1*$^+$ expression relative to *act1*$^+$ was measured by quantitative RT-PCR. RNA was extracted from a *pmt1*Δ strain carrying either *pmt1*$^+$ expressed from the *nmt1* promoter (pAE1890) or from the native *pmt1* promoter (pAE1891). Furthermore, RNA was extracted from a wild-type strain (wt, AEP1) grown either in YES or in YPD medium. The inset graph shows the same data as in the large graph, but on a different scale and without expression from the *nmt1* promoter, for better representation of the low expression range. The experiment was performed by and the figure is courtesy of Karolin Nicklasch. (B) Pmt1 protein levels were indistinguishable in YES and YPD medium. TAP-tagged Pmt1 (AEP10) was detected using PAP antibody (peroxidase anti-peroxidase, Sigma). Nuclear pore complex protein (Nup) served as a loading control and was detected using Mab414 antibody (Covance).

We observed a 100-fold increase of the *pmt1*$^+$ mRNA level when the gene was expressed from a vector with the *nmt1* promoter compared to expression from a vector with the endogenous promoter (Figure 27A). The expression from the vector with the endogenous promoter was still 10-fold higher than the genomic expression. Significantly, the genomic expression level of *pmt1*$^+$ was not altered between the two different complete media YES and YPD. From this experiment, we concluded that the increased tRNA methylation levels in cells carrying the *pmt1*$^+$-overexpression vector

compared to cells expressing genomic *pmt1*$^+$ in the same medium could be attributed to the strongly increased levels of *pmt1*$^+$ expression. Combined with our observations on tRNA methylation levels, these results indicate that even the low amounts of genomically expressed *pmt1*$^+$ are sufficient to methylate $tRNA^{Asp}$ to 100% (wt in YPD, Figure 17) or at least partially (wt + control vector in EMM, Figure 13) in cells that do not carry a copy of *pmt1*$^+$ on a plasmid.

Because the observed *pmt1*$^+$ mRNA levels were very low, we next asked whether the protein level of Pmt1 was detectable and whether it was altered in the two different complete media. Therefore, we sought to investigate, if we could detect protein levels in the yeast cells that expressed *pmt1*$^+$ from the genomic locus by immunoblotting. Western blot analysis of genomically expressed TAP-tagged Pmt1 revealed a detectable amount of protein in the extracts from cells cultured in YES medium (Figure 27B). Significantly, the protein level was not altered when the cells were cultured in YPD medium. The protein level of nuclear pore complex proteins served as a loading control. These results indicated that the differences in the Pmt1-dependent tRNA methylation in YES and YPD medium were not caused by an increase in the amount of Pmt1 protein upon growth in YPD medium.

5.9 Overexpressed Pmt1 localized to the cytoplasm and the nucleus

To determine the subcellular localization of Pmt1, we wanted to visualize the protein using the green-fluorescent protein (GFP) tag. In a first approach, we integrated a GFP tag into the genomic *pmt1*$^+$ locus. The cells were cultured in YES or YPD medium and the protein localization was analyzed by fluorescence microscopy. As a result, we were unable to detect the localization of Pmt1 using GFP-tagged genomic Pmt1 (data not shown). The autofluorescence of the *S. pombe* cells was more prominent than a possible specific GFP signal. Taking into account the low expression level that we determined previously (see above), this could be explained by the low amount of protein in the cells.

To increase the amount of protein within the yeast cells, we created an overexpression vector containing the intron-less *pmt1*$^+$ sequence under the control of the *nmt1*-promoter in front of a GFP tag. The tagged protein was expressed in the *S. pombe* cells and visualized using fluorescence microscopy (Figure 28). The

overexpressed gene product Pmt1-GFP could be detected in the whole cell, in the nucleus as well as in the cytoplasm. This observation was in agreement with previous findings (Matsuyama et al. 2006) and was also consistent with a tRNA methyltransferase activity of Pmt1.

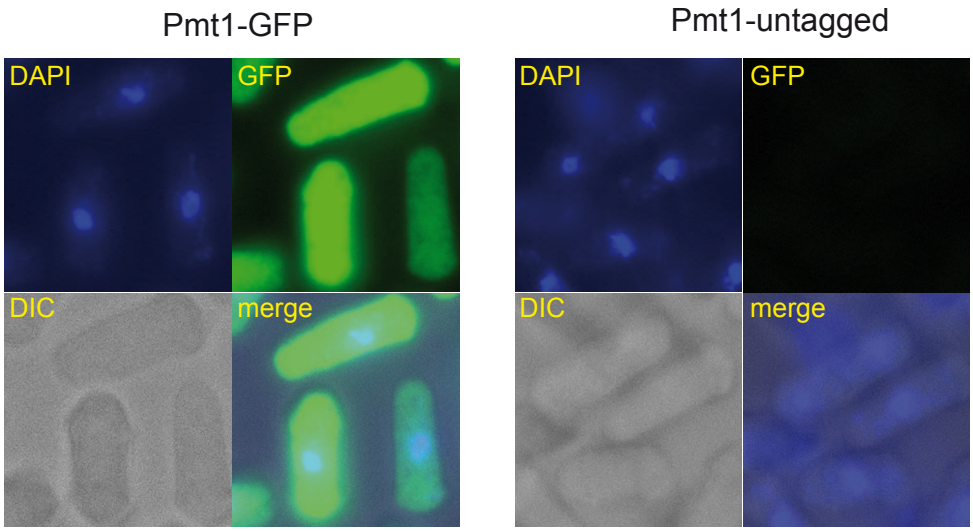

Figure 28: Localization of GFP-tagged Pmt1
Pmt1-GFP was expressed from the overexpression vector pSGP572a-pmt1 in *S. pombe* cells cultured in minimal medium (EMM) and the protein was visualized using fluorescence microscopy. Cells expressing Pmt1 from the overexpression vector REP4X-pmt1 served as a negative control (Pmt1-untagged).

5.10 Endogenous Pmt1 was purified without associated factors

The previous experiment demonstrated that the amount of Pmt1 protein was not altered in YES and YPD medium, yet the activity of Pmt1 varied significantly, because we detected 0 % $tRNA^{Asp}$ methylation in a wild-type strain cultured in YES medium and 100 % methylation when this strain was cultured in YPD medium. We hypothesized that Pmt1 might work in a complex with other proteins and might be regulated in this context. To test this hypothesis, we sought to purify a putative Pmt1-containing complex from *S. pombe* cells.

An established method to purify endogenous protein from yeast cells is the Tandem-Affinity Purification (TAP (Rigaut et al. 1999)). The native conditions of this purification method allow for copurification of associated proteins that subsequently can be identified using mass spectrometry. The TAP method was therefore used to purify TAP-tagged Pmt1 from *S. pombe* cells cultured in YES medium. We successfully purified Pmt1 by the TAP purification, but the amount of purified protein

was comparatively low, since CBP-tagged Pmt1 was only detectable using silver staining to visualize Pmt1 at the expected size of approximately 43 kDa (Figure 29). There were no obvious additional prominent bands in the Pmt1 purification. All bands other than Pmt1-CBP were also present in a parallel purification using a strain lacking Pmt1-TAP. This result suggested that either the amount of associated factors was below the detection limit, that Pmt1 may not be a member of a large protein complex, or that interactions with other proteins may be temporary. Considering the different activity of Pmt1 in the different complete media, it would also be possible that a complex formation was inhibited in YES medium.

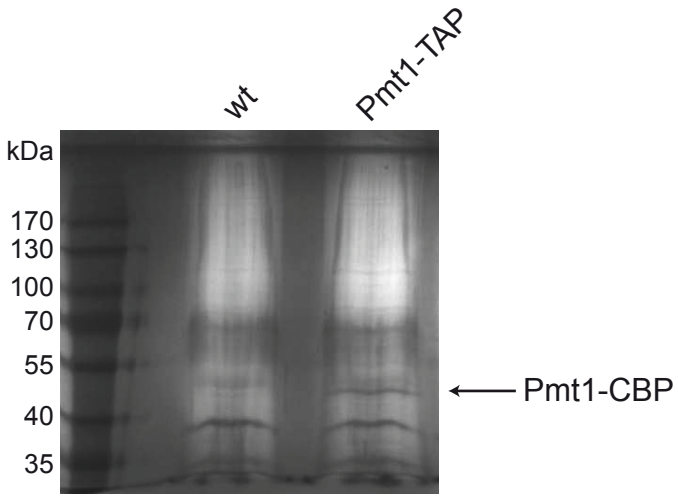

Figure 29: Tandem-Affinity-Purification of Pmt1
TAP-tagged Pmt1 was purified from *S. pombe* cells (AEP10). The eluate from a purification from a 6L culture in YES medium was separated by SDS-PAGE and silver stained. A protein band that migrated at approximately 43 kDa was identified as Pmt1-CBP, because it was not present in the wild type strain.

5.11 A synthetic genetic array to identify factors that are synthetically lethal with *pmt1Δ*

Synthetic lethality is a form of negative genetic interaction that occurs if two genes are deleted or mutated that work in parallel pathways. If only one of the two genes is deleted, the cells are viable, since the parallel pathway compensates the effect of the missing gene product. If the second gene additionally is deleted, the cells become sick or are not even viable at all. Since little is known about the function of Pmt1 in *S. pombe*, we reasoned that we could use a synthetic lethality screen to identify factors that function in a pathway parallel to Pmt1.

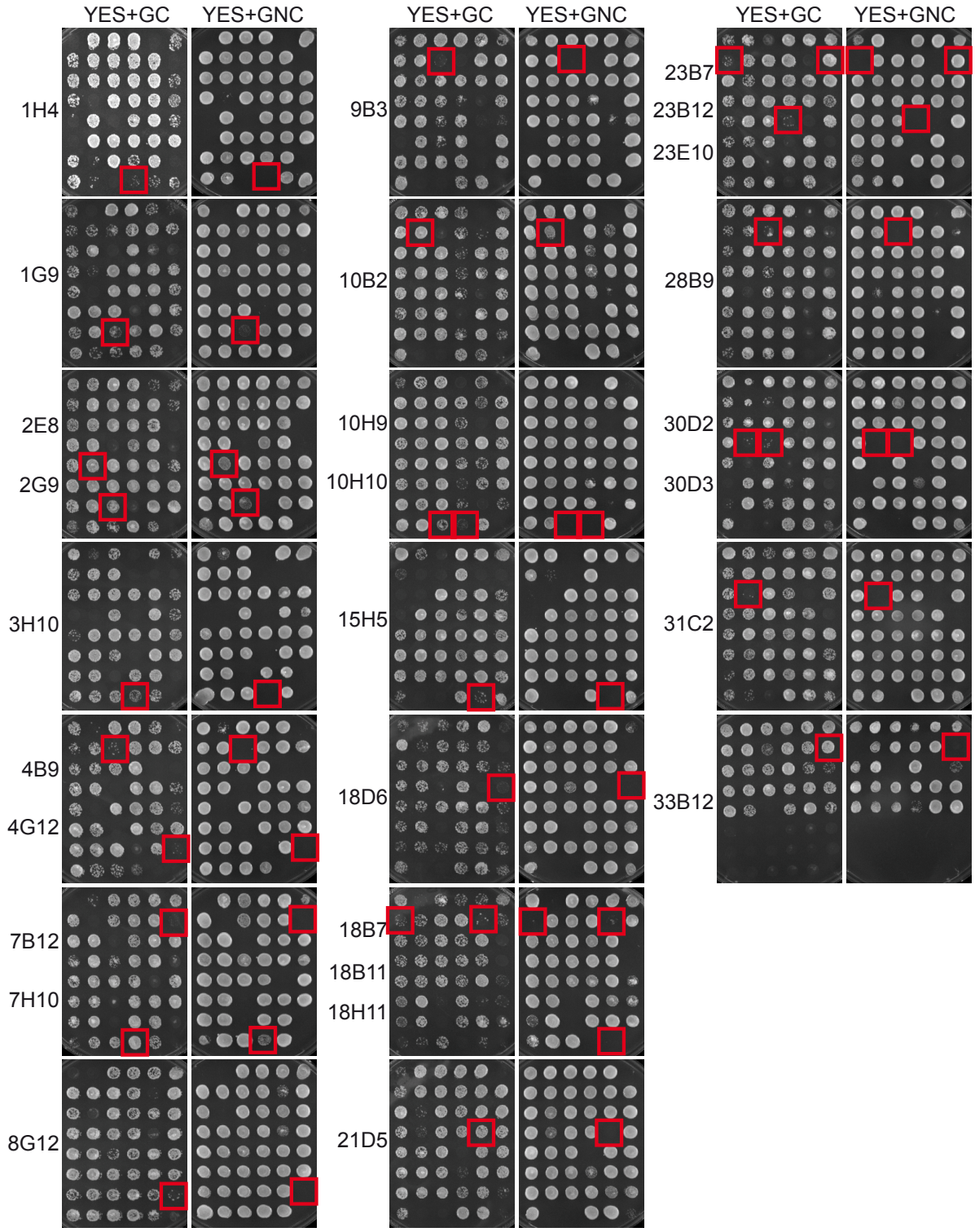

Figure 30: The synthetic genetic array identified candidate genes for synthetic genetic interactions
A *pmt1Δ* strain (AEP37) was crossed with strains from a deletion library on SPAS medium. Selection for haploid single mutants on YES+GC medium and subsequent selection for haploid double mutants on YES+GNC medium identified genes that affect cell growth only upon *pmt1*$^{+}$-deletion. The figure shows the selection plates of candidate genes. Each spot on the plates represents an individual cross. The first number of each label represents the number of the 96 well plate of the deletion library that was used for the cross. The capital letter gives the lane and the second number gives the column on that 96-well plate that identifies the candidate gene.

Among others, one way to identify synthetic lethal interactions is a synthetic genetic array (SGA). A synthetic genetic array is based on a library of deletions of all nonessential genes in an organism, in this case *S. pombe*. In this assay, a *pmt1Δ* strain was crossed with every strain from the deletion library. The selection procedure of the assay allowed us in a first step to isolate haploid cells with the deletion from the library, and in a second step, to isolate double mutants that carried both the deletion from the library and the *pmt1*$^{+}$ deletion. If there were sporulation products with the deletion from the library, but no viable double deletions, then we would have identified a gene that is probably synthetic lethal with the *pmt1*$^{+}$ deletion.

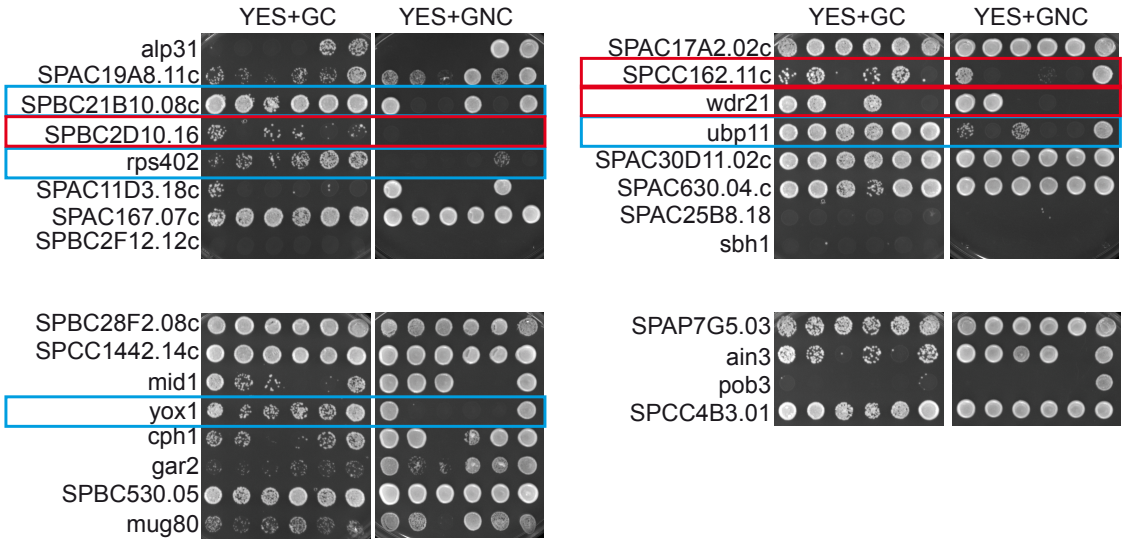

Figure 31: Validation of primary candidates identifies 3 secondary candidates
The procedure of the SGA was repeated with the primary candidate genes. The figure shows the selection plates of candidate genes. The spots in each lane of the plates represent independent crosses of the same candidate deletion with the *pmt1Δ* strain. The lanes are labeled with the name of the deleted gene according to the Bioneer Deletion Library Version 2.0. Boxes mark genes that show a reduced growth on YES+GNC compared to YES+GC. The boxes are color-coded: blue = genes linked to *pmt1*$^{+}$, red = secondary candidates.

We screened the Bioneer Deletion Library, which includes approximately 3000 gene deletions for deletions that are lethal in combination with *pmt1Δ*. The selection procedure was performed according to the established protocol (see material and methods). We were thus able to identify 28 primary candidate gene deletions (Figure 30). To validate the candidates from the initial screen, we repeated the screening procedure with these candidate gene deletions. In this experiment, we performed the selection procedure for each candidate six times in parallel. Seven of the initial 28 candidates (SPBC21B10.08c, SPBC2D10.16, rps402, yox1, SPAC17A2.02c, wdr21, ubp11) showed an impaired growth upon selection for

haploid double mutants in this validation experiment (Figure 31), whereas the other candidate deletions produced viable double mutants with the *pmt1Δ* strain.

To validate that a candidate gene was synthetic lethal with our deletion of interest, we first had to check whether the two genes are linked. This was important, because the whole array was based on crossovers between the sister chromatids when cells undergo meiosis. These crossovers can produce spores with both deletions. If two genes were located at some distance on the same chromosome, the crossover could happen between them. However, if the two genes were located in very close proximity, then the probability for a crossover between the two genes was low. In such a case, the two genes would be linked, and this would impede the development of double mutants. In this case the lack of double mutants would not show a synthetic lethality of the two genes, but linkage to each other.

Table 10: Localization of candidate genes

Gene	Chromosome	Position on chromosome II	Distance to *pmt1*$^+$ in bp	Distance to *pmt1*$^+$ in cM
pmt1	2	1674066-1675102	-	-
SPBC21B10.08c	2	1655946-1656777	17289	2.9
SPBC2D10.16	2	2996452-2996879	1321350	220
rps402	2	1651022-1651810	22256	3.7
yox1	2	1648235-1648840	25226	4.2
SPCC162.11c	3	-	-	-
wdr21	1	-	-	-
ubp11	2	1676524-1677576	1422	0.2

To evaluate the location of the candidate genes that are located on the same chromosome as *pmt1*$^+$, the distance of the two gene loci is calculated by basepairs and centimorgan (cM). A centimorgan gives an estimate about the probability of a crossover between two genes; 1 cM represents a probability of 1% per meiosis. In *S. pombe*, 1 cM is approximately 6 kbp of genomic DNA (Sunnerhagen et al. 1990). Analysis of the gene location revealed that four of the seven candidate genes (SPBC21B10.08c, rps402, yox1, ubp11) are located close to the *pmt1*$^+$ gene locus with distances between 0.2 and 4.2 cM (Table 10) and are therefore linked to *pmt1*$^+$.

A synthetic lethal interaction of these genes with *pmt1*$^{+}$ cannot be identified with the applied assay.

The other three candidate genes could display synthetic lethal interactions with *pmt1Δ* and were further validated. A classical genetic cross of two strains with each deletion and tetrad dissection should be used to further analyze the remaining three secondary candidates, wdr21, SPCC162.11c and SPBC2D10.16. This approach was used as an independent method to show synthetic lethal interactions. Tetrad dissection should yield single mutants for each of the two gene deletions, wild-type spores and double mutants. The double mutants should not be viable, if the combination of the two tested gene deletions is synthetic lethal, and therefore they should not develop on complete medium (YES) plates.

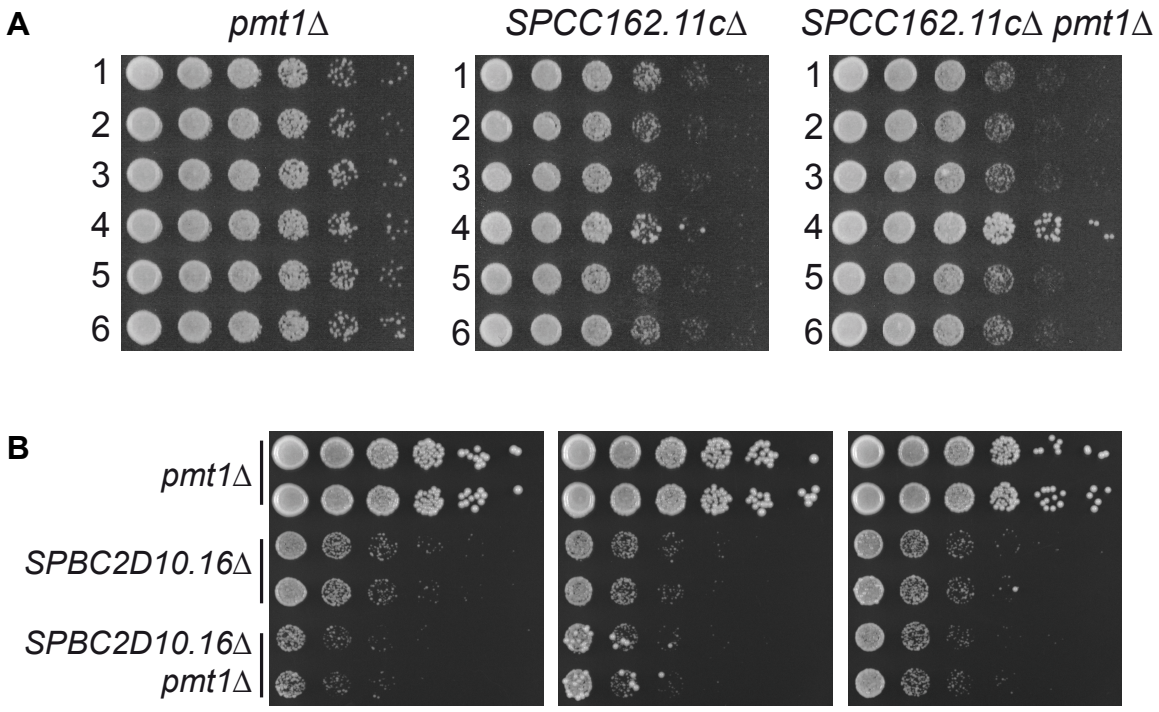

Figure 32: Growth of spores obtained from cross of *pmt1Δ* with a secondary candidate gene
(A) A *pmt1Δ* strain (AEP37) was crossed with a strain deleted for a secondary candidate gene of the SGA (*SPCC162.11cΔ*). After sporulation tetrads were dissected and the spores were analyzed for their ability to grow on standard complete medium (YES). Six spores were analyzed for each genotype (1-6). (B) Like (A), but for the deletion of the candidate gene SPBC2D10.16. Growth of 3 segregants for each genotype is displayed.

For unknown reasons, we were unable to obtain sporulation products from the cross of *pmt1Δ* and *wdr21Δ*. Crosses of the other two gene deletions with a *pmt1Δ* strain resulted in mating and sporulation, which allowed for tetrad dissection. All four spores of a tetrad that developed after the cross of the deletions of the two putative synthetic

lethal interaction partners were analyzed for their ability to grow on *S. pombe* complete medium plates (YES).

Spores that carried both deletions of synthetic lethal interaction partners should be unable to grow on YES medium plates. However, despite the results from the synthetic genetic array, we were able to obtain double mutants from the crosses, and we were unable to detect a growth defect on YES medium for these double mutants (Figure 32). The double mutants did not grow significantly worse than the single mutant of the candidate gene. Thus, we could not verify synthetic interactions with *pmt1*$^{+}$ that were identified using the Synthetic Genetic Array (see discussion).

6 Discussion

Schizosaccharomyces pombe does not contain any detectable methylation in its genomic DNA (Antequera et al. 1984). Despite this notion, a putative DNA methyltransferase called Pmt1 is annotated in the genome of the fission yeast (Wilkinson et al. 1995). Sequence comparisons revealed a membership to the Dnmt2 family of DNA methyltransferases (Yoder and Bestor 1998) that were shown to have only weak DNA methyltransferase activity, but to have a robust and specific tRNA methyltransferase activity (Goll et al. 2006). Pmt1 possesses no DNA methyltransferase activity, which was attributed to a proline-to-serine mutation in DNA methyltransferase motif IV next to the catalytic cysteine (Wilkinson et al. 1995; Pinarbasi et al. 1996).

6.1 The proline-to-serine mutation in the Pmt1 sequence does not inactivate the enzyme

In this study, we demonstrated that Pmt1 is a tRNA methyltransferase that modified the cytosine at position 38 of $tRNA^{Asp}$. This was expected for a Dnmt2 homolog and showed that Pmt1 is an active enzyme, despite the deviation from the consensus sequence of Dnmt2 enzymes that was claimed to be responsible for the absence of detectable methyltransferase activity (Wilkinson et al. 1995; Pinarbasi et al. 1996). The proline residue that is found next to the catalytic cysteine in motif IV of other Dnmt2 enzymes is a special amino acid, because its cyclic structure makes the side chain less flexible and introduces a different angle into the peptide chain than other amino acids. This is associated with a turn in the chain and explains why proline disrupts α-helices and β-sheets and is often found in loops. This is also the reason why proline is often solvent-exposed, although it is a hydrophobic amino acid with a completely aliphatic side chain. In Dnmt2 enzymes, this proline residue of motif IV is located in a loop right next to the catalytic cysteine and positions the catalytic residue next to a turn (Dong et al. 2001). If a serine residue replaces this proline residue, the loop will gain some flexibility. However, there is a second proline in motif IV (PPCQ in Dnmt2, PSCQ in Pmt1), which would prevent a complete disruption of the turn, and the motif is located in a loop, which naturally is a flexible region of a protein and might reduce the importance of the angle of a turn at this position of the peptide

chain. Taken together, these observations would indicate that a proline-to-serine mutation at this position of Dnmt2 proteins is not destined to disrupt the activity of the enzyme, as was previously assumed (Wilkinson et al. 1995). Our results demonstrate catalytic activity of the "mutant" protein Pmt1 and support the considerations on a proline-to-serine mutation at this position.

We were also able to identify a further target for methylation at C38 by Pmt1. This second substrate, $tRNA^{Glu}$, was methylated to a lesser extent than the major target, $tRNA^{Asp}$. The comparison of the sequences of these two tRNAs revealed that $tRNA^{Asp}$ matches a proposed target recognition pattern (Mark Helm, unpublished data), but the $tRNA^{Glu}$ sequence matches only at three out of four sites of this pattern. If these four bases (Table 8) were required for target recognition by Dnmt2 proteins, this explains the lower activity of Pmt1 on $tRNA^{Glu}$, because not all of the necessary recognition sites were present. This could result in a more flexible association of the substrate to the catalytic pocket, which could set the substrate free before the methylation reaction is completed. Another reason for a reduced catalytic activity could be the orientation of the tRNA inside the enzyme. If the mismatch in the target recognition pattern causes a repositioning of the substrate, this would impede the contact of the catalytic amino acids to the substrate, leading to impaired substrate methylation.

6.2 Is Pmt1 activity specific for $tRNA^{Asp}$ and $tRNA^{Glu}$?

In this study, we present evidence for the tRNA methyltransferase activity of Pmt1 on $tRNA^{Asp}$ and $tRNA^{Glu}$ of the fission yeast *S. pombe*. We did not identify other targets for the methylation by Pmt1. However, could additional substrates for Pmt1-dependent methylation exist? We identified $tRNA^{Glu}$ as a substrate by sequence specific RNA bisulfite sequencing. In this experiment, we also investigated other tRNAs that partially match the recognition pattern of Dnmt2 enzymes. For technical reasons, we were unable to obtain data for these additional tRNAs. Therefore, it is possible that one of these tRNAs might be a target for Pmt1.

The results obtained from the methylation assay displayed a methylation signal at the size of tRNAs. We cannot exclude that in the bulk of RNAs in this band of the gel there are additional RNA species of similar size present. These RNAs could be Pmt1 targets, but they could not be identified with the assay applied here. Putative target

RNAs would have to exhibit a tertiary structure that is similar to the L-shaped 3D-structure of tRNAs, because this structure is probably required for target recognition by Dnmt2 enzymes. Interesting candidates for additional methylation targets could be centromeric RNAs or other transcripts that could be used by the RNAi machinery. Such targets might imply a function for Pmt1 in gene silencing.
Furthermore, RNAs of sizes that differ from the size of a tRNA could also be targets of Pmt1-dependent methylation. These possibly larger targets should display a local structure that is similar to the tRNA structure. They could be methylated in the *in vitro* reaction, but not be detected, because they might be less abundant and their methylation signal therefore would be below the detection limit of the methylation assay.

6.3 The impact of C38 methylation on tRNA function

We have demonstrated that Pmt1 is able to methylate tRNAs in the anticodon loop. What influence could this modification of the tRNA have on its function? The methylation at position 38 of the anticodon loop can have an influence on the tertiary structure of tRNA molecules. Nucleotide modification in RNAs often leads to structural and metabolic stabilization (Helm 2006). Furthermore, m^5C residues can be important for appropriate Mg^{2+} binding and thus can induce conformational changes of the whole anticodon loop (Chen et al. 1993). This could also be true for the C38 methylation by Pmt1. Structural stabilization of target RNAs could be a reason for the strong conservation of Dnmt2 enzymes, but there are probably additional benefits from this methylation, because single tRNA modifications only slightly influence tRNA structure (Derrick and Horowitz 1993; Vermeulen et al. 2005).
One of these benefits could be the protection from the rapid tRNA decay (RTD) pathway. This pathway degrades m^5C-deficient tRNA molecules in *S. cerevisiae* when the methyltransferases for 5-methylcytosine and 7-methylguanosine are absent (Alexandrov et al. 2006). This pathway seems to be rather specific for $tRNA^{Val}$ of the budding yeast, but similar pathways could exist for other tRNAs or different tRNAs could be targeted by such a pathway in other organisms like *S. pombe*.
Studies on mRNA translation have revealed that the disruption of Trm4 function in *S. cerevisiae* leads to an increased sensitivity to the antibiotic paromomycin, which

affects the precision of ribosome decoding (Wu et al. 1998). This indicates that methylation of tRNAs could affect translation efficiency.

Another interesting aspect of m^5C in tRNAs has been described previously (Schaefer et al. 2010). Methylation by Dnmt2 protects *Drosophila* tRNAs against stress-induced cleavage and cleavage by angiogenin. This could also be the case for Pmt1 substrates in *S. pombe*. There are several RNases annotated in the genome of the fission yeast and tRNA fragments have been implicated to be involved in several cellular processes (Thompson and Parker 2009; Phizicky and Hopper 2010; Ivanov et al. 2011). A modulation of tRNA fragments by modification of the tRNA could influence these processes. tRNAs were also shown to interact with cytochrome c and thus inhibit caspase activation (Mei et al. 2010). Whether this process might be influenced by methylation of the tRNAs is worth investigating.

6.4 Nutrient components as a cause for changes in tRNA methylation

A major discovery of this study was the induction of tRNA methylation levels upon addition of peptone to the medium. Peptone is an enzymatic digest of animal protein that serves as amino acid and nitrogen source in yeast cultures. A typical peptone contains small peptides (less than 15 % are larger than 5 kDa) and amino acids, but peptic digestion of animal tissue also leaves vitamins and growth factors in the mixture. The complex composition of this media component might be the reason for the strong effect that it has on tRNA methylation by Pmt1, and it will be interesting to identify a single component within the peptone mixture that induces Pmt1 activity.

The natural habitat of *Schizosaccharomyces pombe* cells is the surface of several fruits. The nutrients that are available under such conditions vary significantly from the culture media that are used in the laboratory. Therefore, it is likely that protein expression and protein activity in laboratory strains differ from the situation in cells that grow in their natural environment. Thus, the inactivation of a protein as highly conserved during evolution as the Dnmt2 homolog Pmt1 in laboratory strains could be attributed to the altered requirements under the optimized growth conditions in the laboratory. The requirement for a possibly stabilizing tRNA modification like the methylation at cytosine 38 in $tRNA^{Asp}$ (Motorin et al. 2009) might also be reduced in a

complete medium like YES that provides the yeast cells with enough nutrients to replace degraded tRNAs.

When peptone was added to the *S. pombe* complete medium (YES), Pmt1 was activated and $tRNA^{Asp}$ was methylated. In this modified medium, the cells still had all other nutrients that they also had in YES medium. Therefore, the cause for the activation of Pmt1 could not be the absence of required nutrients. It would rather be the presence of a component of peptone that induces Pmt1 activation. Whether this component activates or inactivates a cellular factor upstream of Pmt1 will be of interest in future experiments. Furthermore, it would be possible that the presence of this peptone component somehow mimics the nutrient availability in the natural environment of *S. pombe*. This would cause the cells to adapt the tRNA methylation levels to the ones needed in the natural habitat. This possible explanation needs further support and it would be important to determine the tRNA methylation state of cells that were isolated from their natural environment.

A second explanation for tRNA methylation upon peptone addition might be that the cells are stressed by this media component in some way. Cellular stress can cause various changes in protein activity (Kourtis and Tavernarakis 2011). This assumption is supported by the observation that *S. pombe* cells are able to mate and sporulate on YPD medium. This process is usually induced under starvation conditions. This suggests that YPD might not really serve as a “complete medium” for *S. pombe* cells. Thus, it is possible that the cells undergo nutritional stress in this medium. Therefore, it is also plausible that the tRNA methylation level is increased by an altered Pmt1 activity upon peptone addition as a means of cellular stress response.

Independently of the cause, natural level or stress response, the methylation of tRNA molecules could contribute to the efficiency of protein translation either by enhanced recognition by the ribosome or by altered tRNA stability (Motorin et al. 2009; Schaefer et al. 2010).

Another nutritional component that could be important for Dnmt2 function is glucose. Studies on the *Entamoeba histolytica* homolog of Dnmt2 revealed an interaction with the glycolytic enzyme enolase (Tovy et al. 2010b). Nuclear Dnmt2 is inhibited by the interaction with enolase upon glucose starvation, and this inhibition can be reversed by the enolase substrate 2-phosphoglycerate. These results indicate that glucose starvation might influence the methyltransferase activity of Dnmt2 enzymes, a fact that could also have an impact on caloric restriction effects in yeast cells. Low glucose growth conditions are known to influence aging in yeast cells due to the

beneficial effects of caloric restriction on chronological lifespan (Smith et al. 2007). If low glucose levels would result in inhibition of Pmt1 activity in *S. pombe* cells, this would provide a possible explanation for the lifespan extension we observed in *pmt1Δ* cells.

6.5 How does the serine/threonine kinase Sck2 influence Pmt1 activity?

During our study, we observed a reduction of Pmt1-dependent RNA methylation upon deletion of the serine/threonine kinase Sck2 (Fujita and Yamamoto 1998). These results suggested that Pmt1 activity was regulated either directly or indirectly via phosphorylation. We hypothesize that in the presence of Sck2, Pmt1 would be phosphorylated and fully active. Conversely, when Sck2 is missing, Pmt1 would not be phosphorylated, and the activity of Pmt1 would be reduced, but not completely inhibited. We did not determine whether this modulation of Pmt1 activity is carried out directly by Sck2 or by downstream targets that are activated by Sck2 (Zuin et al. 2010).

Next to other possible phosphorylation sites within Pmt1, an interesting target for phosphorylation by Sck2 would be the serine residue located next to the catalytic cysteine in motif IV (PSCQ). This serine residue represents a deviation from the consensus sequence of Dnmt2 enzymes. In the structure of Dnmt2, the catalytic cysteine in motif IV is situated in a loop (Dong et al. 2001). Due to the similarities in the amino acid sequence, we can assume that Pmt1 folds in a similar way as Dnmt2. This would imply that the serine residue in the Pmt1 sequence would also be located in this loop structure. Thus, it would be easily accessible for modification by Sck2. A phosphorylation right next to a catalytic amino acid side chain might influence the position of this side chain and could therefore also influence the activity of the enzyme. If the phosphorylation would shift the position of the cysteine closer to the substrate, this would provide a possible explanation for an increased activity of Pmt1 upon phosphorylation by Sck2.

A second residue that would be an interesting target for phosphorylation is the threonine in the target recognition motif. The CFT motif is well conserved among Dnmt2 enzymes (Dong et al. 2001), but is not found in other DNA methyl-transferases. A phosphorylation at this site could influence the positioning of the target base within the catalytic pocket, which could increase the activity of Pmt1.

An interesting aspect of these two possible phosphorylation sites is that the first one is unique to Pmt1 and the second one is found in all Dnmt2 enzymes (Figure 7). Regulation at the serine that is unique to Pmt1 would be found exclusively in the *S. pombe* homolog, whereas regulation in the target recognition domain would then also be possible in the other Dnmt2 homologs.

Apart from these considerations, analysis of potential phosphorylation sites by NetPhos (http://www.cbs.dtu.dk/services/NetPhos/ (Blom et al. 1999)) predicted 8 serine phosphorylation sites, 4 threonine phosphorylation sites and one tyrosine phosphorylation site. Neither the serine residue in the catalytic motif IV nor the threonine in the target recognition motif were indicated as potential targets for phosphorylation, but interestingly the serine residue directly N-terminal to the catalytic motif PSCQ was identified as a candidate phosphorylation site. This residue was also identified as potential phosphorylation site by NetPhosYeast (http://www.cbs.dtu.dk/services/NetPhosYeast/ (Ingrell et al. 2007)). However, this prediction implied 11 serine phosphorylation sites that included the serine residue within the catalytic motif as target for phosphorylation, which supports the considerations on Pmt1 activity described above. This analysis tool did not predict any threonine phosphorylation sites.

Taken together, Pmt1 activity could be regulated by posttranslational phosphorylation of a variety of potential target amino acids. This phosphorylation could be performed by the serine/threonine kinase Sck2 or by a downstream target of Sck2 signaling.

6.6 How could rapamycin affect tRNA methylation by Pmt1?

When we treated *S. pombe* cells with rapamycin, we observed a reduction of the Pmt1-mediated methylation signal in the *in vitro* methylation assay. In other experiments, we always interpreted reduced signal strength as an indicator for an increased *in vivo* methylation of the RNA substrates of Pmt1. However, when we treated *pmt1Δ* cells with rapamycin, we also observed a reduction of the autoradiography signal. Due to the absence of Pmt1 in these cells, a reduction of the signal in *pmt1Δ* cells is unlikely to represent an increased methylation in the cells. Therefore, we asked what other explanations there might be for a decrease in signal strength after *in vitro* methylation of total RNA extracts.

One reason for this could be that upon treatment with rapamycin, another m^5C methyltransferase becomes activated and starts methylating Pmt1 target sites. Since there is no other Dnmt2 homolog annotated in the fission yeast genome, this methyltransferase could only be an RNA methyltransferase. Trm4 performs methylation at position 5 of cytosines in tRNAs of *Saccharomyces cerevisiae*, and there are two putative Trm4-homologs annotated in the *S. pombe* genome (SPAC17D4.04, SPAC23C4.17). However, Trm4 has only been shown to methylate the positions 48 and 49 in the T-stem, position 40 in the anticodon stem and position 34 in the anticodon loop of various tRNAs in *S. cerevisiae* (Motorin and Grosjean 1999), but has never been associated with methylation of position C38 in the anticodon loop.

On the other hand, a reduced *in vitro* methylation could also be explained by the absence of target tRNAs in the total RNA extracts. The EtBr staining in these experiments confirmed that an equal amount of total RNA was used in the control reaction as well as in the reaction with RNA from rapamycin treated cells. Therefore, the reduced signal is not due to reduction of global RNA amount. However, it is possible that within the bulk of small RNAs that comprise the RNA band containing $tRNA^{Asp}$, the amount of Pmt1 substrate is decreased. In a mixture of tRNAs, the absence of one tRNA species cannot be observed by EtBr staining. In this scenario, a reduced amount of Pmt1 substrates in the total RNA could be explained by a specific cleavage or degradation of unmethylated Pmt1 substrates. This degradation would be induced by the addition of rapamycin and would probably be indirect and mediated by an inhibition of the TOR complex (Heitman et al. 1991).

Addition of rapamycin could also be responsible for a reduced level of tRNA transcription. It has been shown that mTOR binds to tRNA genes and thus controls tRNA synthesis via inhibition of the RNA polymerase III inhibitor Maf1 (Kantidakis et al. 2010; Tsang et al. 2010). In this scenario, inhibition of Tor could result in inhibition of tRNA transcription and subsequent reduction of cellular tRNA levels. The reduced tRNA levels would then be detected as reduced *in vitro* methylation signals in the methylation assay that was used in our study, regardless of the presence of Pmt1.

To determine which of the discussed possibilities is the probable cause for our observations, this has to be the subject of further investigations. The activation of a C38 methylation activity of Trm4 homologs would be supported by the broad spectrum of target sites and RNA substrates of these methyltransferases. Substrate degradation, on the other hand, would be in agreement with the protection of Dnmt2

substrates against cleavage by the RNase angiogenin (Schaefer et al. 2010). If an RNase is activated upon rapamycin treatment, the unmethylated Pmt1 substrates of a *pmt1Δ* strain would be degraded. The inhibition of tRNA translation, as a third possibility, could be determined by Northern Blot analysis.

6.7 Pmt1-dependent tRNA methylation and chronological aging

The results of this study provided evidence for a role of Pmt1 activity in the chronological aging process in fission yeast. We were able to show that the deletion of the *pmt1*$^{+}$ gene elongated the lifespan of *S. pombe* cells when they were cultured in minimal medium (EMM). This is contradictory to the data that were obtained from Drosophila. Fruit flies were shown to have a shortened lifespan upon disruption of Dnmt2 function (Lin et al. 2005; Schaefer et al. 2010). This points towards an interesting species-specific difference in the control of lifespan. Combined with the observation that Pmt1 activity is partially regulated by the serine/threonine kinase Sck2, this led us to hypothesize that *sck2Δ*-mediated lifespan extension (Roux et al. 2006) can at least partially be attributed to reduced Pmt1 activation in *sck2Δ* cells. However, equivalent aging experiments in complete medium containing peptone (YPD), which activates Pmt1-dependent tRNA methylation, displayed an elongated lifespan of the wild-type strain. As we were able to show, wild-type cells carry completely methylated $tRNA^{Asp}$ under these culture conditions. Therefore, the results from the second aging experiment were in conflict with the results obtained in minimal medium. However, it is not unprecedented that aging effects depend on media conditions. For instance, different minimal media were demonstrated to influence chronological lifespan and alter the effects of caloric restriction in *S. pombe* (Chen and Runge 2009).

We speculated that nutrient availability might influence the requirement of tRNA methylation for the cellular aging process. Longevity in complete medium might thus require methylation of $tRNA^{Asp}$, whereas it can be omitted in minimal medium. The conditions in minimal medium might render the aging process such that it requires the resources needed for tRNA methylation in other cellular processes that are more important for survival than tRNA methylation. In this case, the absence of a tRNA methylation process would be beneficial for cell survival. In complete medium these resources could be obtained from the medium, and the presence of the tRNA

methylation machinery would not disrupt other processes required for cell survival. In such a case, tRNA methylation could provide a minor beneficial effect on cellular aging, possibly through increased tRNA stability, protection against cleavage or other regulatory functions that might be unrelated to the tRNA function in protein translation.

The nutritional status and nutritional stress response have been implicated in the regulation of tRNA localization (Huynh et al. 2010). The nuclear reexport of mature tRNAs into the cytoplasm is mediated by the amino acid-sensitive tRNA exporter Xpo-t. We could therefore also hypothesize that the different nutrient conditions in the minimal media could induce nuclear accumulation of unmethylated charged tRNAs upon aging and thus prevent the amino acids that are bound to the tRNAs to act as activators of the TOR complex (Sancak et al. 2008). Reduced TOR activity would then result in an increased lifespan. However, to date there are no indications for an influence of tRNA methylation on nuclear reexport of tRNAs, which might be an interesting aspect of further research.

6.8 Is Pmt1-dependent tRNA methylation an isolated process?

During the course of this study, we failed to identify direct or synthetic lethal interaction partners of Pmt1. Do these observations suggest that Pmt1 does not interact with other proteins or that there are no pathways that act in parallel to Pmt1? Our own results on Pmt1 regulation by Sck2 suggest otherwise. No matter if the regulation is directly through Sck2 or if a downstream target of Sck2 regulates Pmt1 activity, it is likely that the regulation is done by posttranslational modification of the Pmt1 protein. This requires physical contact of the modifying enzyme and Pmt1, and therefore suggests that there are physical interaction partners of Pmt1. We also demonstrated that the activity of Pmt1 was altered by the applied culture medium. Therefore, protein interactions might occur when cells cultured in YPD medium are used for protein purification, whereas the purifications here were performed in YES medium.

The same is true for synthetic lethal interaction partners that could point towards pathways that act parallel to Pmt1. The interaction might only be essential under conditions that require Pmt1-dependent tRNA methylation. Therefore, it seems to be promising to include the new knowledge on Pmt1 activation in YPD medium in the

strategy to identify synthetic lethal interactions. The identification of both physical interaction partners and synthetic lethal interactions will provide valuable insight into the biological function of Pmt1 and might provide data that place Pmt1 into known signaling pathways.

6.9 The impact of this study on previous observations concerning Pmt1

A major aspect of the investigation of Pmt1 activity in the fission yeast was the apparent absence of detectable DNA methylation despite the presence of a putative DNA methyltransferase (Antequera et al. 1984). These results were obtained from yeast cells cultured in a medium that does not induce Pmt1 activity (2 % yeast extract, 2 % glucose). Combined with observations from other Dnmt2 homologs that display a low DNA methyltransferase activity (Hermann et al. 2003; Kuhlmann et al. 2005), this suggests that *in vivo* Pmt1 activity on DNA substrates should be reinvestigated under inducing conditions. Other studies reported that recombinant Pmt1 was unable to methylate DNA substrates (Wilkinson et al. 1995; Pinarbasi et al. 1996), but our discovery of a possible regulation of Pmt1 activity by phosphorylation could indicate that the recombinant protein lacks the essential activating phosphorylation. Comparison of phosphorylation site prediction from NetPhosYeast (Ingrell et al. 2007) and NetPhosBac (http://www.cbs.dtu.dk/services/NetPhosBac-1.0/ (Miller et al. 2009)), a predictor for bacterial phosphorylation sites, revealed that only 5 out of 11 phosphorylation sites predicted by NetPhosYeast were also included in the prediction from NetPhosBac. Significantly, the interesting phosphorylation sites in motif IV are absent in the NetPhosBac prediction. This could indicate that essential modifications for Pmt1 activation are missing in the recombinant protein. Taken together, our study revealed the possibility that the absence of DNA methyltransferase activity of Pmt1 could be due to a lack of phosphorylation under the previously investigated conditions and supports a reinvestigation of this DNA methyltransferase activity, both *in vitro* and *in vivo*.

7 Outlook

In this study, we have investigated the Dnmt2 homolog Pmt1 from fission yeast and have found that Pmt1 is an active tRNA methyltransferase, and that it is activated under certain nutritional conditions. The activity of the enzyme is partially regulated by the serine/threonine kinase Sck2 and might be an effector of Sck2-mediated lifespan extension, because we observed an elongated lifespan upon deletion of *pmt1*$^{+}$. The results of this project open up several possibilities for gaining further insight into the activity and biological function of Pmt1.

We found Pmt1 to be activated by addition of peptone to *S. pombe* complete medium. Furthermore, 25 % $tRNA^{Asp}$ methylation was observed in cells cultured in minimal medium. In the future, the conditions leading to Pmt1 activation could be further refined by the identification of distinct compounds that activate the enzyme. For this purpose, minimal medium lacking individual components could be used to culture *S. pombe* cells, and RNA bisulfite sequencing and *in vitro* methylation of total RNA extracts by recombinant Pmt1 could then be used to determine tRNA methylation levels. The effect of excess amounts of these nutritional components could additionally be analyzed. Time course experiments upon switching cells from inducing medium to non-inducing medium and *vice versa* will provide essential information on the establishment and persistence of the tRNA methylation mark. Assuming that reduced nutrient availability provides a stress condition for the cells, the influence of various stresses like heat stress and oxidative stress could also be investigated.

The nutrient dependency of Pmt1 activity also sheds new light on previous results on the genome-wide DNA methylation activity of Pmt1. DNA bisulfite sequencing could be employed to identify DNA methylation in cells cultured under inducing conditions. Additionally, our results on physical and synthetic lethal interaction partners have to be reevaluated by application of inducing conditions in the respective experiments.

Our observation that Sck2 is required for Pmt1 activity suggests that Pmt1 may be a phosphorylation target. This could be investigated by mass spectrometry of Pmt1 protein that has been purified from *S. pombe* cells. Furthermore, site-directed mutagenesis could be utilized to analyze the impact of putative phosphorylation sites. Mutation to alanine would render the putative phosphorylation sites unmodifiable,

and the impact of these mutants on tRNA methylation could be determined via RNA bisulfite sequencing or *in vitro* methylation by recombinant Pmt1/Pmt1 mutants.

The results of this work not only implicate modifications on the protein level, but they also suggest that the substrate tRNAs may be targeted by certain degradation pathways. The impact of rapamycin on the results of the *in vitro* methylation assay suggested that specific RNases could degrade unmethylated Pmt1 substrates upon rapamycin treatment. This could be due to cleavage of the tRNAs in the anticodon loop. To test this, Northern blot analysis could identify tRNA fragments. If these fragments can be identified, the next step would be to determine the RNase responsible for the cleavage. For this purpose, candidate RNases could be deleted in the *S. pombe* cells and the double mutant lacking both Pmt1 and the RNase should display the same *in vitro* tRNA methylation levels as untreated *pmt1Δ* cells, when they are treated with increasing amounts of rapamycin. Northern Blot analysis could also be utilized for the investigation of changes in the RNA transcription level, when RNases were inhibited in the cell culture.

Another important finding of this study was the lifespan alterations in *pmt1Δ* cells. Future experiments could be designed to investigate if Pmt1 activity is involved in the lifespan regulation by other factors known to be involved in aging like sirtuins (Kaeberlein 2010), the TOR pathway (Sharp and Richardson 2011) or the glucose sensing pathway (Roux et al. 2006). The combination of *pmt1Δ* with other lifespan extending mutants could place Pmt1 in one of these pathways.

8 Abstract

DNA nucleotide methyltransferases (Dnmts) are the enzymes responsible for the conversion of cytosine to 5-methylcytosine in eukaryotes. The fission yeast *Schizosaccharomyces pombe* contains a putative DNA methyltransferase, termed pombe methyltransferase1 (Pmt1) that belongs to the Dnmt2 family of cytosine methyltransferases, but intriguingly has no DNA methylation. Dnmt2 family members from several organisms have been demonstrated to methylate $tRNA^{Asp}$ at position C38 rather than cytosines in DNA, but the biological function of this tRNA modification has remained largely unknown.

In this study, we found that Pmt1 is able to methylate position C38 of $tRNA^{Asp}$ and to a lesser extent $tRNA^{Glu}$ *in vitro* using methylation of tRNA transcripts by recombinant Pmt1. RNA bisulfite sequencing of tRNAs showed that Pmt1 is also active *in vivo*. These results show that mt1 in principle has methyltransferase activity, although it was previously thought to be inactive due to a deviation in catalytic motif IV from other Dnmt2 enzymes. Furthermore, *in vivo* Pmt1 activity was strongly influenced by a nutritional factor in the growth medium. Induction of Pmt1 methyltransferase activity was observed upon the addition of peptone to *S. pombe* growth medium. Furthermore, the induction of Pmt1 activity required the serine/threonine kinase Sck2 and was independent of the kinases Sck1, Pka1 and Tor1. Significantly, cells with full tRNA methylation displayed a shortened chronological lifespan, whereas the deletion of $pmt1^{+}$ lead to an elongated lifespan in fission yeast.

In summary, out data show that Pmt1 is an active tRNA methyltransferase. Furthermore, Pmt1 function is regulated in a nutrient-dependent manner by the serine/threonine kinase Sck2, and it is involved in the regulation of chronological aging in the fission yeast *Schizosaccharomyces pombe*.

9 Zusammenfassung

DNA Methyltransferasen (Dnmts) in Eukaryoten katalysieren die Umwandlung von Cytosin zu 5-Methylcytosin. Die Spalthefe *Schizosaccharomyces pombe* besitzt eine mögliche DNA Methyltransferase namens Pombe Methyltransferase1 (Pmt1), die zur Familie der Dnmt2 Enzyme gehört, besitzt jedoch keine nachweisbare DNA Methylierung. Dnmt2 Homologe aus verschiedenen Organismen sind in der Lage, $tRNA^{Asp}$ an Position C38 zu methylieren und zeigen vergleichsweise geringe DNA Methylierungsaktivität. Die biologische Funktion dieser tRNA-Modifikation ist bisher kaum erforscht.

Unsere Ergebnisse aus *in vitro* Methylierungsanalysen mit rekombinantem Pmt1 zeigen, dass das *S. pombe* Homologe von Dnmt2 in der Lage ist, $tRNA^{Asp}$ und $tRNA^{Glu}$ aus der Spalthefe zu methylieren. Diese Resultate demonstrieren, dass Pmt1 ein aktives Enzym ist, obwohl frühere Untersuchungen nahe legten, dass eine Abweichung von der Konsensussequenz der Dnmt2 Enzyme im katalytischen Motiv IV zu einer Inaktivierung des Enzyms geführt hat. Mittels der RNA Bisulfit-Sequenzierung konnten wir diese Aktivität auch *in vivo* zeigen. Interessanterweise zeigten unsere Untersuchungen, dass die Aktivität von Pmt1 durch die Nährstoffe im Kultivierungsmedium reguliert wird. Die Methyltransferaseaktivität von Pmt1 wurde induziert, wenn dem *S. pombe* Vollmedium Pepton zugesetzt wurde. Des Weiteren konnten wir zeigen, dass für die Induktion der Pmt1-Aktivität die Serin/Threonin-Kinase Sck2 benötigt wird, wohingegen die Kinasen Sck1, Pka1 und Tor1 keinen Einfluß auf die Pmt1-abhängige tRNA-Methylierung hatten. Schließlich konnten wir außerdem zeigen, dass Hefezellen, die eine starke tRNA-Methylierung aufweisen, eine verkürzte chronologische Lebensspanne besitzen. Die Deletion des $pmt1^{+}$-Gens führt hingegen zu einer Verlängerung der Lebensspanne der *S. pombe* Zellen.

Zusammengefasst zeigen unsere Daten, dass Pmt1 eine aktive tRNA Methyltransferase ist, dass die Funktion von Pmt1 nährstoffabhängig von der Serin/Threonin kinase Sck2 reguliert wird, und dass Pmt1 an der Regulation der chronologischen Alterung in der Spalthefe *Schizosaccharomyces pombe* beteiligt ist.

10 References

Alexandrov, A., Chernyakov, I., Gu, W., Hiley, S.L., Hughes, T.R., Grayhack, E.J., and Phizicky, E.M. 2006. Rapid tRNA decay can result from lack of nonessential modifications. *Mol Cell* **21**(1): 87-96.

Allen, M.D., Grummitt, C.G., Hilcenko, C., Min, S.Y., Tonkin, L.M., Johnson, C.M., Freund, S.M., Bycroft, M., and Warren, A.J. 2006. Solution structure of the nonmethyl-CpG-binding CXXC domain of the leukaemia-associated MLL histone methyltransferase. *EMBO J* **25**(19): 4503-4512.

Antequera, F., Tamame, M., Villanueva, J.R., and Santos, T. 1984. DNA methylation in the fungi. *J Biol Chem* **259**(13): 8033-8036.

Bacolla, A., Pradhan, S., Roberts, R.J., and Wells, R.D. 1999. Recombinant human DNA (cytosine-5) methyltransferase. II. Steady-state kinetics reveal allosteric activation by methylated dna. *J Biol Chem* **274**(46): 33011-33019.

Banerjee, S., Fisher, O., Lohia, A., and Ankri, S. 2005. Entamoeba histolytica DNA methyltransferase (Ehmeth) is a nuclear matrix protein that binds EhMRS2, a DNA that includes a scaffold/matrix attachment region (S/MAR). *Mol Biochem Parasitol* **139**(1): 91-97.

Beard, C., Li, E., and Jaenisch, R. 1995. Loss of methylation activates Xist in somatic but not in embryonic cells. *Genes Dev* **9**(19): 2325-2334.

Bestor, T., Laudano, A., Mattaliano, R., and Ingram, V. 1988. Cloning and sequencing of a cDNA encoding DNA methyltransferase of mouse cells. The carboxyl-terminal domain of the mammalian enzymes is related to bacterial restriction methyltransferases. *J Mol Biol* **203**(4): 971-983.

Bird, A., Taggart, M., Frommer, M., Miller, O.J., and Macleod, D. 1985. A fraction of the mouse genome that is derived from islands of nonmethylated, CpG-rich DNA. *Cell* **40**(1): 91-99.

Bjork, G.R. 1995. Genetic dissection of synthesis and function of modified nucleosides in bacterial transfer RNA. *Prog Nucleic Acid Res Mol Biol* **50**: 263-338.

Blom, N., Gammeltoft, S., and Brunak, S. 1999. Sequence and structure-based prediction of eukaryotic protein phosphorylation sites. *J Mol Biol* **294**(5): 1351-1362.

Bostick, M., Kim, J.K., Esteve, P.O., Clark, A., Pradhan, S., and Jacobsen, S.E. 2007. UHRF1 plays a role in maintaining DNA methylation in mammalian cells. *Science* **317**(5845): 1760-1764.

Bourc'his, D. and Bestor, T.H. 2004. Meiotic catastrophe and retrotransposon reactivation in male germ cells lacking Dnmt3L. *Nature* **431**(7004): 96-99.

Bujnicki, J.M., Feder, M., Ayres, C.L., and Redman, K.L. 2004. Sequence-structure-function studies of tRNA:m5C methyltransferase Trm4p and its relationship to DNA:m5C and RNA:m5U methyltransferases. *Nucleic Acids Res* **32**(8): 2453-2463.

Byrne, S.M. and Hoffman, C.S. 1993. Six git genes encode a glucose-induced adenylate cyclase activation pathway in the fission yeast Schizosaccharomyces pombe. *J Cell Sci* **105 (Pt 4)**: 1095-1100.

Chang, S.C., Tucker, T., Thorogood, N.P., and Brown, C.J. 2006. Mechanisms of X-chromosome inactivation. *Front Biosci* **11**: 852-866.

Chen, B.R. and Runge, K.W. 2009. A new Schizosaccharomyces pombe chronological lifespan assay reveals that caloric restriction promotes efficient cell cycle exit and extends longevity. *Exp Gerontol* **44**(8): 493-502.

Chen, Y., Sierzputowska-Gracz, H., Guenther, R., Everett, K., and Agris, P.F. 1993. 5-Methylcytidine is required for cooperative binding of Mg2+ and a conformational transition at the anticodon stem-loop of yeast phenylalanine tRNA. *Biochemistry* **32**(38): 10249-10253.

Cheng, X., Kumar, S., Posfai, J., Pflugrath, J.W., and Roberts, R.J. 1993. Crystal structure of the HhaI DNA methyltransferase complexed with S-adenosyl-L-methionine. *Cell* **74**(2): 299-307.

Chuang, L.S., Ian, H.I., Koh, T.W., Ng, H.H., Xu, G., and Li, B.F. 1997. Human DNA-(cytosine-5) methyltransferase-PCNA complex as a target for p21WAF1. *Science* **277**(5334): 1996-2000.

Delaval, K. and Feil, R. 2004. Epigenetic regulation of mammalian genomic imprinting. *Curr Opin Genet Dev* **14**(2): 188-195.

Derrick, W.B. and Horowitz, J. 1993. Probing structural differences between native and in vitro transcribed Escherichia coli valine transfer RNA: evidence for stable base modification-dependent conformers. *Nucleic Acids Res* **21**(21): 4948-4953.

Dong, A., Yoder, J.A., Zhang, X., Zhou, L., Bestor, T.H., and Cheng, X. 2001. Structure of human DNMT2, an enigmatic DNA methyltransferase homolog that displays denaturant-resistant binding to DNA. *Nucleic Acids Res* **29**(2): 439-448.

Fabrizio, P., Pozza, F., Pletcher, S.D., Gendron, C.M., and Longo, V.D. 2001. Regulation of longevity and stress resistance by Sch9 in yeast. *Science* **292**(5515): 288-290.

Fatemi, M., Hermann, A., Pradhan, S., and Jeltsch, A. 2001. The activity of the murine DNA methyltransferase Dnmt1 is controlled by interaction of the catalytic domain with the N-terminal part of the enzyme leading to an allosteric activation of the enzyme after binding to methylated DNA. *J Mol Biol* **309**(5): 1189-1199.

Feldmann, H., Dutting, D., and Zachau, H.G. 1966. Analyses of some oligonucleotide sequences and odd nucleotides from serine transfer ribonucleic acids. *Hoppe Seylers Z Physiol Chem* **347**(4): 236-248.

Fisher, O., Siman-Tov, R., and Ankri, S. 2004. Characterization of cytosine methylated regions and 5-cytosine DNA methyltransferase (Ehmeth) in the protozoan parasite Entamoeba histolytica. *Nucleic Acids Res* **32**(1): 287-297.

Flynn, J., Fang, J.Y., Mikovits, J.A., and Reich, N.O. 2003. A potent cell-active allosteric inhibitor of murine DNA cytosine C5 methyltransferase. *J Biol Chem* **278**(10): 8238-8243.

Fontana, L., Partridge, L., and Longo, V.D. 2010. Extending healthy life span--from yeast to humans. *Science* **328**(5976): 321-326.

Fujita, M. and Yamamoto, M. 1998. S. pombe sck2+, a second homologue of S. cerevisiae SCH9 in fission yeast, encodes a putative protein kinase closely related to PKA in function. *Curr Genet* **33**(4): 248-254.

Fuks, F., Burgers, W.A., Brehm, A., Hughes-Davies, L., and Kouzarides, T. 2000. DNA methyltransferase Dnmt1 associates with histone deacetylase activity. *Nat Genet* **24**(1): 88-91.

Fuks, F., Hurd, P.J., Deplus, R., and Kouzarides, T. 2003. The DNA methyltransferases associate with HP1 and the SUV39H1 histone methyltransferase. *Nucleic Acids Res* **31**(9): 2305-2312.

Goll, M.G. and Bestor, T.H. 2005. Eukaryotic cytosine methyltransferases. *Annu Rev Biochem* **74**: 481-514.

Goll, M.G., Kirpekar, F., Maggert, K.A., Yoder, J.A., Hsieh, C.L., Zhang, X., Golic, K.G., Jacobsen, S.E., and Bestor, T.H. 2006. Methylation of tRNAAsp by the DNA methyltransferase homolog Dnmt2. *Science* **311**(5759): 395-398.

Gowher, H. and Jeltsch, A. 2001. Enzymatic properties of recombinant Dnmt3a DNA methyltransferase from mouse: the enzyme modifies DNA in a non-processive manner and also methylates non-CpG [correction of non-CpA] sites. *J Mol Biol* **309**(5): 1201-1208.

Gowher, H., Loutchanwoot, P., Vorobjeva, O., Handa, V., Jurkowska, R.Z., Jurkowski, T.P., and Jeltsch, A. 2006. Mutational analysis of the catalytic domain of the murine Dnmt3a DNA-(cytosine C5)-methyltransferase. *J Mol Biol* **357**(3): 928-941.

Goyal, R., Reinhardt, R., and Jeltsch, A. 2006. Accuracy of DNA methylation pattern preservation by the Dnmt1 methyltransferase. *Nucleic Acids Res* **34**(4): 1182-1188.

Hata, K., Okano, M., Lei, H., and Li, E. 2002. Dnmt3L cooperates with the Dnmt3 family of de novo DNA methyltransferases to establish maternal imprints in mice. *Development* **129**(8): 1983-1993.

Heitman, J., Movva, N.R., Hiestand, P.C., and Hall, M.N. 1991. FK 506-binding protein proline rotamase is a target for the immunosuppressive agent FK 506 in Saccharomyces cerevisiae. *Proc Natl Acad Sci U S A* **88**(5): 1948-1952.

Helm, M. 2006. Post-transcriptional nucleotide modification and alternative folding of RNA. *Nucleic Acids Res* **34**(2): 721-733.

Helm, M., Giege, R., and Florentz, C. 1999. A Watson-Crick base-pair-disrupting methyl group (m1A9) is sufficient for cloverleaf folding of human mitochondrial tRNALys. *Biochemistry* **38**(40): 13338-13346.

Hengesbach, M., Meusburger, M., Lyko, F., and Helm, M. 2008. Use of DNAzymes for site-specific analysis of ribonucleotide modifications. *RNA* **14**(1): 180-187.

Hermann, A., Schmitt, S., and Jeltsch, A. 2003. The human Dnmt2 has residual DNA-(cytosine-C5) methyltransferase activity. *J Biol Chem* **278**(34): 31717-31721.

Hochuli, E. 1988. Large-scale chromatography of recombinant proteins. *J Chromatogr* **444**: 293-302.

Hore, T.A., Rapkins, R.W., and Graves, J.A. 2007. Construction and evolution of imprinted loci in mammals. *Trends Genet* **23**(9): 440-448.

Hotchkiss, R.D. 1948. The quantitative separation of purines, pyrimidines, and nucleosides by paper chromatography. *J Biol Chem* **175**(1): 315-332.

Howard, G., Eiges, R., Gaudet, F., Jaenisch, R., and Eden, A. 2008. Activation and transposition of endogenous retroviral elements in hypomethylation induced tumors in mice. *Oncogene* **27**(3): 404-408.

Howell, C.Y., Bestor, T.H., Ding, F., Latham, K.E., Mertineit, C., Trasler, J.M., and Chaillet, J.R. 2001. Genomic imprinting disrupted by a maternal effect mutation in the Dnmt1 gene. *Cell* **104**(6): 829-838.

Huynh, L.N., Thangavel, M., Chen, T., Cottrell, R., Mitchell, J.M., and Praetorius-Ibba, M. 2010. Linking tRNA localization with activation of nutritional stress responses. *Cell Cycle* **9**(15): 3112-3118.

Ingrell, C.R., Miller, M.L., Jensen, O.N., and Blom, N. 2007. NetPhosYeast: prediction of protein phosphorylation sites in yeast. *Bioinformatics* **23**(7): 895-897.

Ivanov, P., Emara, M.M., Villen, J., Gygi, S.P., and Anderson, P. 2011. Angiogenin-induced tRNA fragments inhibit translation initiation. *Mol Cell* **43**(4): 613-623.

Jackman, J.E., Montange, R.K., Malik, H.S., and Phizicky, E.M. 2003. Identification of the yeast gene encoding the tRNA m1G methyltransferase responsible for modification at position 9. *RNA* **9**(5): 574-585.

Jackson-Grusby, L., Beard, C., Possemato, R., Tudor, M., Fambrough, D., Csankovszki, G., Dausman, J., Lee, P., Wilson, C., Lander, E. et al. 2001. Loss of genomic methylation causes p53-dependent apoptosis and epigenetic deregulation. *Nat Genet* **27**(1): 31-39.

Janke, C., Magiera, M.M., Rathfelder, N., Taxis, C., Reber, S., Maekawa, H., Moreno-Borchart, A., Doenges, G., Schwob, E., Schiebel, E. et al. 2004. A versatile toolbox for PCR-based tagging of yeast genes: new fluorescent proteins, more markers and promoter substitution cassettes. *Yeast* **21**(11): 947-962.

Jeltsch, A. 2002. Beyond Watson and Crick: DNA methylation and molecular enzymology of DNA methyltransferases. *Chembiochem* **3**(4): 274-293.

Johansson, M.J. and Bystrom, A.S. 2004. The Saccharomyces cerevisiae TAN1 gene is required for N4-acetylcytidine formation in tRNA. *RNA* **10**(4): 712-719.

Jurkowska, R.Z., Jurkowski, T.P., and Jeltsch, A. 2011. Structure and function of mammalian DNA methyltransferases. *Chembiochem* **12**(2): 206-222.

Jurkowski, T.P., Meusburger, M., Phalke, S., Helm, M., Nellen, W., Reuter, G., and Jeltsch, A. 2008. Human DNMT2 methylates tRNA(Asp) molecules using a DNA methyltransferase-like catalytic mechanism. *RNA* **14**(8): 1663-1670.

Kaeberlein, M. 2010. Lessons on longevity from budding yeast. *Nature* **464**(7288): 513-519.

Kalhor, H.R. and Clarke, S. 2003. Novel methyltransferase for modified uridine residues at the wobble position of tRNA. *Mol Cell Biol* **23**(24): 9283-9292.

Kantidakis, T., Ramsbottom, B.A., Birch, J.L., Dowding, S.N., and White, R.J. 2010. mTOR associates with TFIIIC, is found at tRNA and 5S rRNA genes, and targets their repressor Maf1. *Proc Natl Acad Sci U S A* **107**(26): 11823-11828.

Kariko, K., Buckstein, M., Ni, H., and Weissman, D. 2005. Suppression of RNA recognition by Toll-like receptors: the impact of nucleoside modification and the evolutionary origin of RNA. *Immunity* **23**(2): 165-175.

Katoh, M., Curk, T., Xu, Q., Zupan, B., Kuspa, A., and Shaulsky, G. 2006. Developmentally regulated DNA methylation in Dictyostelium discoideum. *Eukaryot Cell* **5**(1): 18-25.

Kim, D.U., Hayles, J., Kim, D., Wood, V., Park, H.O., Won, M., Yoo, H.S., Duhig, T., Nam, M., Palmer, G. et al. 2010. Analysis of a genome-wide set of gene deletions in the fission yeast Schizosaccharomyces pombe. *Nat Biotechnol* **28**(6): 617-623.

Kim, G.D., Ni, J., Kelesoglu, N., Roberts, R.J., and Pradhan, S. 2002. Co-operation and communication between the human maintenance and de novo DNA (cytosine-5) methyltransferases. *EMBO J* **21**(15): 4183-4195.

Kimura, H. and Shiota, K. 2003. Methyl-CpG-binding protein, MeCP2, is a target molecule for maintenance DNA methyltransferase, Dnmt1. *J Biol Chem* **278**(7): 4806-4812.

Klimasauskas, S., Kumar, S., Roberts, R.J., and Cheng, X. 1994. HhaI methyltransferase flips its target base out of the DNA helix. *Cell* **76**(2): 357-369.

Kourtis, N. and Tavernarakis, N. 2011. Cellular stress response pathways and ageing: intricate molecular relationships. *EMBO J* **30**(13): 2520-2531.

Krauss, V. and Reuter, G. 2011. DNA methylation in Drosophila--a critical evaluation. *Prog Mol Biol Transl Sci* **101**: 177-191.

Kuhlmann, M., Borisova, B.E., Kaller, M., Larsson, P., Stach, D., Na, J., Eichinger, L., Lyko, F., Ambros, V., Soderbom, F. et al. 2005. Silencing of retrotransposons in Dictyostelium by DNA methylation and RNAi. *Nucleic Acids Res* **33**(19): 6405-6417.

Kunert, N., Marhold, J., Stanke, J., Stach, D., and Lyko, F. 2003. A Dnmt2-like protein mediates DNA methylation in Drosophila. *Development* **130**(21): 5083-5090.

Laemmli, U.K. 1970. Cleavage of structural proteins during the assembly of the head of bacteriophage T4. *Nature* **227**(5259): 680-685.

Lande-Diner, L., Zhang, J., Ben-Porath, I., Amariglio, N., Keshet, I., Hecht, M., Azuara, V., Fisher, A.G., Rechavi, G., and Cedar, H. 2007. Role of DNA methylation in stable gene repression. *J Biol Chem* **282**(16): 12194-12200.

Laurent, L., Wong, E., Li, G., Huynh, T., Tsirigos, A., Ong, C.T., Low, H.M., Kin Sung, K.W., Rigoutsos, I., Loring, J. et al. 2010. Dynamic changes in the human methylome during differentiation. *Genome Res* **20**(3): 320-331.

Leupold, U. 1950. Die Vererbung von Homothallie und Heterothallie bei Schizosaccharomyces pombe. *CR Lab Carlsberg* **24**: 381-475.

Li, E., Beard, C., and Jaenisch, R. 1993. Role for DNA methylation in genomic imprinting. *Nature* **366**(6453): 362-365.

Li, E., Bestor, T.H., and Jaenisch, R. 1992. Targeted mutation of the DNA methyltransferase gene results in embryonic lethality. *Cell* **69**(6): 915-926.

Lin, M.J., Tang, L.Y., Reddy, M.N., and Shen, C.K. 2005. DNA methyltransferase gene dDnmt2 and longevity of Drosophila. *J Biol Chem* **280**(2): 861-864.

Lindner, P. 1893. Schizosaccharomyces pombe n. sp., ein neuer Gärungserreger. *Wochenschrift für Brauerei* **10**: 1298-1300.

Lister, R., Pelizzola, M., Dowen, R.H., Hawkins, R.D., Hon, G., Tonti-Filippini, J., Nery, J.R., Lee, L., Ye, Z., Ngo, Q.M. et al. 2009. Human DNA methylomes at base resolution show widespread epigenomic differences. *Nature* **462**(7271): 315-322.

Liu, Y. and Santi, D.V. 2000. m5C RNA and m5C DNA methyl transferases use different cysteine residues as catalysts. *Proc Natl Acad Sci U S A* **97**(15): 8263-8265.

Lyko, F., Ramsahoye, B.H., and Jaenisch, R. 2000. DNA methylation in Drosophila melanogaster. *Nature* **408**(6812): 538-540.

Margot, J.B., Aguirre-Arteta, A.M., Di Giacco, B.V., Pradhan, S., Roberts, R.J., Cardoso, M.C., and Leonhardt, H. 2000. Structure and function of the mouse DNA methyltransferase gene: Dnmt1 shows a tripartite structure. *J Mol Biol* **297**(2): 293-300.

Margot, J.B., Ehrenhofer-Murray, A.E., and Leonhardt, H. 2003. Interactions within the mammalian DNA methyltransferase family. *BMC Mol Biol* **4**: 7.

Matsuyama, A., Arai, R., Yashiroda, Y., Shirai, A., Kamata, A., Sekido, S., Kobayashi, Y., Hashimoto, A., Hamamoto, M., Hiraoka, Y. et al. 2006. ORFeome cloning and global analysis of protein localization in the fission yeast Schizosaccharomyces pombe. *Nat Biotechnol* **24**(7): 841-847.

Mei, Y., Yong, J., Liu, H., Shi, Y., Meinkoth, J., Dreyfuss, G., and Yang, X. 2010. tRNA binds to cytochrome c and inhibits caspase activation. *Mol Cell* **37**(5): 668-678.

Mertineit, C., Yoder, J.A., Taketo, T., Laird, D.W., Trasler, J.M., and Bestor, T.H. 1998. Sex-specific exons control DNA methyltransferase in mammalian germ cells. *Development* **125**(5): 889-897.

Miller, M.L., Soufi, B., Jers, C., Blom, N., Macek, B., and Mijakovic, I. 2009. NetPhosBac - a predictor for Ser/Thr phosphorylation sites in bacterial proteins. *Proteomics* **9**(1): 116-125.

Moreno, S., Klar, A., and Nurse, P. 1991. Molecular genetic analysis of fission yeast Schizosaccharomyces pombe. *Methods Enzymol* **194**: 795-823.

Motorin, Y. and Grosjean, H. 1999. Multisite-specific tRNA:m5C-methyltransferase (Trm4) in yeast Saccharomyces cerevisiae: identification of the gene and substrate specificity of the enzyme. *RNA* **5**(8): 1105-1118.

Motorin, Y., Lyko, F., and Helm, M. 2009. 5-methylcytosine in RNA: detection, enzymatic formation and biological functions. *Nucleic Acids Res* **38**(5): 1415-1430.

Okano, M., Bell, D.W., Haber, D.A., and Li, E. 1999. DNA methyltransferases Dnmt3a and Dnmt3b are essential for de novo methylation and mammalian development. *Cell* **99**(3): 247-257.

Okano, M., Xie, S., and Li, E. 1998a. Cloning and characterization of a family of novel mammalian DNA (cytosine-5) methyltransferases. *Nat Genet* **19**(3): 219-220.

-. 1998b. Dnmt2 is not required for de novo and maintenance methylation of viral DNA in embryonic stem cells. *Nucleic Acids Res* **26**(11): 2536-2540.

Ooi, S.K., Qiu, C., Bernstein, E., Li, K., Jia, D., Yang, Z., Erdjument-Bromage, H., Tempst, P., Lin, S.P., Allis, C.D. et al. 2007. DNMT3L connects unmethylated lysine 4 of histone H3 to de novo methylation of DNA. *Nature* **448**(7154): 714-717.

Otani, J., Nankumo, T., Arita, K., Inamoto, S., Ariyoshi, M., and Shirakawa, M. 2009. Structural basis for recognition of H3K4 methylation status by the DNA methyltransferase 3A ATRX-DNMT3-DNMT3L domain. *EMBO Rep* **10**(11): 1235-1241.

Panning, B. and Jaenisch, R. 1996. DNA hypomethylation can activate Xist expression and silence X-linked genes. *Genes Dev* **10**(16): 1991-2002.

Phalke, S., Nickel, O., Walluscheck, D., Hortig, F., Onorati, M.C., and Reuter, G. 2009. Retrotransposon silencing and telomere integrity in somatic cells of Drosophila depends on the cytosine-5 methyltransferase DNMT2. *Nat Genet* **41**(6): 696-702.

Phizicky, E.M. and Alfonzo, J.D. 2010. Do all modifications benefit all tRNAs? *FEBS Lett* **584**(2): 265-271.

Phizicky, E.M. and Hopper, A.K. 2010. tRNA biology charges to the front. *Genes Dev* **24**(17): 1832-1860.

Pinarbasi, E., Elliott, J., and Hornby, D.P. 1996. Activation of a yeast pseudo DNA methyltransferase by deletion of a single amino acid. *J Mol Biol* **257**(4): 804-813.

Pradhan, M., Esteve, P.O., Chin, H.G., Samaranayke, M., Kim, G.D., and Pradhan, S. 2008. CXXC domain of human DNMT1 is essential for enzymatic activity. *Biochemistry* **47**(38): 10000-10009.

Pradhan, S., Bacolla, A., Wells, R.D., and Roberts, R.J. 1999. Recombinant human DNA (cytosine-5) methyltransferase. I. Expression, purification, and comparison of de novo and maintenance methylation. *J Biol Chem* **274**(46): 33002-33010.

Puig, O., Caspary, F., Rigaut, G., Rutz, B., Bouveret, E., Bragado-Nilsson, E., Wilm, M., and Seraphin, B. 2001. The tandem affinity purification (TAP) method: a general procedure of protein complex purification. *Methods* **24**(3): 218-229.

Rai, K., Chidester, S., Zavala, C.V., Manos, E.J., James, S.R., Karpf, A.R., Jones, D.A., and Cairns, B.R. 2007. Dnmt2 functions in the cytoplasm to promote liver, brain, and retina development in zebrafish. *Genes Dev* **21**(3): 261-266.

Rassoulzadegan, M., Grandjean, V., Gounon, P., Vincent, S., Gillot, I., and Cuzin, F. 2006. RNA-mediated non-mendelian inheritance of an epigenetic change in the mouse. *Nature* **441**(7092): 469-474.

Reinisch, K.M., Chen, L., Verdine, G.L., and Lipscomb, W.N. 1995. The crystal structure of HaeIII methyltransferase convalently complexed to DNA: an extrahelical cytosine and rearranged base pairing. *Cell* **82**(1): 143-153.

Rigaut, G., Shevchenko, A., Rutz, B., Wilm, M., Mann, M., and Seraphin, B. 1999. A generic protein purification method for protein complex characterization and proteome exploration. *Nat Biotechnol* **17**(10): 1030-1032.

Riggs, A.D. 1975. X inactivation, differentiation, and DNA methylation. *Cytogenet Cell Genet* **14**(1): 9-25.

Robertson, K.D., Ait-Si-Ali, S., Yokochi, T., Wade, P.A., Jones, P.L., and Wolffe, A.P. 2000. DNMT1 forms a complex with Rb, E2F1 and HDAC1 and represses transcription from E2F-responsive promoters. *Nat Genet* **25**(3): 338-342.

Robertson, K.D. and Wolffe, A.P. 2000. DNA methylation in health and disease. *Nat Rev Genet* **1**(1): 11-19.

Roguev, A., Wiren, M., Weissman, J.S., and Krogan, N.J. 2007. High-throughput genetic interaction mapping in the fission yeast Schizosaccharomyces pombe. *Nat Methods* **4**(10): 861-866.

Rountree, M.R., Bachman, K.E., and Baylin, S.B. 2000. DNMT1 binds HDAC2 and a new co-repressor, DMAP1, to form a complex at replication foci. *Nat Genet* **25**(3): 269-277.

Roux, A.E., Quissac, A., Chartrand, P., Ferbeyre, G., and Rokeach, L.A. 2006. Regulation of chronological aging in Schizosaccharomyces pombe by the protein kinases Pka1 and Sck2. *Aging Cell* **5**(4): 345-357.

Rozenski, J., Crain, P.F., and McCloskey, J.A. 1999. The RNA Modification Database: 1999 update. *Nucleic Acids Res* **27**(1): 196-197.

Sado, T., Fenner, M.H., Tan, S.S., Tam, P., Shioda, T., and Li, E. 2000. X inactivation in the mouse embryo deficient for Dnmt1: distinct effect of hypomethylation on imprinted and random X inactivation. *Dev Biol* **225**(2): 294-303.

Sambrook, J., Fritsch, E.F., and Maniatis, T. 1989. *Molecular Cloning: A Laboratory Manual*. Cold Spring Harbor Laboratory Press.

Sancak, Y., Peterson, T.R., Shaul, Y.D., Lindquist, R.A., Thoreen, C.C., Bar-Peled, L., and Sabatini, D.M. 2008. The Rag GTPases bind raptor and mediate amino acid signaling to mTORC1. *Science* **320**(5882): 1496-1501.

Santi, D.V., Norment, A., and Garrett, C.E. 1984. Covalent bond formation between a DNA-cytosine methyltransferase and DNA containing 5-azacytosine. *Proc Natl Acad Sci U S A* **81**(22): 6993-6997.

Schaefer, M., Hagemann, S., Hanna, K., and Lyko, F. 2009a. Azacytidine inhibits RNA methylation at DNMT2 target sites in human cancer cell lines. *Cancer Res* **69**(20): 8127-8132.

Schaefer, M. and Lyko, F. 2009. Solving the Dnmt2 enigma. *Chromosoma* **119**(1): 35-40.

-. 2010. Lack of evidence for DNA methylation of Invader4 retroelements in Drosophila and implications for Dnmt2-mediated epigenetic regulation. *Nat Genet* **42**(11): 920-921; author reply 921.

Schaefer, M., Pollex, T., Hanna, K., and Lyko, F. 2009b. RNA cytosine methylation analysis by bisulfite sequencing. *Nucleic Acids Res* **37**(2): e12.

Schaefer, M., Pollex, T., Hanna, K., Tuorto, F., Meusburger, M., Helm, M., and Lyko, F. 2010. RNA methylation by Dnmt2 protects transfer RNAs against stress-induced cleavage. *Genes Dev* **24**(15): 1590-1595.

Schaefer, M., Steringer, J.P., and Lyko, F. 2008. The Drosophila cytosine-5 methyltransferase Dnmt2 is associated with the nuclear matrix and can access DNA during mitosis. *PLoS One* **3**(1): e1414.

Sharp, Z.D. and Richardson, A. 2011. Aging and cancer: can mTOR inhibitors kill two birds with one drug? *Target Oncol* **6**(1): 41-51.

Shen, J.C., Rideout, W.M., 3rd, and Jones, P.A. 1994. The rate of hydrolytic deamination of 5-methylcytosine in double-stranded DNA. *Nucleic Acids Res* **22**(6): 972-976.

Smith, D.L., Jr., McClure, J.M., Matecic, M., and Smith, J.S. 2007. Calorie restriction extends the chronological lifespan of Saccharomyces cerevisiae independently of the Sirtuins. *Aging Cell* **6**(5): 649-662.

Sprinzl, M. and Vassilenko, K.S. 2005. Compilation of tRNA sequences and sequences of tRNA genes. *Nucleic Acids Res* **33**(Database issue): D139-140.

Sunnerhagen, P., Seaton, B.L., Nasim, A., and Subramani, S. 1990. Cloning and analysis of a gene involved in DNA repair and recombination, the rad1 gene of Schizosaccharomyces pombe. *Mol Cell Biol* **10**(7): 3750-3760.

Takashima, S., Takehashi, M., Lee, J., Chuma, S., Okano, M., Hata, K., Suetake, I., Nakatsuji, N., Miyoshi, H., Tajima, S. et al. 2009. Abnormal DNA methyltransferase expression in mouse germline stem cells results in spermatogenic defects. *Biol Reprod* **81**(1): 155-164.

Tang, L.Y., Reddy, M.N., Rasheva, V., Lee, T.L., Lin, M.J., Hung, M.S., and Shen, C.K. 2003. The eukaryotic DNMT2 genes encode a new class of cytosine-5 DNA methyltransferases. *J Biol Chem* **278**(36): 33613-33616.

Tatematsu, K.I., Yamazaki, T., and Ishikawa, F. 2000. MBD2-MBD3 complex binds to hemi-methylated DNA and forms a complex containing DNMT1 at the replication foci in late S phase. *Genes Cells* **5**(8): 677-688.

Thompson, D.M. and Parker, R. 2009. The RNase Rny1p cleaves tRNAs and promotes cell death during oxidative stress in Saccharomyces cerevisiae. *J Cell Biol* **185**(1): 43-50.

Tovy, A., Hofmann, B., Helm, M., and Ankri, S. 2010a. In vitro tRNA methylation assay with the Entamoeba histolytica DNA and tRNA methyltransferase Dnmt2 (Ehmeth) enzyme. *J Vis Exp*(44).

Tovy, A., Siman Tov, R., Gaentzsch, R., Helm, M., and Ankri, S. 2010b. A new nuclear function of the Entamoeba histolytica glycolytic enzyme enolase: the metabolic regulation of cytosine-5 methyltransferase 2 (Dnmt2) activity. *PLoS Pathog* **6**(2): e1000775.

Tsang, C.K., Liu, H., and Zheng, X.F. 2010. mTOR binds to the promoters of RNA polymerase I- and III-transcribed genes. *Cell Cycle* **9**(5): 953-957.

Vermeulen, A., McCallum, S.A., and Pardi, A. 2005. Comparison of the global structure and dynamics of native and unmodified tRNAval. *Biochemistry* **44**(16): 6024-6033.

Vicens, Q. and Westhof, E. 2001. Crystal structure of paromomycin docked into the eubacterial ribosomal decoding A site. *Structure* **9**(8): 647-658.

Weisman, R. and Choder, M. 2001. The fission yeast TOR homolog, tor1+, is required for the response to starvation and other stresses via a conserved serine. *J Biol Chem* **276**(10): 7027-7032.

Wilkinson, C.R., Bartlett, R., Nurse, P., and Bird, A.P. 1995. The fission yeast gene pmt1+ encodes a DNA methyltransferase homologue. *Nucleic Acids Res* **23**(2): 203-210.

Wood, V. Gwilliam, R. Rajandream, M.A. Lyne, M. Lyne, R. Stewart, A. Sgouros, J. Peat, N. Hayles, J. Baker, S. et al. 2002. The genome sequence of Schizosaccharomyces pombe. *Nature* **415**(6874): 871-880.

Wu, J.C. and Santi, D.V. 1987. Kinetic and catalytic mechanism of HhaI methyltransferase. *J Biol Chem* **262**(10): 4778-4786.

Wu, P., Brockenbrough, J.S., Paddy, M.R., and Aris, J.P. 1998. NCL1, a novel gene for a non-essential nuclear protein in Saccharomyces cerevisiae. *Gene* **220**(1-2): 109-117.

Xie, S., Wang, Z., Okano, M., Nogami, M., Li, Y., He, W.W., Okumura, K., and Li, E. 1999. Cloning, expression and chromosome locations of the human DNMT3 gene family. *Gene* **236**(1): 87-95.

Yoder, J.A. and Bestor, T.H. 1998. A candidate mammalian DNA methyltransferase related to pmt1p of fission yeast. *Hum Mol Genet* **7**(2): 279-284.

Yoder, J.A., Soman, N.S., Verdine, G.L., and Bestor, T.H. 1997a. DNA (cytosine-5)-methyltransferases in mouse cells and tissues. Studies with a mechanism-based probe. *J Mol Biol* **270**(3): 385-395.

Yoder, J.A., Walsh, C.P., and Bestor, T.H. 1997b. Cytosine methylation and the ecology of intragenomic parasites. *Trends Genet* **13**(8): 335-340.

Zuin, A., Carmona, M., Morales-Ivorra, I., Gabrielli, N., Vivancos, A.P., Ayte, J., and Hidalgo, E. 2010. Lifespan extension by calorie restriction relies on the Sty1 MAP kinase stress pathway. *EMBO J* **29**(5): 981-991.

11 Danksagung

Ich möchte zunächst Frau Prof. Ann Ehrenhofer-Murray dafür danken, dass ich meine Promotion in diesem interessanten Themengebiet erarbeiten konnte, und dass sie sich immer die Zeit genommen hat mich bei der Projektplanung und beim experimentellen Vorgehen zu unterstützen.

Mein besonderer Dank gilt außerdem den Mitgliedern der Forschergruppe „Biochemistry and biological function of Dnmt2 methyltransferases“ (DFG FOR1082), im speziellen Wolfgang Nellen und Albert Jeltsch für die Unterstützung bei der Etablierung des *in vitro* Methylierungsassays und das zur Verfügung stellen des Dnmt2-Expresssionsplasmids und Matthias Schaefer für Hilfe bei der RNA-Bisulfitsequenzierung. Der DFG danke ich für die finanzielle Unterstützung während der Promotion. Außerdem danke ich Sara Müller dafür, dass sie mir den Methylierungsassay beigebracht hat, dass ich mit ihr über Dnmt2 diskutieren konnte und für die nette Unterhaltung bei all den Meetings.

Ich bedanke mich bei allen Mitgliedern des Genetik Labors für die Unterstützung bei Labor- und Schreibtischarbeit und für das angenehme Arbeitsklima in der Gruppe und auch bei Stefan und Chrissi, die mittlerweile anderswo ihren Platz gefunden haben. Ein besonderes Dankeschön geht an Martin für kleine Pausen und an die „Mittagsgruppe“, Gesine, Jan, Karo, Rita, Tanja: Wenn einer von uns mal einen Marauder und ein X-phone hat, dann treffen wir uns und hören im Radio „Friday“.

Bei meinen Eltern möchte ich mich von ganzem Herzen dafür bedanken, dass sie mir das Studium und damit all die resultierenden Herausforderungen und Erfahrungen ermöglicht haben und dass sie mich immer unterstützt haben. Meinem Bruder Martin danke ich dafür, dass er mich als einziger in der Familie noch versteht, wenn es um die Wissenschaft geht.

Mein ganz besonderer Dank gilt Boris, der in den letzten 10 Jahren jeden Tag für mich da war, immer an mich geglaubt hat und die Gabe besitzt mich immer wieder daran zu erinnern, wie viel Spaß man im Leben haben kann.

Der Lebenslauf ist in der Online-Version aus Gründen des Datenschutzes nicht enthalten.

Erklärung:

Hiermit erkläre ich, gem. §6 Abs. (2) f) der Promotionsordnung der Fakultäten für Biologie, Chemie und Mathematik zur Erlangung des Dr. rer. nat., dass ich das Arbeitsgebiet, dem das Thema „Characterization of the Dnmt2 homolog Pmt1 in *Schizosaccharomyces pombe*“ zuzuordnen ist, in Forschung und Lehre vertrete und den Antrag von Maria Becker befürworte und die Betreuung auch im Falle eines Weggangs, wenn nicht wichtige Gründe dem entgegenstehen, weiterführen werde.

Essen, den 03.07.2012 _____

Unterschrift eines Mitglieds der Universität Duisburg-Essen

Erklärung:

Hiermit erkläre ich, gem. § 7 Abs. (2) c) + e) der Promotionsordnung der Fakultäten für Biologie, Chemie und Mathematik zur Erlangung des Dr. rer. nat., dass ich die vorliegende Dissertation selbstständig verfasst und mich keiner anderen als der angegebenen Hilfsmittel bedient habe.

Essen, den 03.07.2012 _____

Unterschrift des/r Doktoranden/in

Erklärung:

Hiermit erkläre ich, gem. § 7 Abs. (2) d) + f) der Promotionsordnung der Fakultäten für Biologie, Chemie und Mathematik zur Erlangung des Dr. rer. nat., dass ich keine anderen Promotionen bzw. Promotionsversuche in der Vergangenheit durchgeführt habe und dass diese Arbeit von keiner anderen Fakultät/Fachbereich abgelehnt worden ist.

Essen den 03.07.2012 _____

Unterschrift des/r Doktoranden/in